WIFI Integration with LTE in the Roadmap of 5G Networks

Danielle Saliba

UNIVERSITE BRETAGNE LOIRE / MATHSTIC

IMT Atlantique
Bretagne-Pays de la Loire
École Mines-Télécom

Thèse de doctorat de

L'ÉCOLE NATIONALE SUPERIEURE MINES-TELECOM ATLANTIQUE
BRETAGNE PAYS DE LA LOIRE - IMT ATLANTIQUE

COMUE UNIVERSITE BRETAGNE LOIRE

ECOLE DOCTORALE N° 601
Mathématiques et Sciences et Technologies de l'Information et de la Communication
Spécialité : *Télécommunications*

Par
Danielle Saliba

WiFi Integration with LTE in the Roadmap of 5G Networks

Thèse présentée et soutenue à Brest, le 18 Dec 2019

Unité de recherche : IMT Atlantique, Lab-STICC,UBL, F-29238 Brest, France

Thèse N° : 2019IMTA0168

Rapporteurs avant soutenance :

Guillaume Ferré, Maître de Conférences, Enseirb-Matmeca, Talence, France
Joumana Farah, Professeure, Université Libanaise, Liban

Composition du Jury :

Président :	Samir Saoudi, Professeur, IMT Atlantique, Brest, France
Rapporteurs :	Guillaume Ferré, Maître de Conférences, Enseirb-Matmeca, Talence, France Joumana Farah, Professeure, Université Libanaise, Liban
Dir. de thèse :	Sebastien Houcke, Professeur, IMT Atlantique, Brest, France
Co-dir. de thèse :	Rodrigue Imad, Maître de Conférences, Université de Balamand, Liban

Declaration

I declare that I have written this PhD thesis entitled “WiFi Integration with LTE towards 5G Networks” independently, under the supervision and guidance of the advisors and referring exclusively the technical references, thesis publications and other sources of information cited at the end of this document and listed in the detailed bibliography. As the author, I furthermore state that, with respect to the development of this PhD thesis, I have not breached any copyright or violated anyone’s personal and/or ownership rights.

Contents

Acknowledgment

The research work described herein has been conducted at Signal and Communication department, Mines Telecom Atlantique Institute Brest, France.

I would like to acknowledge the support received from Mines Telecom Atlantique Institute which allowed me to continue my Ph.D study in telecommunications. It was a challenge for me to start the PhD thesis following 10 years of university graduation and in parallel to my work in the Telecom industrial field and in parallel to my duties toward my family and children in my personal life. When I reflect upon the last four years, I feel particularly proud of what I have achieved.

However, I would not have got this far without the support of many people. To all of them I dedicate this work. There are two people in particular I would like to thank, my supervisors Pr. Sebastien Houcke and Dr. Rodrigue Imad. I am extremely grateful for their unconditional support and constructive criticism offered throughout this thesis. It has been a pleasure to work with both of them. I am also grateful to the co-authors of the papers included in this thesis, Pr. Bachar El Hassan for his advices and guidance. I have very much enjoyed the experience of working collaboratively and publishing together.

Finally, and most importantly, I would like to take this opportunity to express my cordial gratitude and appreciation to my husband, my daughters and my parents for their continual support, and overall understanding. I am thankful to them for always being present to support me, at any time, in any place, and in any situation. Their encouragement has shown me many times the right way and gave me the perseverance to resolve difficult situations. They believed in me and pushed me to explore new directions in my life.

"*Challenges are what make life interesting, and overcoming them is what makes life meaningful*", Joshua Marine

List of Abbreviations

3G	Third generation of mobile networks
4G	Fourth generation of mobile networks
5G	Fifth generation of mobile networks
AP	Access Point
BPSK	Binary Shift Keying
BS	Base Station
CA	Collision Avoidance
CAPEX	capital expenditures
CCA	Clear Channel Assessment
CCA-CS	CCA Carrier Sense
CCA-ED	CCA Energy Detection
CDD	Cyclic Delay Diversity
CDMA	Code Division Multiple Access
CP	Cyclic Prefix
CQI	Channel Quality Indicator
CSAT	Carrier Sensing and Adaptive Transmission
CSI	Channel State Information
CSMA	Carrier Sense Multiple Access
DCF	Distributed Coordination Function
DFT	Discrete Fourier Transform
DL	Downlink
eICIC	Enhanced Inter-Cell Interference Coordination
EPC	Evolved Packet Core
EPS	Evolved Packet System
E-UTRAN	Evolved UTRAN (used as synonym for LTE)
FDM	Frequency Division Multiplex
FFT	Fast Fourier Transform

GI	Guard Interval
GSM	Global System for Mobile Communication
HCF	Hybrid Coordination Function
HetNet	Heterogeneous network
HT STA	High Throughput Stations
IFFT	inverse Fast Fourier Transform
IOT	Internet of things
IP	Internet Protocol
ISI	Inter Symbol Interference
ISM	Industrial, Scientific and Medical (radio band)
LAA	Licensed Assisted Access
LBT	Listen Before Talk protocol
LMS	Least Mean Square
LTE	Long term evolution
LTE-A	LTE Advanced
M2M	Machine to Machine
MAC	Media Access Control
MCS	modulation and coding schemes
MIMO	Multiple-input and multiple-output
MLE	Maximum Likelihood Estimation
MSE	Mean Squared Error
NAV	Network Allocation Vector
OFDM	Orthogonal Frequency Division Multiplexing
OFDMA	Orthogonal Frequency Division Multiple Access
OPEX	operational expenditures
PCF	Point Coordination Function
PDF	Probability Density Function
PHY	physical

PLCP	Physical Layer Convergence Procedure
PMD	Physical Medium Dependent
PRB	Physical Resource Block
PS	Power Spectrum
PSD	Power Spectrum Density
QAM	Quadrature Amplitude Modulation
QoE	Quality of Experience
QoS	Quality of Service
QPSK	Quadrature Phase Shift Keying
RAT	Radio Access Technologies
RB	Resource Block
RNC	Radio Network Controller
ROI	Return on Investment
RRC	Radio Resource Connection
RRM	Radio Resource Management
RSSI	Received Signal Strength Indication
SC-FDMA	Single Carrier Frequency Division Multiple Access
SINR	Signal to Interference Noise Ratio
SNR	Signal to Noise Ratio
STA	Stations
TCO	Total Cost of Ownership
TTI	Transmission Time Interval
UE	User equipment
UL	Uplink
UMTS	Universal Mobile Telecommunication System
UTRAN	UMTS Terrestrial Radio Access Network
WCDMA	Wideband Code Division Multiple Access
Wi-Fi	Wireless Fidelity
WLAN	Wireless Local Area Network

List of Figures

List of Tables

Scope of the Thesis

Inspired by the new and challenging additional capacity and higher throughput requirements for mobile data traffic, the main objectives of this thesis are:

a) Understand what current Wireless solutions can offer to advanced mobile technologies by analyzing the additional capacity that could be offered by Wireless-Fidelity (WiFi) to Long Term Evolution Advanced (LTE-A) networks.

b) Propose new solution in WiFi networks Load times attenuation measurement and thus estimate the available idle capacity of the physical layer

c) Define the heavy users in Long term evolution (LTE) network based on the measured high data consumption or average needed throughput.

d) Dimension the WiFi Network in order to support the transferred heavy traffic of LTE network

e) Estimate the profit share between LTE and WiFi following the cooperation through the proposed solutions.

General Introduction

Mobile data traffic is revealing an ongoing exponential growth due to the increasing number of mobile broadband devices and with the deployment of the IOT. This increase of data traffic necessitates new architecture and visions in the roadmap of the 5G networks in order to ensure a suitable mobile infrastructure that will be able to support the 10 times expected increase in the throughput and needed mobile capacity. However, there is a lack of available licensed spectrum, noting that most of the current mobile data traffic comes from indoor locations or mobile users with fixed positions. For those reasons, the cooperation between LTE and WiFi is an alleviating solution which aims to distribute the connected users efficiently between the Het-Nets and ensure throughput equilibration for the best QoS and capacity limitations management.

WiFi could be considered as a good technology to support LTE systems and enhance the capacity in the 5G roadmap for many technical reasons. Basically, the data rates of WiFi systems are comparable with the ones of cellular networks, where WiFi could achieve higher energy saving than the cellular networks. In addition, WiFi APs can be easily and quickly deployed in many suburban areas and indoor environments, with very reasonable cost of investment and without limitations in the hardware size or needed practical or environmental customization.

In addition, the majority of smart devices handsets are equipped with WiFi connectivity, and according to different studies, above 80% of the mobile traffic came from indoor locations [1][2]. Therefore, WiFi could have advantage to establish a communication infrastructure over other wireless communication technologies [1].

In order to ensure efficient coexistence between WiFi and LTE, we are tackling the basic challenges faced in WiFi systems.

One of those challenges, is the channel assignment process for the end user within a minimum response time and optimal spectrum utilization from the suitable AP. As per WiFi systems technical specifications, to perform the channel assignment when a device is first switched on, the software above the Media Access Control (MAC) layer stimulates the device to establish a contact message to select the most suitable AP [3]. The device will be in either active or passive

scanning mode based on the AP response type. For IEEE specifications, different implementations are allowed, therefore different characteristics may exist between devices. The time of the scanning mode could increase significantly depending on the channels load, and the status of the APs, where basic timers exist to assure minimum and maximum times for interrogation requests.

In our thesis, we propose a novel algorithm that estimates the load times attenuation of the WiFi 802.11n physical layer by taking the overlapping characteristic of the physical channels. This algorithm estimates the average load times attenuation of all the overlapped physical channels over a certain observation time instead of the non-overlapped ones only, independently from all system timers. Therefore, our algorithm is increasing the capacity of WiFi channels assignment based on their minimum load value in highly populated networks, where with the presence of the increasing spectrum demand constraint for future WiFi and 5G systems, the number of available non-overlapped channels may not be enough, thus devices need to share different channels (overlapped and non-overlapped) or to check for a new spectrum if it becomes available.

In addition, once the values of the estimated load are collected on a higher control node level, we could evaluate the load of the entire WiFi network APs channels, facilitating by that the aggregation and processing time of the capacity calculations.

Another challenge faced in WiFi systems, is that almost all WiFi networks are constituted of randomly deployed WiFi cells, and this is due to the fact that there are no limitations or regulations on WiFi cell deployment [3].The random installation of WiFi APs may cause WiFi networks to be implemented without optimal planning.

Obviously, cellular traffic can be partially offloaded if both WiFi and LTE cooperate together. However, it is essential to dimension efficiently the WiFi APs needed to support a proper number of transferred LTE users while ensuring a suitable user experience.

In addition, it is apparent that when extra APs are installed, a WiFi network will gain additional available capacity, and thus will achieve higher throughput. Nevertheless, increasing the number of APs and consequently the related Capital Expenditures (CAPEX) and Operational Expenditures (OPEX) without any constraint is not a good solution.

Therefore, we address in our proposed second algorithm, the two aforementioned constraints:

LTE efficient offload to WiFi networks, and the optimal WiFi network planning to support LTE. In this algorithm, we first define the LTE heavy users that are consuming the top data traffic in LTE network, and transfer or offload them to the WiFi network. The proposed solution will mitigate the energy consumption of the LTE cell related to the heavy users, and therefore, instead of increasing the number of LTE BSs or expanding their capacity, we are proposing to introduce new WiFi APs in the heterogenous network. This new architecture can ensure a low-cost solution compared to other solutions where we may increase the LTE macro or small cells that necessitate additional cost of investment. In this case, the investment in hardware implementation and maintenance costs, CAPEX and OPEX, will be reduced due to the fact that the needed cost for expanding WiFi networks is much less than the one needed for LTE sites.

Then, having the total number of users that are transferred to WiFi with the related volume of data consumption, the existing WiFi network, initially constituted of minimum one AP, will be handling this LTE offloaded traffic on top of its initial one. We estimate the WiFi network remaining available capacity based on the first proposed algorithm that estimates the load times attenuation value of the WiFi overlapped physical channels. Consequently, any needed additional capacity will be reflected by incrementing the number of WiFi APs, that are able to handle this new traffic, an ensure an optimal planning of the WiFi network.

Finally, the profit analysis of the cooperation between both systems is analyzed in this thesis for two different scenarios: in case the same operator owns both WiFi and LTE systems, or in case those systems are owned by two different operators. This analysis is based on the cooperative game theory Shapley value that proved its efficiency in profit sharing in the context of multiplayers that involves several types of relationships. Its main concept is that each player will have a profit share proportional to its contribution in the network setting and the added value it brings to the overall value chain as it will be explained in the related chapter.

Document Organization:

The remaining of this report is organized as follows. In Chapter 1, IEEE 802.11 standards of the different releases and amendments have been presented. The modulation and coding schemes of the 5th amendment 802.11n adopted in the analysis and simulations of this thesis are presented in detail, along with the physical layer architecture and functions (carrier sense

function, transmit function, receive function). The adopted modulation technique Orthogonal Frequency Division Multiplexing (OFDM) of 802.11n is analyzed, along with the structure of the overlapped physical channels and transmitter and receiver block diagrams. In addition, the MAC layer basic functions are described to clarify the WiFi systems medium access basic technique Carrier Sense Multiple Access/Collision Avoidance (CSMA/CA) in addition to the network connections and scanning methods, where our proposed algorithms in this thesis are essential to facilitate and enhance the quality and performance of the network and channel assignment model between the end user (or station) and the WiFi Access Points (APs).

In Chapter 2, our first algorithm which aims to estimate the WiFi Channels load times attenuation during a channel observation time is analyzed. In fact, we have presented the overlapped architecture of 802.11n physical channels, where we have analyzed the model of observing the three non-overlapped channels, and by those observations we can estimate the load times the attenuation of the remaining overlapped channels to have in total the estimated value over the twelve channels. Once the attenuation value is normalized, an estimated value for the channels load could be measured.

A five channels observations model has been analyzed as well, where we have noticed additional accuracy level. The study has been presented with a normalized attenuation model, however it has been analyzed in presence of a normalized white Gaussian noise environment, where we have demonstrated that the estimated load is almost equal to the real load of the channels with a negligible Mean Squared Error (MSE) value for the obtained results.

In Chapter 3, LTE system channel allocation according to the available resource blocks on the radio interface are described. This resources allocation defines the capacity of the LTE radio interface, where we can conclude the throughput value of the subscribers on the Downlink (DL) interface. According to this capacity, the throughput by user has been defined, where we have selected a top number of users that have the most significant volume of downloaded data on the LTE network, to be transferred to the WiFi network, thus freeing the related capacity on LTE network for more users and better throughput. The definition of heavy users and users transfer schemes are described in detailed in this chapter.

In Chapter 4, we refer to our first algorithm, to calculate the load of the channels of WiFi physical layer with normalized attenuation, to have a global average value per peak hours for

a certain number of days. Having this value, we can estimate the occupation of the WiFi network and thus estimate the remaining available free capacity that will be able to handle the transferred traffic of the heavy users from LTE to WiFi. Knowing the available capacity of WiFi network, any extra needed capacity will be reflected by adding more WiFi APs that will be able to support the amount of transferred data. This dimensioning of the minimum needed number of WiFi APs, represents the new needed WiFi hardware or investment to support LTE, instead of adding or investing in the extra needed LTE BSs, that will necessitate definitely extra amount of CAPEX and OPEX.

Chapter 5 describes the profit estimation for the WiFi and LTE coexistence based on the previously proposed dimensioning method to pinpoint the benefit of the cooperation. We have analyzed the coexistence through the gaming theory where we have two players WiFi and LTE willing to cooperate or not based on the resulted profit. The profit is calculated using Shapley value, as the difference between the revenue shares and the cost shares and based on two different scenarios respectively: if both LTE and WiFi systems are owned by the same operator, or if they are owned by two separate operators. The results have shown the benefit of cooperation, where definitely they are optimal in case where the same operator owns both systems.

Finally, Chapter 6 concludes the thesis work, to summarize the advantage of the proposed algorithms, and elaborate on the future needed extra possibilities and research areas.

CHAPTER 1 –

WiFi Access Medium

In this chapter the Physical and MAC layers of the WiFi systems are described in addition to the basic functionalities and features, in order to pinpoint the channel assignment and channel occupation time or channels load measurement in 802.11 physical layer.

1.1 IEEE 802.11 Standards

Wireless Local Area Network (WLAN) WiFi is based on IEEE 802.11 standards designed for indoor Wireless Local Area Networks for bandwidths of up to 100 MHz, at frequencies of 2.4 and 5 GHz.

The most common set of standards encountered in the IEEE 802.11 Wireless LAN till the time of writing are basically: 802.11a, 802.11b, 802.11g, 802.11n, 802.11ac and 802.11ax with maximum data rate extended from 54 Mbps, 11 Mbps, 54 Mbps, 600 Mbps, 1.3 Gbps and 12 Gbps respectively. The current highest data rate of WiFi standard is 802.11ac (1.3 Gbps). The next generation 802.11ax is in the process of rolling out [4]. Basically, the main physical layer standards of 802.11n or 802.11ac are based on Orthogonal Frequency Division Multiplexing (OFDM) that will be explained in detail in the next paragraph.

The Fifth Amendment 802.11n, operating in 2.4 GHz Industrial Scientific and Medical (ISM) unlicensed band, is adopted in this thesis algorithms and simulations, where we will be building our first proposed algorithm based on the overlapping characteristic of the 802.11n physical channels.

Other basic characteristics of 802.11n are MIMO concepts and channel bonding. Legacy WLANs communicate through a single spatial stream and single antenna, whereas MIMO enables transmission over two or more spatial streams with multiple transmitters and receivers. In addition, 802.11n operates over 20 MHz or 40 MHz channels. Channel bonding can be deployed to merge two 20 MHz channels into one that is 40 MHz wide, which will increase the data rates (theoretically double).

In 20 MHz mode, there are 64 subcarriers, while there are 128 subcarriers in 40 MHz mode. The basic MCS used in IEEE 802.11n are Binary Phase Shift Keying (BPSK), Quadrature Phase Shift Keying (QPSK), 16-Quadrature Amplitude Modulation (QAM), and 64-QAM, as per Table 1.1 [5].

Table. 1.1 Modulation and Coding Schemes in 802.11n (Data rate in Mbps).

MCS	Code rate	Modulation	Number of spatial streams	Data rate in 20 MHz	Data rate in 40 MHz
0	1/2	BPSK	1	6.5	13.5
1	1/2	QPSK	1	13	27
2	3/4	QPSK	1	19.5	40.5
3	1/2	16-QAM	1	26	54
4	3/4	16-QAM	1	39	81
5	2/3	64-QAM	1	52	108
6	3/4	64-QAM	1	58.5	121.5
7	5/6	64-QAM	1	65	135
8	1/2	BPSK	2	13	27
9	1/2	QPSK	2	26	54
10	3/4	QPSK	2	39	81
11	1/2	16-QAM	2	52	108
12	3/4	16-QAM	2	78	162
13	2/3	64-QAM	2	104	216
14	3/4	64-QAM	2	117	243
15	5/6	64-QAM	2	130	270

We will explain in detail in the next paragraphs the characteristic of the Physical and MAC layers of 802.11n standard in order to visualize the overlapping characteristic and the standard channels allocation scheme, that will be analyzed in our next proposed algorithm in this thesis.

1.2 WiFi Physical and MAC Layers

In order to describe into details, the channels load measurement and the channel assignment scheme in 802.11n, we represent in this paragraph the Physical and MAC layer functions responsible of the carrier sensing and channels assignment methods.

1.2.1 Structure and basic functions

The 802.11 wireless networks physical layer is divided into two sublayers: The Physical Layer Convergence Procedure (PLCP) sub layer and the Physical Medium Dependent (PMD) sublayer, whereas the second Data link layer is the MAC layer as shown in Fig. 1.1.

<table>
<tr><td>OSI Layer 2: Data Link</td><td>MAC</td></tr>
<tr><td rowspan="2">OSI Layer 1: Physical</td><td>PLCP</td></tr>
<tr><td>PMD</td></tr>
</table>

Fig 1.1 802.11 wireless networks Physical layer logical architecture

The PLCP sub layer is the link between the frames of the MAC layer and the radio transmissions in the air [6]. Basically, PLCP frames include a preamble to help synchronize incoming transmissions. The PMD is responsible for transmitting any bit it receives from the PLCP into the air using the antenna. Under the direction of the PLCP, the PMD sublayer provides actual transmission and reception of 802.11 frames. To provide this service, the PMD interfaces directly with the wireless medium, that is the air, and provides modulation and demodulation of the frame transmissions. The PLCP and PMD communicate with each other to govern the transmission and reception functions [7].

In addition, one of the basic general operations of the 802.11 physical layer is carrier-sensing [7]. The physical layer implements a carrier-sense operation by directing the PMD to check whether the medium is busy or idle. This involves activating a receiver that receives and demodulates radio frequency signals at specific frequencies. The PLCP performs the following sensing operations if the station is not transmitting or receiving a frame:

• **Detection of incoming signals:** The PLCP within the station senses the medium continually. When the medium becomes busy, the PLCP reads in the PLCP preamble and header of the frame to attempt synchronization of the receiver to the data rate of the signal.

• **Clear Channel Assessment (CCA):** The CCA operation determines whether the wireless medium is busy or idle. The PMD measures the energy on the medium that exceeds a specific level, which is the energy detection threshold. If the medium is idle, the PLCP will send an “idle”

notification to the MAC layer. If the medium is busy, the PLCP will send a “busy” notification to the MAC layer. The MAC layer can then make a decision whether to send a frame or not.

The 802.11 MAC layer interfaces with a specific 802.11 physical (PHY) layer, such as 802.11n, to perform the tasks of carrier sensing, transmission, and receiving of 802.11 frames [7]. The basic function of carrier sensing is the ability of an AP receiver to detect and decode an incoming WiFi signal preamble. CCA reports BUSY status when another WiFi signal is detected and must be held as BUSY for the length of the received frame as indicated in the frame's PLCP Length field. If the medium is busy, the PLCP will send a “busy” notification to the MAC layer. The MAC layer can then make the decision in case to send a frame or not [7].

CCA involves two related functions: CCA Carrier Sense (CCA-CS) and CCA Energy Detection (CCA-ED).

CCA-CS: Ability of the receiver to decode and detect a WiFi preamble. From the PLCP header field, the time duration for which the medium will be occupied can be inferred and when such WiFi preamble is detected the CCA flag is held busy until the end of data transmission.

CCA-ED: Ability of the receiver to detect non-WiFi energy in the operating channel and back off data transmission. The ED threshold is typically defined to be 20 dB above the minimum Rx sensitivity of the PHY. If the in-band signal energy crosses this threshold, CCA is held busy until the medium energy is below the threshold.

To understand the channel assignment scheme, we analyze into details the channel or medium access principle. A station wanting to transmit data, senses first the medium, and if idle, it can transmit the data depending on additional rules that 802.11 defines. If the medium is busy (which indicates that another station is transmitting), the station holds off transmission. This protocol is referred to as Carrier-Sense Multiple Access (CSMA) [7].

The main type of medium access used in 802.11n is Distributed Coordination Function (DCF) access. The DCF access method is part of the original 802.11 standard and uses a carrier sensing access method similar to Ethernet, which provides distributed asynchronous (unpredictable) access to the medium [7].

The DCF implements Carrier-Sense Multiple Access with Collision Avoidance CSMA/CA, a contention-based protocol to enable stations to decide upon their own when to access the

medium based on the presence or absence of traffic. The DCF is a mandatory medium access protocol that was introduced in the original 802.11 specification.

The DCF uses a combination of both physical and virtual carrier-sense mechanisms to determine whether the medium is busy or idle. If both physical and virtual mechanisms indicate an idle medium, the station can transmit data. If not, the station must wait. The Physical layer provides a physical means of sensing the channel. The result of the physical channel assessment from the Physical layer is sent to the MAC layer as part of the information in deciding the status of the channel. The MAC layer carries out the virtual carrier-sense protocol based on reservation information found in the Duration field of all frames. This information announces (to all other stations) a station's impending use of the medium. The MAC layer monitors the Duration field in all MAC frames and places this information in the station's Network Allocation Vector (NAV) if the value is greater than the current NAV value. The NAV operates like a timer, starting with a value equal to the Duration field value of the last frame transmission sensed on the medium and counting down to zero.

As a condition to accessing the medium, the MAC layer checks the value of its NAV. If the NAV equals zero and the PHY layer indicates a clear channel (that is, Received Signal Strength Indication (RSSI) is below a specific threshold), the station can transmit a frame. Just before sending a frame, a station calculates the amount of time necessary to send the frame based on the frame's length and data rate. The station places a value representing this time in the Duration field in the header of the frame. This process reserves the medium for the sending station because the Duration field causes the MAC layers in other stations to hold off transmissions until the sending station finishes sending its frame [7].

An important aspect of the DCF is a random backoff that a station must wait if it detects a busy medium. If the channel is in use, the station must wait a random period of time before attempting to access the medium. Thus, if the PHY layer indicates that the medium is not clear (that is, RSSI threshold is above a specific threshold), the MAC layer implements a backoff algorithm, regardless of the status of the NAV. This avoids the probability of collisions among stations waiting to transmit.

From the other side, before checking the medium access, stations must first connect to an 802.11 network prior to sending any data. This process is automatic and involves the following actions: Scanning for network (necessary for the station to identify an AP that he can connect to), Authenticating with the network (to announce the desire to associate with another station or AP, or to ensure that the requesting station is authentic to be connected to the network), and Associating with the AP (to synchronize the client station and access point with important information, such as beacon interval and supported data rates). Once the client radio completes these steps, it can begin sending data frames [7].

During the scanning for the network, the station will use either active or passive scanning mode based on the response type from the AP. For IEEE specifications, different implementations are allowed; therefore, different characteristics may exist between stations or devices. The time of the scanning mode could increase significantly depending on the channels load.

Currently, in the channel selection principle of WiFi systems, two scanning modes could be used to assure a systematic channel assignment as mentioned before: passive and active scanning. In the case of passive scanning, the client has to wait to receive a Beacon Frame from the AP [8]. A Beacon is transmitted from an AP and contains information about the AP along with a timing reference. The device then searches for a network just by listening for beacons until it finds a suitable network to join. This procedure is similar for the 11 channels.

With active scanning the device tries to locate an AP by transmitting Probe Request Frames, and waits for Probe Response from the AP [8]. The probe request frame can be either a directed or a broadcast probe request. The probe response frame from the AP is similar to the beacon frame. The client station records the signal strength of the beacon frame or probe response to make a decision on which AP to associate with. In general, the client station chooses the AP that sent the beacon or response having the strongest signal [7].

While active scanning is a faster way to establish the contact, it consumes more battery power. In addition, the delay of the probe response from the AP is variable and depends on the load of the AP. If the station waits for the Probe Response for a significant period of time, it will affect the average of the total scan duration. However, if it waits for a short duration, the probability of finding the suitable AP is decreased.

802.11n standard defines two timers to assure the optimal control: MinChannelTime and MaxChannelTime. If the Probe Response is not received between those two timers, the terminal assumes the channel is empty, thus no available AP exists.

Each vendor implements scanning differently, but many use both passive and active scanning. For example, the client station might initially and periodically thereafter perform a passive scan of all radio frequency channels. Between passive scans, the client station may perform an active scan if the signal strength of the AP that the client station is connected is declining rapidly, such as when the client station is moving away from the AP.

1.2.2 Used Modulation scheme

We will describe in this paragraph, the used modulation scheme and the channels architecture in order to visualize the 802.11n overlapped physical channels needed in the analysis of our first proposed algorithm.

OFDM is a combination between multiplexing and modulation [5]. Multiplexing is the combination of independent signals that are produced by different sources. Modulation refers to mapping the original information into new symbol which has frequency, phase and amplitude. Therefore, OFDM can be understood as a method that first split the original data into independent channels, modulate the data and re-multiplex it to create OFDM carriers. OFDM is the special case of Frequency Division Multiplex (FDM). In FDM, the data comes in one stream and cannot be divided. In OFDM, the information is made up by many smaller streams where a large number of overlapping, orthogonal, narrow band sub channels or subcarriers, transmitted in parallel, divide the available transmission bandwidth into several orthogonal subcarriers, and each subcarrier is modulated with the modulation technique in the same bandwidth [5].

The separation of subcarriers is theoretically minimal so that there is a very compact spectral utilization. The spacing is basically 15 kHz (i.e. the spacing between the peaks of each sub-carrier is 15 kHz). However, the phenomenon that hangouts most of the radio access technologies is the Inter Symbol Interference (ISI). ISI is caused by multipath propagations.

This basically causes the bits to interfere with each other and degrade the received signal. To prevent this, a Cyclic Prefix (CP) is added to the symbol which is simply a copy of the tail of the same symbol added at the start of the symbol. CP is preferred to Guard Interval (GI) which is the separation of the symbols in time domain by a time interval to neutralize the delay spread caused by the multipath. With the use of CP, data stream becomes continuous and this shortens the receiver filter delay [5]. Below are the multicarrier modulation techniques of FDM and OFDM respectively.

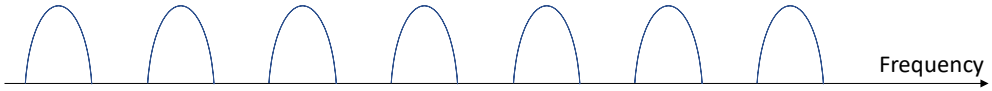

Fig 1.2. Conventional FDM multicarrier modulation technique

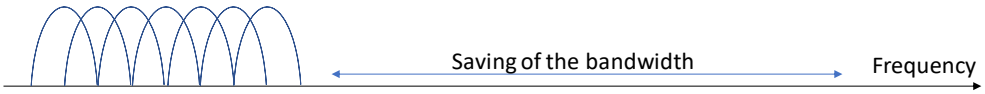

Fig 1.3. Conventional OFDM multicarrier modulation technique

In our study, we have considered in our Matlab simulations, 802.11n in 2.4 GHz band, with 20 MHz channel bandwidth, with 16 QAM modulation, 64 subcarriers, one spatial stream, and different number of symbols varying between 100 to 1000 symbols as signal length. The QAM modulation is a digital modulation technique that maps binary information using the gray code maps. The output after modulation is a complex signal which can be used to transfer through the physical channel.

Based on the adopted OFDM configuration in WLAN 802.11n standard in 20 MHz, the physical layer is constituted basically of 14 channels spaced with 5 MHz, where the adjacent channels are overlapping. In Europe, the first 11 channels remain available, and only three channels are non-overlapping in frequency at the same time [10], (e.g. channels 1, 5 and 9) as presented in Fig. 1.4:

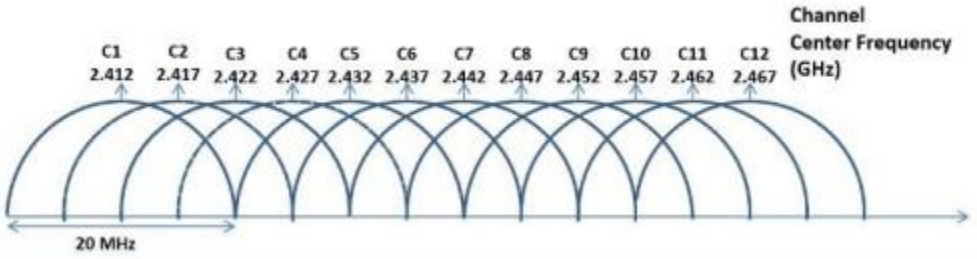

Fig 1.4. 802.11n physical overlapped channels

The use of multiple channels often increases the capacity of a wireless network, especially, if those channels are orthogonal. However, the challenge lies when we have less available orthogonal channels than the number of existing nodes. In practical cases, the overlapped channels are not considered usable, and are not selectable on most hardware in order to avoid the co-channel interference. Thus, to avoid this interference and maximize the throughput, only non-overlapped channels are used. Nevertheless, in this thesis, we are expecting that in densely populated networks, and with the constraints of increasing spectrum demand for future WiFi and mobile communication technologies such as 5G, the number of available non-overlapped channels may not be enough, thus devices might have to share both overlapped and non-overlapped channels or to check for a new spectrum if it becomes available. For these considerations, we are proposing an algorithm that calculates the load of the entire overlapped channels and not only the non-overlapped ones in order to ensure a proper channel selection during the data session between the end user and the WiFi AP.

Under the same concept, the study could be extended to 5 GHz band with 20 MHz channel width (or with wider channel width e.g. 40 MHz in channel bonding), constituted basically of 42 overlapped channels spaced with 5 MHz, with only 24 non-overlapping channels used in practical scenarios. Similarly, using the overlapped channels in 5 GHz (such as in 802.11 ac or 802.11 ax) could be considered due to the expected dense arrangement of APs, therefore overlapping or non-overlapping channels option could be a solution for the future increasing demand of the WLAN spectrum.

Finally, the theoretical Power Spectral Density (PSD) of an OFDM signal is needed to be calculated in our first proposed algorithm. We represent here below the formula to calculate the theoretical spectrum $S(f)$ or the PSD of the OFDM signal as given by [11]:

$$S(f) = \frac{\sigma_c^2}{MT_S} \sum_{k=0}^{N-1} \left(sinc\left[\left(f - k\Delta_f \right) MT_S \right] \right)^2 \quad (1.1)$$

where $sinc(\alpha) = sin(\pi\alpha) / (\pi\alpha)$, M is the symbol length (or duration in µs), σ_c variance of the data symbols $C(k;l)$ (complex value) modulated on the k^{th} subcarrier of the l^{th} symbol, k discrete frequency index, N is the number of subcarriers, and Δ_f the frequency spacing between subcarriers. The theoretical Power Spectrum Density (PSD) is shown in Fig. 1.5. To assure the OFDM orthogonal relationship between subcarriers, Δ_f is set as $W/N = 1/M$, where W is the total bandwidth of the signal, and T_s is the sampling interval employed in the OFDM transmitter.

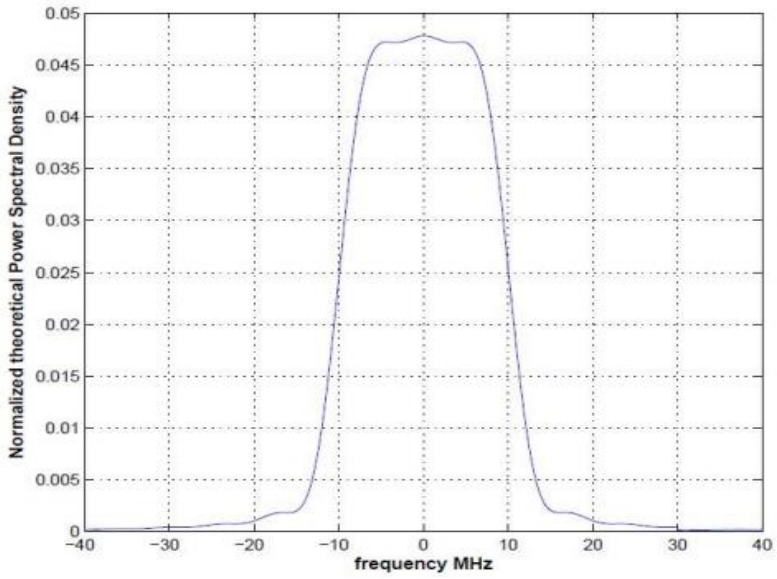

Fig. 1.5 Normalized theoretical Power Spectral Density of the 802.11n physical channel

1.2.3 Physical Layer Block Diagrams

In the below paragraph, we explain the needed functions of the 802.11n OFDM transmitter and receiver, that is adopted in our Matlab simulation to generate the 802.11n signal.

To build up our 802.11n physical layer simulation, we define a list of frame blocks with the appropriate modulation and coding schemes or sub standards (physical modes) as shown in Fig. 1.6 that represents the block diagram of an IEEE 802.11n transmitter, with Cyclic Delay Diversity (CDD) as space-time frequency (STF) technique that can exploit spatial diversity or generate transmit diversity.

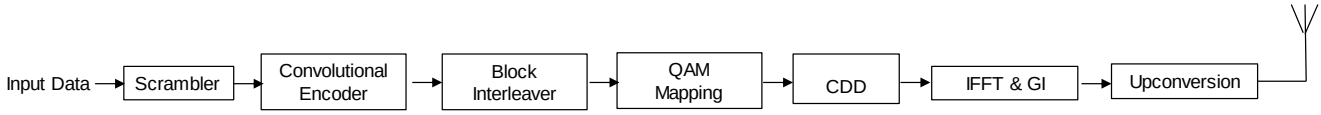

Fig. 1.6 Block diagram of an IEEE802.11n transmitter

Input data is first scrambled using the pseudo-noise scrambler before applying the convolutional encoder [5]. After encoding, a parser sends consecutive blocks of bits to different spatial streams. The bits are then interleaved by a block interleaver with a block size equal to the number of bits in a single OFDM symbol of the nth spatial stream. By interleaving, the bits across both spatial streams and subcarriers, the link performance benefits from both spatial diversity and frequency diversity. After interleaving, the bits are modulated into QAM symbols. Inverse Fast Fourier Transform (IFFT) is then applied to perform OFDM at the end before transmitting.

Based on the 802.11n draft, we come up in our Matlab simulation in this thesis with the design for our wireless system. The system is described in the block diagram for both the transmitter and receiver sides as shown in Fig. 1.7.

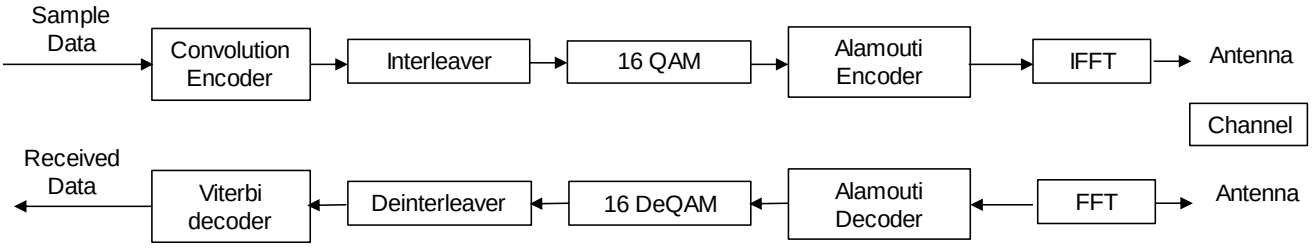

Fig 1.7. 802.11n Wireless communication system adopted Block Diagram

For the block diagram of Fig. 1.7, first the convolution encoder is a type of error-correction method [8] in which each m-bit information input in will be encoded to n-bit information symbol at the output. m/n is the code rate, and the transformation is a function of the k information symbol, k is the constraint length of the encoder. Convolution code usually used to improve the performance of digital radio. We use the Matlab convolution function to create the Convolution Encoder. Then the interleaver is applied to improve the error-correcting code. It will prevent the loss of data during the transmitting and receiving process. De-interleaver just rearranges the data to get the original signal. The Matlab function for Interleaver strictly follows the 802.11n draft to create the result.

In addition, 16-QAM modulation is applied. Then Alamouti encoder could be applied based on 2x2 MIMO technique as per Fig. 1.7. The concept of 2x2 MIMO is that the Data from the 16-QAM will be encoded into two separate signals. During the transmitting process, there are two notations for channel from transmit antenna to receive antenna. In our simulation, and for simplicity of signal processing, we have considered only one spatial stream from transmit to receiving signal.

Finally, IFFT and FFT are the main fundamental to implement OFDM, IFFT for transmitter and FFT for receiver [9] (FFT window size used in our Matlab simulation is 64 equal to the number of subcarriers). To implement the OFDM, we use IFFT to arrange data into orthogonal signal assuming there is no noise or interference on the channel.

CHAPTER 2-

Proposed Algorithm for Load Measurement of the WiFi Physical Channels

In order to reduce the time of an AP and channel discovery, and thus to optimize the values of different timers of WiFi systems on MAC and physical layers, we propose in this thesis a novel algorithm that estimates the load times the attenuation of each channel based on the overlapping characteristic of the WiFi physical layer, and thus ensuring to assign a channel based on the minimal load value. This algorithm is based on the overlapping characteristic of the physical channels where through some analytical observations of the non-overlapped channels, we can estimate the load times the attenuation of all the channels of the physical layer.

2.1 The basis of the estimated Load measurements

The channels occupation in WiFi systems is measured through the standard physical carrier sense mechanism CCA as described in the previous chapter.

However, this procedure, might be affected in congested networks and is centralized on an AP level, and depends on the network performance quality.

The accuracy of the CCA method depends on the probabilities of correct detection, and false alarm [12]. The correct detection probability is that a busy channel will be correctly detected as being busy and the false alarm probability is that an idle channel will be incorrectly detected as being busy. Those probabilities depend on the signal-to-noise ratio (SNR), and have significant impact on MAC performance metrics. As previously described, when the MAC layer has a packet to transmit, it requests the PHY layer to perform a CCA. If the CCA indicates an idle channel, MAC informs the PHY to start transmitting the packet. If, on the other hand, a the CCA

indicates a busy channel, MAC waits for a certain period (called backoff) and requests another CCA. If a busy channel had been incorrectly detected by the PHY layer as idle, the subsequent transmission will cause a collision, thus destroy the node's own packet and any others on air. Equally, if an idle channel had been detected incorrectly as busy, the node would postpone a possible alternative transmission and the channel would subsequently go unutilized [13].

In addition, the effectiveness of a CCA method must also consider the consumed power in the process for energy constrained nodes. Collisions caused by missed detection result in energy being wasted in unsuccessful transmissions. False alarms that occur will cause MAC to backoff needlessly and spend more energy in subsequent CCAs. The CCA mechanisms discussed in the previous chapter affect MAC energy efficiency to varying degrees due to their different power consumption characteristics and channel performance. While the poor performance of ED causes MAC energy efficiency to drop on the one hand, its energy consumption causes very little overhead during CCA. Clearly there is a trade-off between energy consumption and channel performance in the manner it impacts MAC throughput and energy efficiency [12].

For all the above considerations, we propose in our thesis a new algorithm that estimates the load times the attenuation of the WiFi 802.11n physical layer channels by analyzing the overlapping characteristic of the physical channels.

The algorithm is applied on the physical layer of WLAN networks, before establishing any connection between the WiFi AP and the user station.

Through the analysis and observation of a minimum of 3 non-overlapped channels (e.g. channels 1, 5 and 9), we can estimate the load times the attenuation of those distinct 3 channels and thus determine simultaneously this value over the remaining overlapped channels of the WiFi physical layer. By this, we can select the channel with the minimum load, and reduce the measurement time of channel load estimation.

Note that by the channel "load", we mean the percentage of the channel usage in time (or busy time) with respect to the total channel measurement time (total busy and idle time). Having the load of each channel facilitates the decision of the user for the channel selection based on the minimal load measurement. In our study, we simulate the WiFi 802.11n in 2.4 GHz radio

band with 20 MHz channel width, constituted basically of 14 overlapped channels spaced with 5 MHz.

Under the same concept, the study could be extended to 5 GHz band with 20 MHz channel width (or with wider channel width e.g. 40 MHz in channel bonding), constituted basically of 42 overlapped channels spaced with 5MHz, with only 24 non-overlapping channels used in practical scenarios. Similarly, using the overlapped channels in 5GHz could be considered due to the expected dense arrangement of APs, therefore overlapping or non-overlapping channels option could be a solution for the future increasing demand of the WLAN spectrum.

2.2 State of the Art

Many research studies were proposed to define the channel selection criteria in wireless networks, in order to minimize the AP or channel discovery time, independently from the medium QoS or SNR, and from the different timers' parameters. An optimal scanning procedure aims to adjust the values of related timers based on the channel conditions and the network characteristics while taking into consideration the user requirements.

Most of the existing proposals on the AP discovery in IEEE 802.11 networks focus on reducing the impact of scanning procedure on other processes, by reducing for example the duration of the scanning procedure during the handover, since MSs cannot send and receive data frames while they are scanning other channels. Basically, the proposed areas for efficient scanning are through limiting the number of channels to probe or to reduce the channel waiting time as was described for example in [13].

Also, authors in [10] proposed an algorithm that splits the complex power optimization and channel assignment problem into two separate solutions: first solution define the problem as pure channel assignment case with constant transmission power. Then in the second solution, after the channels are assigned based on the first one, they approached to the optimization of transmission power in APs. In this way, the power in an AP is increased or decreased in a step by step approach, so that the Signal to Interference Noise Ratio (SINR) is maximized and coverage area threshold is maintained for every AP.

In [14], authors presented a network and an interference models for multiple APs cochannel deployment and proposed a channel assignment scenario which transform the channel assignment problem into a time slot allocation problem. They proposed a multi AP deployment

mechanism, which allows all APs to operate in the same channel and coordinates them to obtain the appropriate channel and reduce the system interference. The core idea of the algorithm is to maintain a moderate cooperation between APs by a Central Access Controller in order to achieve a high channel utilization. They have proposed a basic channel assignment by vertex coloring algorithm which can determine the minimum number of time slots; they constructed a channel assignment by making extra polls for APs to improve the channel utilization; and then they have classified the clients to optimize the polling list of APs and reduce empty polls. In addition, since all APs only operate in one channel, they proposed multiple vertically nonoverlapping channels that can be used to improve the network capacity in high density WLANs.

Channel assignment in multi-rate 802.11n WLANs, to maximize the network throughput was analyzed in [15]. Authors first presented a network model and an interference model and estimated the client throughput based on them. They then formulated the channel assignment problem into a throughput optimization problem where they estimated the throughput for each client and formulated the problem into an integer linear program. They also proposed a distributed channel assignment algorithm that can be formulated into a throughput optimization problem. In fact, they analyzed the interference relationship between any two clients from different APs to estimate the throughput. This information was essential to the proposed channel assignment algorithm. So, they first presented a protocol to obtain the interference relationship among clients from neighboring APs, then gave a distributed channel assignment algorithm, named as throughput-maximizing channel assignment algorithm, that aims to maximize the network throughput.

In [16], authors elaborated the IEEE 802.11 discovery process needed for handovers between MS and WiFi AP. The scanning process consists in probing actively the radio channels to gather APs information and therefore to be able to be connected on the best suitable channel. This discovery is performed initially through the scanning process, where a MS sends a Probe Request management frame and waits for a Probe Response on each channel. This waiting time is managed by two timers in the scanning process: the MinChannelTime (MinCT) and the MaxChannelTime (MaxCT). If no Probe Response is received before MinCT expires, the MS switches to the next channel and sends a new Probe Request. Otherwise, if at least

one Probe Response was received, the MS waits for a longer timer, MaxCT, to receive more responses from other APs that operates in the same channel. The 802.11 standard does not specify the timer values nor the order in which the channels should be scanned (i.e., the channel sequence), even though these parameters impact greatly the scanning performance. Therefore, as analyzed in this paper, there is a tradeoff between keeping the latency short to minimize the impact on applications, and how many APs the MS is able to discover. In order to address this compromise, authors defined the scanning performance according to three metrics: the scanning latency which is the elapsed time for scanning the whole set of channels; the failure rate which is the probability of not finding any AP after completing the scanning; and finally, the discovery rate which is the fraction of discovered APs over the total number of available APs. The same problem is addressed in our proposed algorithm in this chapter, which is how to define the best suitable AP to be connected to a MS in the channel discovery and scanning process. The aim is to propose a scanning algorithm that seeks to discover the maximum number of APs in the shortest period of time, independently from the predefined values of the MAC and physical layers parameters. However, authors in this paper have adopted a probabilistic approach based on the three defined metrics mentioned previously (the scanning latency, the failure rate, and the discovery rate), that aims to find the set of scanning parameters in the decision space (i.e., the channel sequence and the timers) that minimize the scanning latency and the failure rate and maximize the discovery rate. The resolution of this problem provides multiple equivalent tradeoff solutions, where one particular configuration can be selected by taking into account the application needs that may prioritize one of the objectives.

In [17], authors have addressed the problem of the best AP selection in WLANs due to the same challenge of unplanned and unregulated nature of WiFi networks. Usually in WiFi networks, APs which are close to each other often operate on the same channel, especially on the frequently used non-overlapping channels, and therefore resulting in poor performance when the traffic demand exceeds the channel capacity. In this case, it is better for users to join a different network, for instance another AP operating on a different non-saturated channel, or a network using a different access technology (e.g., cellular network, wired network).

In their work, authors showed that it is possible for IEEE 802.11 stations to detect a saturated channel by monitoring passively the beacon frames. Since APs send periodically beacon frames and encode them using the strongest modulation and coding scheme, so that even the stations that are far away from the sending APs can decode them correctly. Therefore, when sending beacons, APs sense the channel in prior and, if it is busy, delay the sending of frames, resulting in unequally spaced beacon frames, whenever other transmitters are active. They proposed a method for stations to detect a saturated channel by passive monitoring of beacon messages, which are available to all stations as part of the IEEE 802.11 standard procedures.

By analyzing their experiments under different traffic loads, they proposed to identify if a channel is saturated based on the distribution of the beacon jitter. Since even though APs send beacon frames periodically, they have to wait for the channel to be idle, resulting in an additional delay that depends on the traffic intensity. They presented empirical results that showed that the beacon jitter follows a similar distribution whenever the channel is saturated. Therefore, their solution analyzes this by comparing the beacon jitter distribution with a reference distribution that corresponds to a saturated channel. This enables stations to passively collect information and to determine whether a channel is saturated or not and therefore to select the best suitable AP.

Furthermore in [18], authors in their work proposed various distributed channel allocation algorithms which are based on QoE oriented allocation. They have studied two innovative distributed channel assignment algorithms that make use of learning automata to explore the QoE measure of associated clients to locally formulate the optimization problem. Between two of the proposed algorithms, first one does not require communication with other APs, while the second algorithm is based on a communication with neighboring APs. After finding QoE level of the clients associated to the serving AP, the algorithms use learning automata mechanism to enhance the proposed performance index that maximize both users perceived quality and user-level fairness

In [19], authors proposed a channel assignment algorithm at the APs in order to maximize Signal-to-Interference Ratio (SIR) at the user level. They started with the channel assignment at the APs, which is based on minimizing the total interference between APs. Based on this initial assignment, they calculated the SIR for each user. They considered assigning channels

to APs based on maximizing the SIR at the user level instead of minimizing the interference between neighboring APs, which quantitatively leads to increase in network throughput as well as the channel reuse factor in some cases.

In [20], similarly authors have measured the interference to assure channel selection, however based on realistic interference scenarios in WLAN environments. They formulated a weighted variant of the graph coloring problem that takes into account realistic channel interference observed in wireless environments, as well as the impact of such interference on wireless users. They proposed scalable distributed algorithms that achieve better performance than existing techniques for channel assignment.

In [21], the study proposed a cloud-assisted channel selection method for multi-node wireless networks. Periodic channel idle airtime measurements of the APs are accumulated at a remote controller that runs various forecasting methods on the aggregated data and finds the best fitting method for each AP channel pair. By using the selected forecasting method, for every channel and every AP, expected idle airtime in the near future is calculated. Channel assignment is carried out by the remote controller, based on the forecasted idle airtime of each AP. While performing the channel assignment, the remote controller considers the available frequency bands in the network.

In addition, other than the scanning procedure and optimal criteria for AP channel selection, in the literature there is not much work focused on load estimation in itself. However, there are many papers that define load in some way, basically based on CCA measurements, and then use this load estimate as an input to their network management subsystems.

In [22], authors focused on analyzing the variation in IEEE 802.11k channel load measurements for neighbor WLAN systems, that allows stations to assess how occupied or idle a frequency channel is. Investigations were based on the variation of the channel load in time (i.e. how does the measurement vary in time for static traffic conditions). Also, measurements were based on the variation between the channel load values reported by different measuring stations, located at varying distances from the AP (i.e. what effect will interference from neighboring nodes have on the calculation of the channel load). Using the channel load report within their simulations, a measuring station reports the fractional duration

over which the CCA indicates that the medium is busy during a measurement period. Simulations have shown that there is a significant variation in channel loads reported by the same station at different times, which may have important effect on the selection of the channel with the minimum load. The variation present in these measurements questions the accuracy of a single channel load measurement; hence considerable attention must be taken when using and interpreting such measurements. Moreover, in this study, there was not an analytical method or algorithm presented to measure the channels load independently from the CCA measurements initially present in WLANs between the PHY and MAC layers.

In [23], a distributed least congested channel selection algorithm is proposed based interference between stations and load information. They analyzed the minimum interfering stations, as well as associated stations, by exchanging with neighbor APs, the beacon frame of the IEEE 802.11 standard with some additional field of channel load information. Authors proposed that the AP can select the least congested channel among all other available channels since this channel has the minimum number of interfering stations based on the measurements of the beacon and probe frames used in IEEE 802.11 standards with some additional fields of channel load information exchanged with neighbor APs.

In [24], authors proposed a load balancing algorithm to enhance the WLAN network performance. The algorithm dynamically balances the network load by distributing the mobile stations among APs, based on their measured load through the channel capacity and SNR values. The proposed Load balancing algorithm assesses periodically the parameters of each AP and distribute the MSs between the available APs. Whenever a station enters, moves and leaves from network, the load balancing server executes this algorithm. After the execution, the results provide the information about the number of associated stations with each AP and the total load measured in APs. This information is stored and updated in the server database. Their proposed load balancing algorithm calculates the load on each AP whenever an association or re-association takes place in the WLAN, based on traffic generated parameters (ON State time, OFF State time, packet size in bytes, number of stations generating traffic).

Other studies, such as [25], [26], [27] are basically parameters adjustments for the WLAN channels load measurements and reporting or traffic management based on network

parameters. In [25], authors proposed a mechanism for a channel monitoring to effectively derive accurate results of channel load. They focused on optimizing the duration of channel monitoring and thus minimize the impact on applications. In [26], authors proposed a resource allocation algorithm using utility functions for heterogeneous traffic and that considers the estimated User Equipment (UE) speed, traffic types and channel quality. In [27], authors performed an analysis of load-based routing metrics based on the interface buffer queue occupancy and contention window level. However, despite their popularity, authors show that metrics based on these parameters were not good bases for load accounting because these metrics do not vary with traffic load despite their ability to sense saturated regions. As an alternative they proposed the channel load metric that accurately accounts for channel load, contention, and interference.

In [28], the load criterion was measured by monitoring a limited number of channels at each measurement time instead of monitoring all channels. As per other studies and WLAN standards, the load measurement in this paper is based on the standard mechanism CCA which can measure the fraction of time in which the channel is idle or busy. However, since the CCA based load measurement may take significant time since the monitoring station should halt its transmission or reception during the duration of the measurement, the proposed algorithm utilizes the Gaussian Process Regression technique, used to estimate the instantaneous load of each channel by utilizing the previous load measurements. In this method, they monitor only a limited number of channels at each measurement time instead of monitoring all channels, and then determine the channel with the minimum traffic load without measuring all channels.

To summarize the different aims and methods adopted in the aforementioned studies, we represent in Table 2.1 the general summary of the analyzed state of the art.

Table 2.1. General summary of the analyzed state of the art

Reference	Aim	Adopted Method
[13]	channels scanning	through limiting the number of channels to probe or to reduce the channel waiting time
[10]	channel assignment	transmission power optimization in APs so that the SINR is maximized and coverage area threshold is maintained for every AP.
[14]	channel assignment	through time slot allocation, which allows all APs to operate in the same channel and coordinates them to obtain the appropriate channel, and reduce the system interference
[15]	channel assignment	the problem was formulated into a throughput optimization problem
[16]	channels scanning	in probing actively, the radio channels to optimize APs information: timers duration and channels sequence, based on the scanning latency, the failure rate, and the discovery rate
[17]	channel assignment	by detecting a saturated channel through monitoring passively the beacon frames, and therefore to determine whether a channel is saturated or not to select the best suitable AP
[18]	channel assignment	based on QoE oriented allocation to maximize both users perceived quality and user-level fairness
[19]	channel assignment	to maximize SIR at the user level instead of minimizing the interference between APs, which leads to increase in network throughput as well as the channel reuse factor
[20]	channel assignment	through measuring the interference to assure channel selection based on realistic interference scenarios in WLAN environments
[21]	channel assignment	forecasting method: expected idle airtime for every channel and every AP is calculated
[22]	channel assignment	channel allocation based on channel load measurement to assess how occupied or idle a frequency channel is. This method was based on the standard CCA method

[23]	channel assignment	based on measuring interference between stations and some additional fields of channel load information exchanged with neighbor APs
[24]	load balancing between APs	by distributing the mobile stations among APs, based on their measured load through the channel capacity and SNR values according to some standard parameters
[25]	channel load	based on channel monitoring standard parameters
[26]	channel assignment	based on UE speed, traffic types and channel quality
[27]	load balancing between APs	based on the interface buffer queue occupancy and contention window level
[28]	load measurement	based on the standard CCA mechanism, by monitoring a limited number of channels at each measurement time instead of monitoring all channels

In this chapter, the same concept of limited number of channels observation is applied in our next proposed algorithm in this thesis, however with different load estimation approach than the standard CCA based load measurement one.

To give an idea of how much time is needed to collect load information of each channel, similarly to the approach presented in [28], we consider the 2.4 GHz frequency band where there are 12 non-overlapping channels with a bandwidth of 20 MHz. If a channel is monitored for a duration of 50 milliseconds (ms) then the total time spent for the monitoring process will equal 600 ms (respectively 1150 ms 1.15 seconds for 23 overlapped channels in 5 GHz frequency band), which can significantly degrade the performance of the monitoring station in terms of both the throughput and delay. If the monitoring station is the AP, then the effect of the monitoring becomes more significant. For the aforementioned reason, monitoring only a certain number of non-overlapped channels in our proposed algorithm, constructs a predefined set of channels to be measured, and only those channels are measured at each measurement time, enabling the estimation of the load of the other overlapped channels as it will be explained in detail in the next sections.

2.3 Channels Observations Model

As we mentioned earlier in this study, our proposed algorithm is able to estimate the load times the attenuation of the 12 overlapped channels of the IEEE 802.11n operating under 2.4 GHz, by performing 3 observations only, and this on the non-overlapped channels, i.e channels 1, 5, and 9.

Noting that by observing the channel 1, our algorithm is able to estimate the load times the attenuation of channel 1 as well as the load times the attenuation of the adjacent overlapped channels, in this case channels 2, 3 and 4. Similarly the observation of channel 5 will lead to estimate the load times the attenuation of the overlapped channels 2, 3, 4 and 5, 6, 7, and 8. The observation of channel 9 will lead to estimate the load times the attenuation of the overlapped channels 6, 7, 8 and 9, 10, 11 and 12.

Let us define $\Gamma^j(f)$ as the baseband spectrum of the signal observed in channel j ($j = 1, 5, 9$ denotes the non-overlapped channels) and $S(f)$ the theoretical baseband PS of the WiFi signal calculated in equation (1.1), which emits in a continuous way. According to CSMA/CA principle, APs are not transmitting their data continuously. Let α_i denotes the load of channel i ($i = 1, \dots, 12$), and $\lambda_i(f)$ is the signal attenuation dependent on the channel frequency due to the propagation model of the same channel i.

α_i is defined as the percentage usage of channels i in time (or busy time) in respect to the total channel measurement time as described previously. The observed baseband spectrum of channel j with respect to all signals transmitted in the overlapped channels i is expressed as:

$$(\lambda_i^2(f).\alpha_i).S(f) \tag{2.1}$$

In the next sections of our algorithm, we assume that the attenuation of channel i, λ_i is constant independently from the frequency in order to facilitate the calculations, however the robustness of the algorithm in presence of multipath fading is demonstrated at the end of the simulations results section. Also, let a_i be the value needed to be calculated as per the equation below:

$$a_i = \lambda_i^2.\alpha_i \tag{2.2}$$

We present in the next sections, the 3 observations models that will lead to the estimation of the load times the attenuation of the entire 12 channels.

2.3.1 Channel 1 Observation and Load times the Attenuation Estimation of the related overlapped channels

To estimate $\Gamma^j(f)$, the baseband spectrum of the signal observed in channel j, we use Welch periodogram method [29]:

Mathematically, it is defined as the Fourier transform of the autocorrelation sequence of the time series. This method outlines the application of the Fast Fourier Transform algorithm to the estimation of the power spectra, which involves sectioning the record, taking modified periodograms of these sections, and averaging these modified periodograms [29] [30].

Let us now derive the expression of the PS of Channel 1, $\Gamma^1(f)$. Channels 1, 2, 3 and 4 contribute to this PS referring to Fig. 1.4.

We are therefore able to estimate the channels load times the attenuation values a_1, a_2, a_3, and a_4 from this observation. The contribution of channels 2, 3, and 4 in the PS of channel 1 is illustrated in Fig. 2.1, taking into consideration that those channels are shifted to the baseband, thus duplicated from both sides while saving the same overlapping proportions.

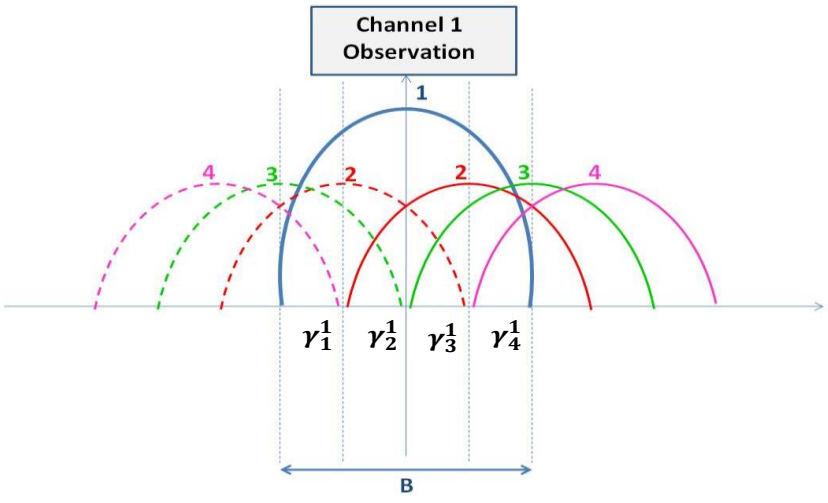

Fig 2.1. Channel 1 Observation Model

The observation of channel 1 reflects the total load times the attenuation of channel 1 in addition to a part of the load times the attenuation of its related overlapped channels 2, 3 and 4, according to the overlapped partitions.

For a bandwidth B of the channel, the total overlapping bandwidth between two consecutive channels is $3(B/4)$. Based on this sectioning, we divide the theoretical PSD $S(f)$ into 4 partitions S_1, S_2, S_3, and S_4 as presented in Fig. 2.2:

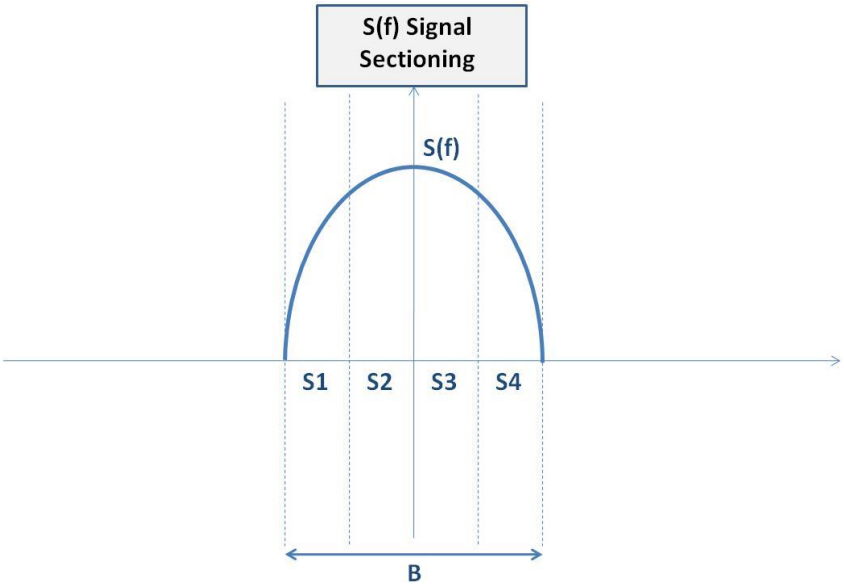

Fig 2.2. Signal Sectioning – Theoretical PSD

$$S_1(f) = S(f)\ for\ f\ \epsilon\ [-B/2; -B/4] \text{ and } 0 \text{ elsewhere}$$
$$S_2(f) = S(f)\ for\ f\ \epsilon\ [-B/4;\ 0] \text{ and } 0 \text{ elsewhere} \quad (2.3)$$
$$S_3(f) = S(f)\ for\ f\ \epsilon\ [0; B/4] \text{ and } 0 \text{ elsewhere}$$
$$S_4(f) = S(f)\ for\ f\ \epsilon\ [B/4; B/2] \text{ and } 0 \text{ elsewhere}$$

The complete theoretical PSD is denoted by the vector $\mathbb{S} = [S_1(f), S_2(f), S_3(f), S_4(f)]$ of size (1x4).

Similarly, $\Gamma^j(f)$, which is the PS of the observed signal in channel *j*, is divided into 4 sections $\gamma_1^j, \gamma_2^j, \gamma_3^j, \gamma_4^j$.

$$\gamma_1^j(f) = \Gamma^j(f)\ for\ f\ \epsilon\ [-B/2; -B/4] \text{ and } 0 \text{ elsewhere}$$

$$\gamma_2^j(f) = \Gamma^j(f)\ for\ f\ \epsilon\ [-B/4; 0] \text{ and } 0 \text{ elsewhere} \quad (2.4)$$

$$\gamma_3^j(f) = \Gamma^j(f)\ for\ f\ \epsilon\ [0; B/4] \text{ and } 0 \text{ elsewhere}$$

$$\gamma_4^j(f) = \Gamma^j(f)\ for\ f\ \epsilon\ [B/4; B/2] \text{ and } 0 \text{ elsewhere.}$$

The complete PS is the vector $\Gamma^j(f) = [\gamma_1^j(f); \gamma_2^j(f); \gamma_3^j(f); \gamma_4^j(f)]\ of$ size (4x1) (j = 1, 5, 9 in our case).

Based on the sectioning described in the previous sections, and based on equations (2.1), (2.3), and (2.4), we need to calculate γ_1^j, γ_2^j, γ_3^j, and γ_4^j in terms of $S(f)$ and a_i (the load times the attenuation of channel i) for the 12 channels, and thus during the 3 non-overlapped channels observations.

In the observation of channel 1 ($j = 1$) referring to Fig. 2.1, γ_1^1 is constituted of 2 times the load of channel 1 corresponding to section 1 (S_1), 1 time the load of channel 2 corresponding to section 2 (S_2), 1 time the load of channel 3 corresponding to section 3 (S_3), and 1 time the load of channel 4 corresponding to section 4 (S_4).

And therefore, based on the sectioning described previously, and referring to equation (2.2), we can have the below system of equations:

$$\gamma_1^1(f) = 2.a_1.S_1(f) + a_2.S_2(f) + a_3.S_3(f) + a_4.S_4(f) \quad (2.5)$$

By applying the same concept for γ_2^1, γ_3^1, and γ_4^1, we can write the below system of equations:

$$\gamma_2^1(f) = 2.a_1.S_2(f) + a_2.\big(S_1(f) + S_3(f)\big) + a_3.S_4(f)$$

$$\gamma_3^1(f) = 2.a_1.S_3(f) + a_2.\big(S_2(f) + S_4(f)\big) + a_3.S_1(f)$$

$$\gamma_4^1(f) = 2.a_1.S_4(f) + a_2.S_3(f) + a_3.S_2(f) + a_4.S_1(f)$$

From the above equations, we can write the Power Spectrum (PS) of the observed signal in channel 1 as:

$$\Gamma^1(f) = \begin{bmatrix} \mathbb{S} & 0 & 0 & 0 \\ 0 & \mathbb{S} & 0 & 0 \\ 0 & 0 & \mathbb{S} & 0 \\ 0 & 0 & 0 & \mathbb{S} \end{bmatrix} \cdot \begin{bmatrix} 2 & 0 & 0 & 0 \\ 0 & 1 & 0 & 0 \\ 0 & 0 & 1 & 0 \\ 0 & 0 & 0 & 1 \\ 0 & 1 & 0 & 0 \\ 2 & 0 & 0 & 0 \\ 0 & 1 & 0 & 0 \\ 0 & 0 & 1 & 0 \\ 0 & 0 & 1 & 0 \\ 0 & 1 & 0 & 0 \\ 2 & 0 & 0 & 0 \\ 0 & 1 & 0 & 0 \\ 0 & 0 & 0 & 1 \\ 0 & 0 & 1 & 0 \\ 0 & 1 & 0 & 0 \\ 2 & 0 & 0 & 0 \end{bmatrix} \cdot \begin{bmatrix} a_1 \\ a_2 \\ a_3 \\ a_4 \end{bmatrix} \tag{2.6}$$

Now let $\mathbb{B}_1$ be equal to:

$$\mathbb{B}_1 = \begin{bmatrix} \mathbb{S} & 0 & 0 & 0 \\ 0 & \mathbb{S} & 0 & 0 \\ 0 & 0 & \mathbb{S} & 0 \\ 0 & 0 & 0 & \mathbb{S} \end{bmatrix} \cdot \begin{bmatrix} 2 & 0 & 0 & 0 \\ 0 & 1 & 0 & 0 \\ 0 & 0 & 1 & 0 \\ 0 & 0 & 0 & 1 \\ 0 & 1 & 0 & 0 \\ 2 & 0 & 0 & 0 \\ 0 & 1 & 0 & 0 \\ 0 & 0 & 1 & 0 \\ 0 & 0 & 1 & 0 \\ 0 & 1 & 0 & 0 \\ 2 & 0 & 0 & 0 \\ 0 & 1 & 0 & 0 \\ 0 & 0 & 0 & 1 \\ 0 & 0 & 1 & 0 \\ 0 & 1 & 0 & 0 \\ 2 & 0 & 0 & 0 \end{bmatrix}, \tag{2.7}$$

then

$$\Gamma^1(f) - \mathbb{B}_1 . a^1 = 0 \tag{2.8}$$

where $a^1 = [a_1, a_2, a_3, a_4]$ denotes the load times the attenuation vector of channels 1, 2, 3 and 4 in the observation of channel 1.

Our aim is to estimate a^1. Since the channel load has a non-negative value, non-negativity constraint should be applied on the load estimations instead of simple non-square matrix inversion. In this algorithm, the non-negative Least Mean Square (LMS) calculation has been applied. It is derived based on a stochastic gradient descent approach [31] combined with a fixed-point iteration strategy that ensures convergence toward a solution to estimate vector a^1 from channel 1.

We denote by:

$$[\hat{a}_1^1, \quad \hat{a}_2^1, \quad \hat{a}_3^1, \quad \hat{a}_4^1]$$

the estimate of the load of channels 1, 2, 3 and 4 obtained from the observation of channel 1.

It is given by:

$$\begin{bmatrix} \hat{a}_1^1 \\ \hat{a}_2^1 \\ \hat{a}_3^1 \\ \hat{a}_4^1 \end{bmatrix} = \underset{a^1}{\text{Argmin}}(\|\Gamma^1(f) - \mathbb{B}_1.a^1\|) \tag{2.9}$$

By applying (2.9), we are now able to estimate the load of channels 1, 2, 3 and 4 from the observation of channel 1.

2.3.2 Channel 5 Observation and Load times the Attenuation Estimation of the related overlapped channels

Same observation principle is applied for channel 5 ($j = 5$). As described previously, let us now derive the expression of the PS $\Gamma^5(f)$. Channels 5, 6, 7 and 8 contribute to this PS as well as the channels 2, 3, and 4 referring to Fig. 1.4. Therefore, we are able to estimate the channels load times the attenuation a_5, a_6, a_7, and a_8 from this observation, as well to confirm in double calculation method the value of a_2, a_3, and a_4. The contribution of all those channels in the PS of channel 5 is illustrated in Fig. 2.3, taking into consideration that those channels are shifted

to the baseband thus duplicated from both sides while saving the same overlapping proportions.

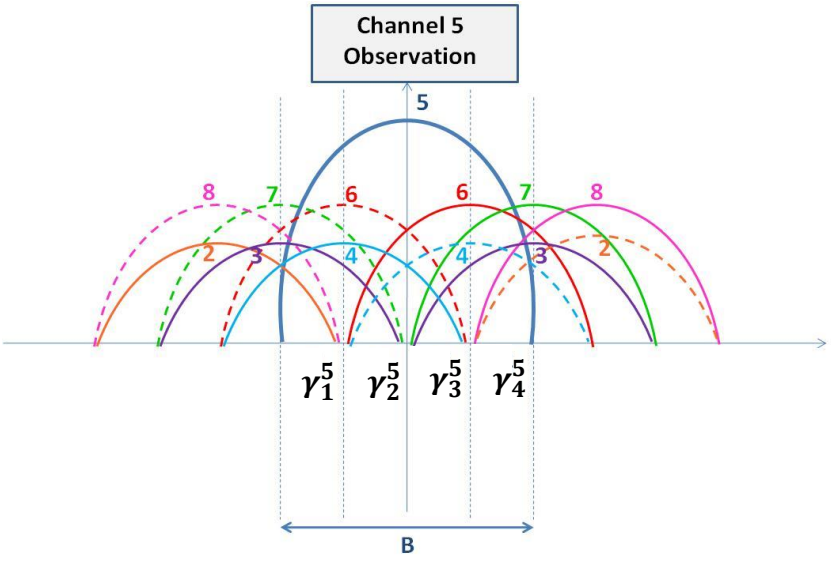

Fig 2.3. Channel 5 Observation Model

For the channel 5 calculations, we proceed similarly as per the observation of channel 1 method, in order to recover the load times the attenuation a_i of the related overlapped channels. For channel 5 observation, we have the below equations:

$$\gamma_1^5(f) = a_2.S_4(f) + a_3.S_3(f) + a_4.S_2(f) + 2a_5.S_1(f) + a_6.S_2(f) + a_7.S_3(f) + a_8.S_4(f)$$

$$\gamma_2^5(f) = a_3.S_4(f) + a_4.\big(S_1(f) + S_3(f)\big) + 2\,a_5.S_2(f) + a_6.\big(S_1(f) + S_3(f)\big) + a_7.S_4(f) \quad (2.10)$$

$$\gamma_3^5(f) = a_3.S_1(f) + a_4.\big(S_4(f) + S_2(f)\big) + 2\,a_5.S_3(f) + a_6.\big(S_4(f) + S_2(f)\big) + a_7.S_1(f)$$

$$\gamma_4^5(f) = a_2.S_1(f) + a_3.S_2(f) + a_4.S_3(f) + 2\,a_5.S_4(f) + a_6.S_3(f) + a_7.S_2(f) + a_8.S_1(f)$$

From the above equations, we can write the PS of the observed signal in channel 5 as:

$$\Gamma^5(f) = \begin{bmatrix} \mathbb{S} & 0 & 0 & 0 \\ 0 & \mathbb{S} & 0 & 0 \\ 0 & 0 & \mathbb{S} & 0 \\ 0 & 0 & 0 & \mathbb{S} \end{bmatrix} \cdot \begin{bmatrix} 0 & 0 & 0 & 2 & 0 & 0 & 0 \\ 0 & 0 & 1 & 0 & 1 & 0 & 0 \\ 0 & 1 & 0 & 0 & 0 & 1 & 0 \\ 1 & 0 & 0 & 0 & 0 & 0 & 1 \\ 0 & 0 & 1 & 0 & 1 & 0 & 0 \\ 0 & 0 & 0 & 2 & 0 & 0 & 0 \\ 0 & 0 & 1 & 0 & 1 & 0 & 0 \\ 0 & 1 & 0 & 0 & 0 & 1 & 0 \\ 0 & 1 & 0 & 0 & 0 & 1 & 0 \\ 0 & 0 & 1 & 0 & 1 & 0 & 0 \\ 0 & 0 & 0 & 2 & 0 & 0 & 0 \\ 0 & 0 & 1 & 0 & 1 & 0 & 0 \\ 1 & 0 & 0 & 0 & 0 & 0 & 1 \\ 0 & 1 & 0 & 0 & 0 & 1 & 0 \\ 0 & 0 & 1 & 0 & 1 & 0 & 0 \\ 0 & 0 & 0 & 2 & 0 & 0 & 0 \end{bmatrix} \cdot \begin{bmatrix} a_2 \\ a_3 \\ a_4 \\ a_5 \\ a_6 \\ a_7 \\ a_8 \end{bmatrix} \tag{2.11}$$

Now let $\mathbb{B}_5$ be equal to:

$$\mathbb{B}_5 = \begin{bmatrix} \mathbb{S} & 0 & 0 & 0 \\ 0 & \mathbb{S} & 0 & 0 \\ 0 & 0 & \mathbb{S} & 0 \\ 0 & 0 & 0 & \mathbb{S} \end{bmatrix} \cdot \begin{bmatrix} 0 & 0 & 0 & 2 & 0 & 0 & 0 \\ 0 & 0 & 1 & 0 & 1 & 0 & 0 \\ 0 & 1 & 0 & 0 & 0 & 1 & 0 \\ 1 & 0 & 0 & 0 & 0 & 0 & 1 \\ 0 & 0 & 1 & 0 & 1 & 0 & 0 \\ 0 & 0 & 0 & 2 & 0 & 0 & 0 \\ 0 & 0 & 1 & 0 & 1 & 0 & 0 \\ 0 & 1 & 0 & 0 & 0 & 1 & 0 \\ 0 & 1 & 0 & 0 & 0 & 1 & 0 \\ 0 & 0 & 1 & 0 & 1 & 0 & 0 \\ 0 & 0 & 0 & 2 & 0 & 0 & 0 \\ 0 & 0 & 1 & 0 & 1 & 0 & 0 \\ 1 & 0 & 0 & 0 & 0 & 0 & 1 \\ 0 & 1 & 0 & 0 & 0 & 1 & 0 \\ 0 & 0 & 1 & 0 & 1 & 0 & 0 \\ 0 & 0 & 0 & 2 & 0 & 0 & 0 \end{bmatrix}, \tag{2.12}$$

then

$$\Gamma^5(f) - \mathbb{B}_5 . a^5 = 0 \tag{2.13}$$

where $a^5 = [a_2, a_3, a_4, a_5, a_6, a_7, a_8]$ denotes the load times the attenuation vector of channels 2, 3, 4, 5, 6, 7, and 8 in the observation of channel 5.

Our aim is to estimate a^5 using the non-negative Least Mean Square (LMS) calculation as described in channel 1 observation calculations.

We denote by:

$$[\hat{a}_2^5, \hat{a}_3^5, \hat{a}_4^5, \hat{a}_5^5, \hat{a}_6^5, \hat{a}_7^5, \hat{a}_8^5]$$

the estimate of the load of channels 2, 3, 4, 5, 6, 7, and 8 obtained from the observation of channel 5.

It is given by:

$$\begin{bmatrix} \hat{a}_2^5 \\ \hat{a}_3^5 \\ \hat{a}_4^5 \\ \hat{a}_5^5 \\ \hat{a}_6^5 \\ \hat{a}_7^5 \\ \hat{a}_8^5 \end{bmatrix} = \underset{a^5}{\text{Argmin}}(\|\Gamma^5(f) - \mathbb{B}_5.a^5\|) \qquad (2.14)$$

By applying (2.14), we are now able to estimate the load of channels 2, 3, 4, 5, 6, 7, and 8 from the observation of channel 5.

2.3.3 Channel 9 Observation and Load times the Attenuation Estimation of the related overlapped channels

Same observation principle is applied for channel 9. We derive the expression of the PS $\Gamma^9(f)$. Channels 9, 10, 11 and 12 contribute to this PS as well as the channels 6, 7, and 8 referring to Fig. 1.4. Therefore, we are able to estimate the channels load times the attenuation a_9, a_{10}, a_{11}, and a_{12} from this observation, as well to confirm in double calculation method the load a_6, a_7, and a_8. The contribution of all those channels in the PS of channel 9 is illustrated in Fig. 2.4, taking into consideration that those channels are shifted to the baseband thus duplicated from both sides while saving the same overlapping proportions.

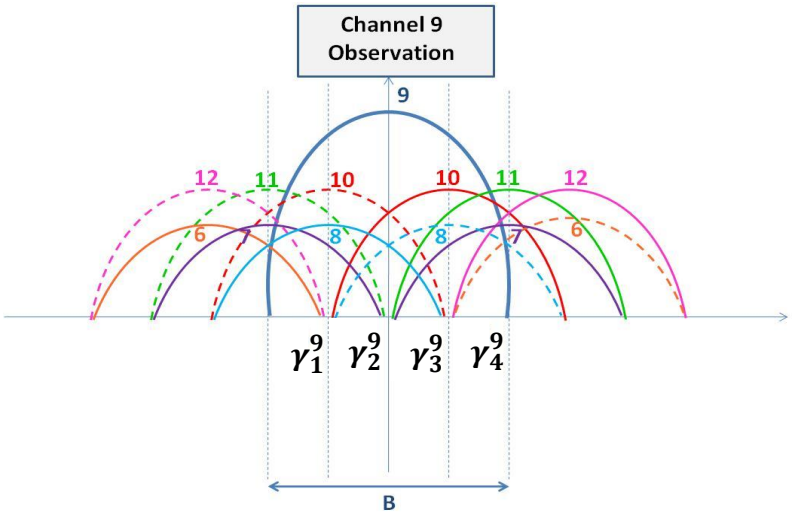

Fig 2.4. Channel 9 Observation Model

For the channel 9 calculations, we proceed similarly as per the observation of channel 1and 5 methods, in order to recover the load times the attenuation a_i of the related overlapped channels. For channel 9 observation, we have the below equations:

$$\gamma_1^9(f) = a_6.S_4(f) + a_7.S_3(f) + a_8.S_2(f) + 2a_9.S_1(f) + a_{10}.S_2(f) + a_{11}.S_3(f) + a_{12}.S_4(f)$$

$$\gamma_2^9(f) = a_7.S_4(f) + a_8.\big(S_1(f) + S_3(f)\big) + 2\,a_9.S_2(f) + a_{10}.\big(S_1(f) + S_3(f)\big) + a_{11}.S_4(f) \quad (2.15)$$

$$\gamma_3^9(f) = a_7.S_1(f) + a_8.\big(S_4(f) + S_2(f)\big) + 2\,a_9.S_3(f) + a_{10}.\big(S_4(f) + S_2(f)\big) + a_{11}.S_1(f)$$

$$\gamma_4^9(f) = a_6.S_1(f) + a_7.S_2(f) + a_8.S_3(f) + 2a_9.S_4(f) + a_{10}.S_3(f) + a_{11}.S_2(f) + a_{12}.S_1(f)$$

From the above equations, we can write the PS of the observed signal in channel 9 as:

$$\Gamma^9(f) = \begin{bmatrix} \mathbb{S} & 0 & 0 & 0 \\ 0 & \mathbb{S} & 0 & 0 \\ 0 & 0 & \mathbb{S} & 0 \\ 0 & 0 & 0 & \mathbb{S} \end{bmatrix} \cdot \begin{bmatrix} 0 & 0 & 0 & 2 & 0 & 0 & 0 \\ 0 & 0 & 1 & 0 & 1 & 0 & 0 \\ 0 & 1 & 0 & 0 & 0 & 1 & 0 \\ 1 & 0 & 0 & 0 & 0 & 0 & 1 \\ 0 & 0 & 1 & 0 & 1 & 0 & 0 \\ 0 & 0 & 0 & 2 & 0 & 0 & 0 \\ 0 & 0 & 1 & 0 & 1 & 0 & 0 \\ 0 & 1 & 0 & 0 & 0 & 1 & 0 \\ 0 & 1 & 0 & 0 & 0 & 1 & 0 \\ 0 & 0 & 1 & 0 & 1 & 0 & 0 \\ 0 & 0 & 0 & 2 & 0 & 0 & 0 \\ 0 & 0 & 1 & 0 & 1 & 0 & 0 \\ 1 & 0 & 0 & 0 & 0 & 0 & 1 \\ 0 & 1 & 0 & 0 & 0 & 1 & 0 \\ 0 & 0 & 1 & 0 & 1 & 0 & 0 \\ 0 & 0 & 0 & 2 & 0 & 0 & 0 \end{bmatrix} \cdot \begin{bmatrix} a_6 \\ a_7 \\ a_8 \\ a_9 \\ a_{10} \\ a_{11} \\ a_{12} \end{bmatrix} \tag{2.16}$$

Now let $\mathbb{B}_9$ be equal to:

$$\mathbb{B}_9 = \begin{bmatrix} \mathbb{S} & 0 & 0 & 0 \\ 0 & \mathbb{S} & 0 & 0 \\ 0 & 0 & \mathbb{S} & 0 \\ 0 & 0 & 0 & \mathbb{S} \end{bmatrix} \cdot \begin{bmatrix} 0 & 0 & 0 & 2 & 0 & 0 & 0 \\ 0 & 0 & 1 & 0 & 1 & 0 & 0 \\ 0 & 1 & 0 & 0 & 0 & 1 & 0 \\ 1 & 0 & 0 & 0 & 0 & 0 & 1 \\ 0 & 0 & 1 & 0 & 1 & 0 & 0 \\ 0 & 0 & 0 & 2 & 0 & 0 & 0 \\ 0 & 0 & 1 & 0 & 1 & 0 & 0 \\ 0 & 1 & 0 & 0 & 0 & 1 & 0 \\ 0 & 1 & 0 & 0 & 0 & 1 & 0 \\ 0 & 0 & 1 & 0 & 1 & 0 & 0 \\ 0 & 0 & 0 & 2 & 0 & 0 & 0 \\ 0 & 0 & 1 & 0 & 1 & 0 & 0 \\ 1 & 0 & 0 & 0 & 0 & 0 & 1 \\ 0 & 1 & 0 & 0 & 0 & 1 & 0 \\ 0 & 0 & 1 & 0 & 1 & 0 & 0 \\ 0 & 0 & 0 & 2 & 0 & 0 & 0 \end{bmatrix}, \tag{2.17}$$

then

$$\Gamma^9(f) - \mathbb{B}_9 . a^9 = 0 \tag{2.18}$$

where $a^9 = [a_6, a_7, a_8, a_9, a_{10}, a_{11}, a_{12}]$ denotes the load times the attenuation vector of channels 6, 7, 8, 9, 10, 11, and 12 in the observation of channel 9.

Our aim is to estimate a^9 using the non-negative Least Mean Square (LMS) calculation as described in channel 1 and 5 calculations.

We denote by:

$$[\hat{a}_6^9, \hat{a}_7^9, \hat{a}_8^9, \hat{a}_9^9, \hat{a}_{10}^9, \hat{a}_{11}^9, \hat{a}_{12}^9]$$

the estimate of the load of channels 6, 7, 8, 9, 10, 11, and 12 obtained from the observation of channel 9. It is given by:

$$\begin{bmatrix} \hat{a}_6^9 \\ \hat{a}_7^9 \\ \hat{a}_8^9 \\ \hat{a}_9^9 \\ \hat{a}_{10}^9 \\ \hat{a}_{11}^9 \\ \hat{a}_{12}^9 \end{bmatrix} = \underset{a^9}{\text{Argmin}}(\|\Gamma^9(f) - \mathbb{B}_9.a^9\|) \tag{2.19}$$

By applying (2.19), we are now able to estimate the load of channels 6, 7, 8, 9, 10, 11, and 12 from the observation of channel 9.

From all the above equations, as already declared, we are able to estimate the load times the attenuation of the entire physical layer channels of 802.11n, by applying only 3 observations methods on the non-overlapped channels (1, 5, 9).

2.4 Estimated Load times Attenuation in respect to different Observations

In the section 2.3, we have defined the matrices to estimate the load times the attenuation value $\hat{a}_i^j$ for the overlapped channels i ($i = 1, \dots, 12$) from the different observations of the 3 non-overlapped ones ($j = 1, 5, 9$). Since as noticed, the estimated load times the attenuation value $\hat{a}_i$ of each channel can be calculated simultaneously from the observation of at least one or more adjacent non-overlapped channels, we propose the below equation to estimate $\hat{a}_i$:

$$\hat{a}_i = \sum_{j \in \{1,5,9\}} \beta_i^j \ \hat{a}_i^j \tag{2.20}$$

where β_i^j is a coefficient defined according to two proposed methods:

- The Direct calculations method: from one channel observation only, we estimate the value $\hat{a}_i$ of the channels that overlap directly with it. We define, for the observation of the 3 non-overlapped channels 1, 5 and 9 respectively, the values of β_i^j as following:

$$\hat{a}_i = \hat{a}_i^1 \qquad for\ i = 1, 2, 3\ and\ 4 \tag{2.21}$$

$$\hat{a}_i = \hat{a}_i^5 \qquad for\ i = 5, 6, 7\ and\ 8$$

$$\hat{a}_i = \hat{a}_i^9 \qquad for\ i = 9, 10, 11\ and\ 12$$

- The Averaged calculations method: each estimated channel load times attenuation value $\hat{a}_i$ is estimated from the observation of at least 2 channels that overlap with it, referring to equation (2.20) and for more than one channel simultaneous observations. In this case, β_i^j is the proportion intersection value of the channel i in the channel j, therefore we can conclude the below values of β_i^j:

$$if\ i = j, \qquad \beta_i^j = 1$$

$$if\ |i - j| > 3, \qquad \beta_i^j = 0$$

$$if\ |i - j| = 3, \qquad \beta_i^j = \frac{1}{4}$$

$$if\ |i - j| = 2, \qquad \beta_i^j = \frac{1}{2}$$

$$if\ |i - j| = 1, \qquad \beta_i^j = \frac{3}{4}$$

For example, the load of channel 1 is estimated from the observation of channel 1, the loads of channels 2, 3 and 4 are estimated from the observations of both channels 1 and 5 as per the following equations:

$$\alpha_1^1 = \alpha_1^1$$

$$\alpha_2^{1,5} = \left(\frac{3}{4}.\alpha_2^1\right) + \left(\frac{1}{4}.\alpha_2^5\right)$$

$$\alpha_3^{1,5} = \left(\frac{1}{2}.\alpha_3^1\right) + \left(\frac{1}{2}.\alpha_3^5\right)$$

$$\alpha_4^{1,5} = \left(\frac{1}{4}.\alpha_4^1\right) + \left(\frac{3}{4}.\alpha_4^5\right)$$

Similarly, the load of channel 5 is estimated from the observation of channel 5, the load of channels 6, 7, and 8 are estimated from the observations of channels 5 and 9, and finally the loads of channels 9, 10, 11, and 12 are estimated from the observation of channel 9.

The performance of the proposed Direct and Averaged calculations methods is presented in the simulations results where we have applied the load calculation based on an averaged method between simultaneous two channels observation, to note that additional channels observations (more than 3) could be applied as previously stated.

2.5 Simulations Results

Simulations were conducted on Matlab to generate the physical signal of 802.11n based on OFDM technique, according to WiFi 802.11n specific parameters shown in Table 2.2.

Table. 2.2 Used 802.11n parameters in the channel load estimation algorithm.

Parameter	Value
Bandwidth	20 MHz
The frequency spacing between subcarriers	312.5Khz
Sampling interval employed in the OFDM transmitter Ts	0.05 µs

Symbol length	3.2 µs
Number of subcarriers	64
FFT Window	64
Modulation	16 QAM
Total number of samples per OFDM symbol	1024
Number of samples zero-padded after 16 QAM	2048
Number of symbols	200

The length of the input signal used in our simulations is equivalent to the duration of 200 OFDM symbols in time (or 200 times the symbol duration t_s = *3.2 µs*), where the channel load is expressed by non-zero symbols value equivalent to the time occupation of the signal (or busy time), and with null symbols value when the channel is empty (or idle time). The channels load predefined on the twelve channels is expressed as the percentage of the channel occupation time between 0% and 100% (or 0 and 1) assumed as following: *20%, 50%, 0%, 40%, 90%, 0%, 60%, 70%, 80%, 40%, 0%, 90%.*

In addition, to simplify the presentation of the algorithm, we consider in the simulation results, that the attenuation $\lambda_i = 1 \ \forall \ i, \ \forall f$; therefore, we represent the calculated load α_i only. However, the robustness of the proposed algorithm in the presence of a multipath fading channel (i.e. $\lambda_i \neq 1$) is analyzed and presented in section (2.5.5) at the end of the simulations section to highlight the accuracy of the algorithm in practical conditions.

2.5.1 Load Estimation in an Ideal Channel

As explained previously, since the physical channels overlap with only 3 distinct channels, an observation of those 3 distinct channels entails to measure the load of the 12 channels.

Therefore, we start first by observing channels 1, 5, and 9. By applying our algorithm presented in the previous section with the assumption that the signal is in ideal channel with $\lambda_i = 1 \ \forall \ i$, $\forall \ f$; , the load of channels 1, 2, 3, and 4 are estimated from the observation of channel 1, the load of channels 5, 6, 7 and 8 are estimated from the observation of channel 5, and the load of channels 9, 10, 11 and 12 are estimated from the observation of channel 9.

As shown in Fig. 2.5, the estimated load is nearly the same comparing to the predefined load.

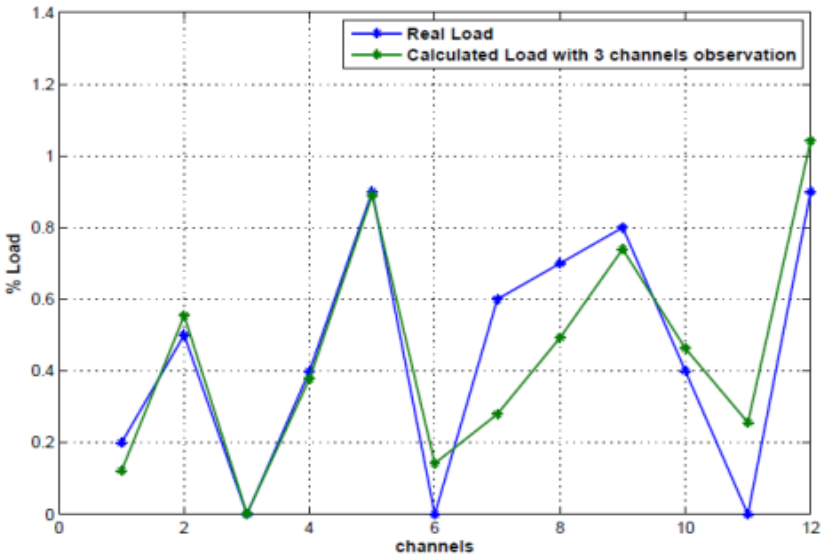

Fig 2.5. Estimated Load versus the real load with 3 channels observation

To check the effect of several additional channels observations, we have applied our algorithm on channels 1, 5, 6, 9, and 12 (optionally 5 channels observation in this case). The loads of channels 1, 2, 3, and 4 are estimated from the observation of channel 1, the load of channel 5 is estimated from the observation of channel 5, the loads of channels 6, 7 and 8 are estimated from the observation of channel 6, the load of channel 9 is estimated from the observation of channel 9 and the loads of channels 10, 11 and 12 are estimated from the observation of channel 12.

A comparison between the 3 channels observation and the 5 channels observation is done, and the results in terms of the value of the Mean Squared Error (MSE), averaged through several repetitive random simulations, is shown in Fig. 2.6 for the two averaged and direct

calculations methods, with a fixed signal length of 100 symbols and SNR of 10 dB. As we can see, the MSE decreases with 5 channels observations; thus we can conclude that with additional number of channels observation, the algorithm accuracy level is increased.

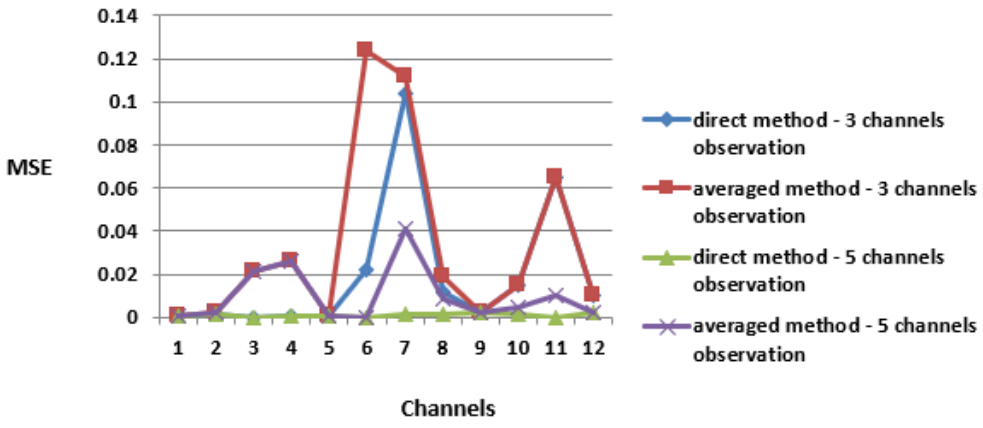

Fig 2.6. Averaged MSE of the estimated load versus the real load values

In addition, we can observe that the averaged calculations method did not bring additional improvement in the MSE values compared to the direct calculations method, thus additional coefficients finetuning could be considered to investigate other calculations that might be subject to further studies.

Finally, we should note that the values of MSE are averaged for several repetitive simulations results in order to have a general average value, however a difference in the values may appear randomly in some channels than the others in each simulation based on the initial considered values of the load.

2.5.2 Load Estimation in presence of a White Gaussian Noise

We assume now that the channel is affected by a White Gaussian Noise. In order to analyze the noise effect on the accuracy of our algorithm, same observations are used to reflect the estimated load versus the real one. The averaged MSE value is represented in respect to SNR in Fig. 2.7, with a fixed signal length of 100 OFDM symbols. We can notice that the precision of the algorithm is affected by a high noise level; however an acceptable error margin can still exist with a SNR around 3 dB.

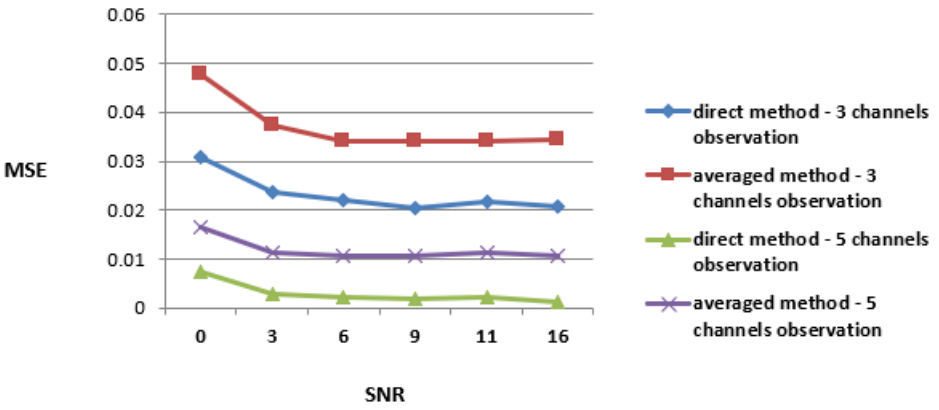

Fig 2.7. Averaged MSE of the estimated load versus SNR

2.5.3 Load Estimation with higher Symbol Length

We have analyzed the effect of signal length (i.e. the number of OFDM symbols) at the input in an Ideal free channel. Different realizations have been performed in order to reflect the averaged MSE with increased number of OFDM symbols duration $100*t_s$ (the symbol duration (t_s) = 3.2 µs), $200*t_s$, $300*t_s$, $400*t_s$ and $1000*t_s$ as can be shown in Fig. 2.8 with a SNR = 10 dB. As we can notice, the averaged MSE value decreases with the highest number of OFDM symbols, since the precision of the estimated load increases for a higher message length where the observations results are more accurate.

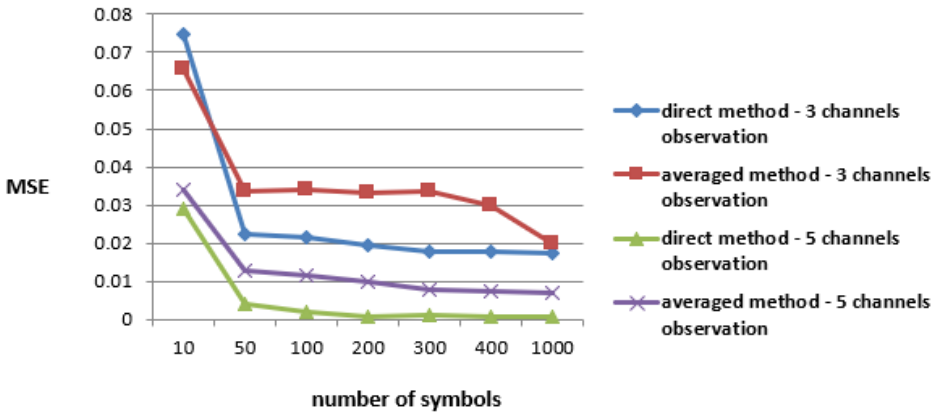

Fig 2.8. Averaged MSE of the estimated load versus Signal Length

2.5.4 Load Estimation in presence of a Multipath Fading

Following the assumption that the attenuation is not affecting our calculations ($\lambda_i = 1;\ \forall i;\ \forall f$), non-perfect conditions are assumed in this subsection in the presence of a multipath fading channels.

In multipath fading, the radio signal propagates from the transmitter to the receiver via different multiple paths due to the obstacles and reflectors existing in the wireless channel. These multipaths are caused by mechanisms of reflection, diffraction, and scattering.

When the user is significantly far from the base station, the LOS signal path does not exist, and reception happens mainly from the indirect signal paths. These multiple paths have different propagation lengths and will cause amplitude and phase fluctuations and time delay in the received signal. Thus, the main effect of multipath propagation can be described in terms of fading and delay spread.

Small scale fading is also called Rayleigh fading because if the multiple reflective paths are large in number and there is no line-of-sight signal component, the envelope of the received signal is statistically described by Rayleigh distribution. When there is a dominant non-fading signal component present, such as a line-of-sight propagation path, the small-scale fading envelope is described by Rician distribution and, thus, is referred to as Rician fading.

In our simulation the channel under consideration can be modeled as a multipath fading channel in which the impulse response may follow distributions like Rayleigh distribution (in which there is no Line of Sight (LOS) ray between transmitter and receiver).

The Rayleigh distribution follow the below Probability Density Function (PDF):

$$f(x;\sigma) = \frac{x}{\sigma^2} \cdot e^{-x^2/(2\sigma^2)} \tag{2.22}$$

where $x, \sigma > 0$, σ is the scale parameter of the distribution.

Let the Rayleigh channel be the vector $H = [h_0, h_1, \dots, h_{K-1}]$ and the transmitted signal S, then the received signal R is as per the equation below:

$$R = H \otimes S \tag{2.23}$$

where the symbol $\otimes$ represents the discrete convolution operator.

Each tap h_k of H would be generated as Rayleigh random variable with scale parameter σ_k.

The mean value $E(X)$ of Rayleigh random variable X is as following:

$$E(X) = \sigma * \sqrt{\frac{\pi}{2}} \tag{2.24}$$

For the k[th] Rayleigh coefficient h_k of the impulse response we define $E(h_k)$ as the mean value of h_k following a multipath decreasing exponential power profile, thus:

$$E(h_k) = e^{-k\lambda} \tag{2.25}$$

With λ is a constant value predefined for each simulation.

To generate the different multipath taps h_k, we calculate the Rayleigh scale parameter referring to equation (2.24) as per the below:

$$\sigma_k = \frac{E(h_k)}{\sqrt{\frac{\pi}{2}}} = \frac{e^{-k\lambda}}{\sqrt{\frac{\pi}{2}}} \tag{2.26}$$

We normalize the vector H to have $||H||^2 = 1$, to reflect the effective PSD and thus calculate the channels load as previously explained in the first algorithm of this thesis.

As we can observe in Fig. 2.9, the accuracy margin has been decreased in respect to the Ideal channel conditions, however our algorithm is still reliable for the different 12 WiFi channels with 10 channel taps and a decreasing exponential power profile for the taps of the channel equal to 1, despite certain attenuation factors.

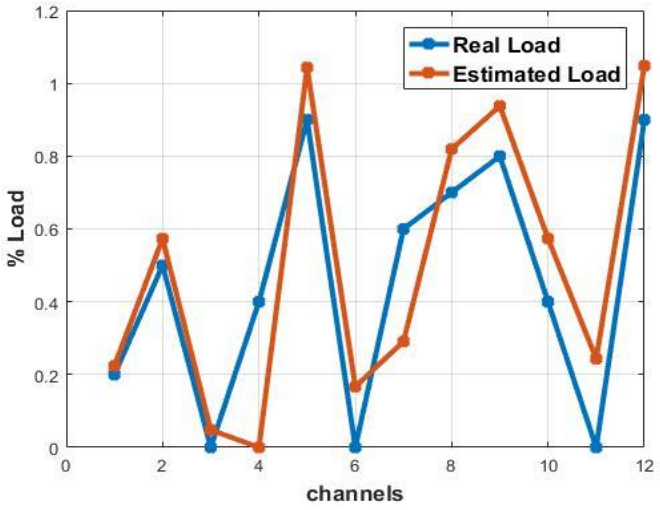

Fig 2.9. Estimated load versus the real load values in presence of a multipath fading channel

By varying λ parameter of the decreasing exponential power profile for the taps of the channel in ascending order within the multipath fading model, the Mean Squared Error (MSE), between the real load value and the estimated one, is decreased as shown in figure 2.10:

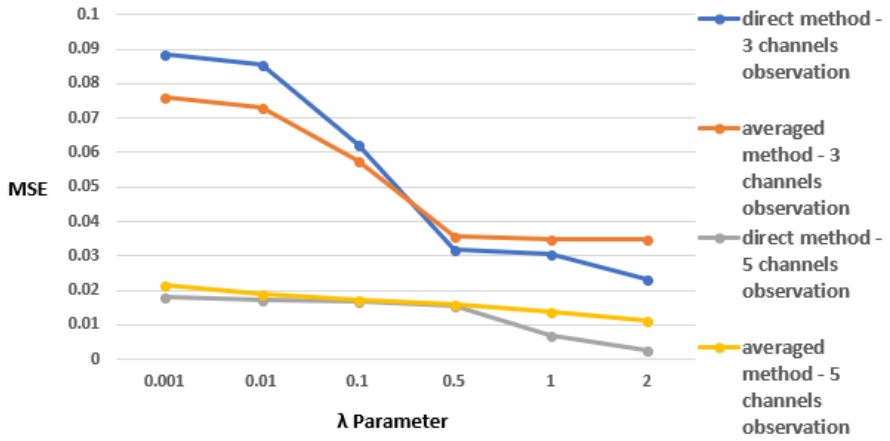

Fig 2.10. Averaged MSE of the estimated load versus the real load values in presence of a multipath fading channel for different scale parameters

In addition, by varying the number of multipath channel taps between 5, 10, 15, 20 and 30 taps, and with $\lambda = 1$, we can notice as shown in figure 2.11, that the MSE value is almost the same for all channels taps.

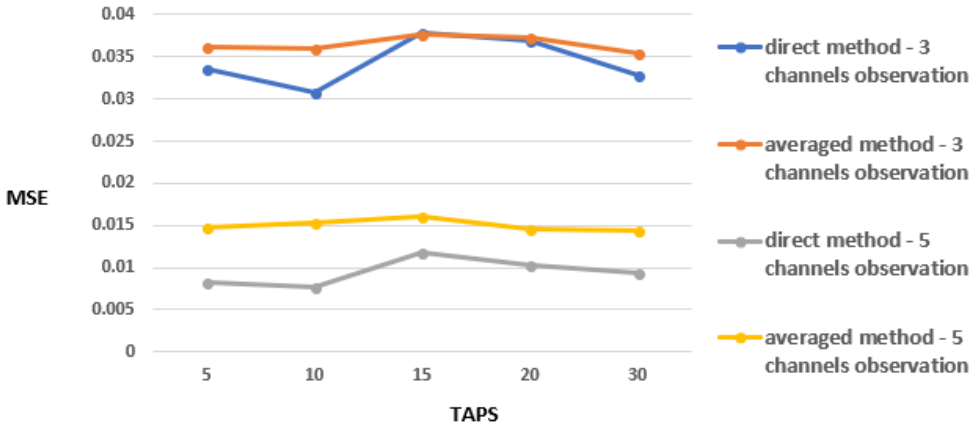

Fig 2.11. Averaged MSE of the estimated load versus the real load values in presence of a multipath fading channel for different number of Taps

Finally, the difference between the averaged MSE with multipath fading channel with 10 taps and with $\lambda = 1$, and with an Ideal channel are represented in figure 2.12, with the same signal length of 100 OFDM symbols, without Gaussian noise, where the simulations results have been averaged for 10 realizations.

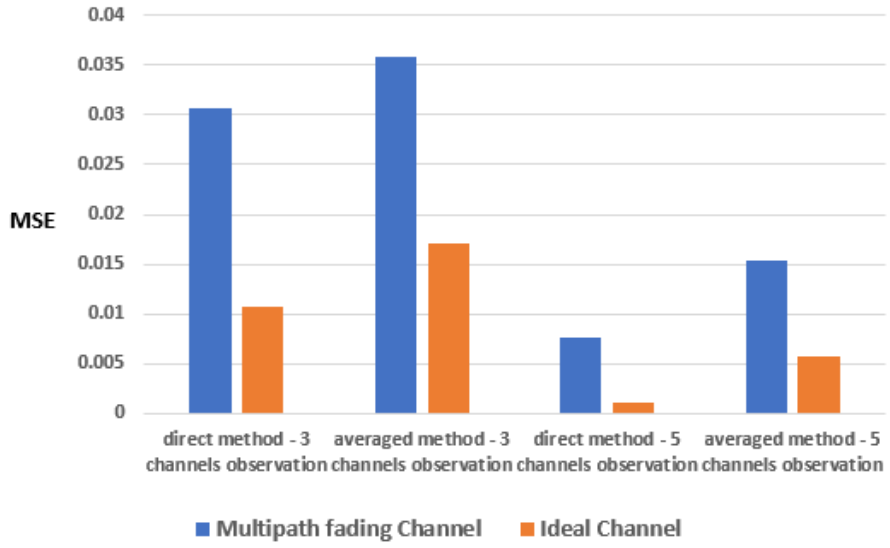

Fig 2.12. Averaged MSE of the estimated load versus the real load values in presence of a multipath fading channel and in an Ideal channel

As it can be noticed, the MSE value in case of multipath fading is higher than the MSE in an Ideal channel.

2.6 Attempt to estimate Channels Load in presence of Rayleigh attenuation model

In this section, we tried to estimate the load of the WiFi 802.11n overlapped channels in presence of a Rayleigh fading model, without considering the attenuation equal to 1 or normalized as per the previous simulation sections.

However, our attempt did not reach a successful result since we get an infinite number of possible solutions of attenuation values. Despite this non-finite result, we will represent here below our approach in details, just for the reference of future related investigations, aiming to calculate the load and the attenuation separately.

As per most real cases, the Rayleigh fading model is normally viewed as a suitable approach to take when analyzing and predicting radio wave propagation performance for areas such as wireless communications in urban environment where there are many reflections and refractions from buildings, obstacles etc...

Thus accordingly, we have tried in this section to formulate a system of equations from the well-known value a_i , where $a_i = \lambda_i^2 . \alpha_i$ calculated in the previous section of this chapter (Referring to equation (2.1) and (2.2)).

2.6.1 Attenuation System Model

As mentioned previously, we consider that the attenuation is the general Rayleigh multipath fading channel model. The Rayleigh fading model uses a statistical approach to analyze the propagation and can be used in a number of environments. In probability theory and statistics, a Rayleigh random variable x follows the Probability Density Function (PDF) presented below [32]:

$$f(x;\sigma') = \frac{x}{\sigma'^2} . e^{-x^2/(2\sigma'^2)} \quad (2.22)$$

where $x, \sigma' > 0$, σ' is the scale parameter of the distribution.

Based on our previous sections, referring to (2.1), we have calculated the load times the attenuation factors $(\alpha_i . \lambda_i^2)$ of the WiFi physical channels where the attenuation was normalized. However, since in this section λ_i is a Rayleigh random variable, thus the squared Rayleigh variable is an exponential random variable that follows the below PDF function [33]:

$$f(X;\sigma) = \sigma . e^{-\sigma x} \quad (2.23)$$

where $x, \sigma > 0$, σ is the scale parameter of the distribution.

2.6.2 Proposed Algorithm

We consider one user measuring the load times the attenuation of the 12 channels i, through K MIMO antennas systems, having K different random paths, thus having K different random attenuations $\lambda_{i,k}$.

We can conclude that this user who is observing and estimating $a_i = (\alpha_i \,.\, \lambda_i^2)$ of one channel i, can initiate K different values of this measurement $a_{i,k}$, with different K attenuation $\lambda_{i,k}^2$ but with the same load α_i .

As previously mentioned, we consider that the attenuation $\lambda_{i,k}$ is a Rayleigh random variable that can be used to describe the form of fading that occurs when Rayleigh multipath propagation exists, thus $\lambda_{i,k}^2$ is an exponential distribution variable with different rate parameters σ_{k} for the different K paths. Therefore, the known variable $a_{i,k}$ is also an exponential random variable, since it is the product of a constant real value α_i times an exponential random variable, with different rate parameter $\sigma_{a,\mathrm{k}}$ for the different K paths.

While calculating the load and attenuation of any random channel from the 12 overlapped ones assigned to one AP, and based on the previous explained algorithm in (2.1), we have the below equation:

$$a_{i,k} = (\alpha_i \,.\, \lambda_{i,k}^2) \tag{2.24}$$

$k = 1, \dots, K$ number of MIMO antennas ($K \geq 2$); α_i is the load of the random channel i to be calculated; $\lambda_{i,k}^2$ is the attenuation value following the PDF of an exponential random variable (with rate parameter σ_k) to be calculated; and $a_{i,k}$ is the known random exponential variable (with rate parameter $\sigma_{a,k}$), calculated in the previous sections.

We consider the minimum number of MIMO antennas, $K = 2$, so we have a system with minimum 2 equations with 3 unknown variables to calculate $(\alpha_i, \lambda_{i,1}, \lambda_{i,2})$, and measuring the load of the same AP channel i via 2 different paths:

$$\alpha_i \,.\, \lambda_{i,1}^2 = a_{i,1} \tag{2.25}$$

$$\alpha_i \,.\, \lambda_{i,2}^2 = a_{i,2} \tag{2.26}$$

with $\sigma_1, \sigma_2, \sigma_{\mathrm{a},1}, \sigma_{\mathrm{a},2}$ the rate parameters of $\lambda_{i,1}^2, \lambda_{i,2}^2, a_{i,1}, a_{i,2}$ respectively as previously described.

The variance of an exponential random variable x with rate parameter σ is:

$$Var(x) = \frac{1}{\sigma^2} \tag{2.27}$$

Thus from (2.24), (2.25), and (2.26) we can conclude the following:

$$\alpha_i^2 . \frac{1}{\sigma_1^2} = \frac{1}{\sigma_{a,1}^2} \tag{2.28}$$

$$\alpha_i^2 . \frac{1}{\sigma_2^2} = \frac{1}{\sigma_{a,2}^2} \tag{2.29}$$

Thus

$$\sigma_1 = \alpha_i \, . \, \sigma_{\mathrm{a},1} \tag{2.30}$$

$$\sigma_2 = \alpha_i \, . \, \sigma_{\mathrm{a},2} \tag{2.31}$$

To calculate $\sigma_{\mathrm{a},1}$ and $\sigma_{\mathrm{a},2}$ knowing that the values of $a1$ and $a2$ are known for $k = 2$ antennas as calculated in previous section, we have 2 exponential PDF functions with $\sigma_{\mathrm{a},1}$ and $\sigma_{\mathrm{a},2}$ unknown, that we can calculate by the Maximum Likelihood Estimation (MLE) based on the rate parameter value that maximize the likelihood of the PDF functions according to the following equations, where we can calculate $\sigma_{\mathrm{a},1}$ and $\sigma_{\mathrm{a},2}$ respectively:

$$MLE_{\sigma_{\mathrm{a},1}} = Argmax_{\sigma_{\mathrm{a},1}}(\sigma_{\mathrm{a},1} \, . \, e^{-\sigma_{\mathrm{a},1} a_1}) \tag{2.32}$$

$$MLE_{\sigma_{\mathrm{a},2}} = Argmax_{\sigma_{\mathrm{a},2}}(\sigma_{\mathrm{a},2} \, . \, e^{-\sigma_{\mathrm{a},2} a_2}) \tag{2.33}$$

Equations (2.32) and (2.33) are resolved using Matlab by applying the derivative of the acquired function in order to get the desired maximum of $\sigma_{\mathrm{a},1}$ and similarly $\sigma_{\mathrm{a},2}$.

Thus, we still need to calculate σ_1 and σ_2 of the exponential attenuation variables to calculate the desired load α. In order to have a system of equations of σ_1 and σ_2, we propose to do the ratio of both equations (2.25) and (2.26) of $k = 2$ MIMO antennas, where we get the following:

$$\frac{\lambda_{i,1}^2}{\lambda_{i,2}^2} = \frac{a_{i,1}}{a_{i,2}} = Y_i \tag{2.34}$$

noting that Y_i is a known random variable (since $a_{i,1}$ and $a_{i,2}$ are known), representing the ratio of two random exponential variables, with rate parameters σ_1 and σ_2 that are needed to be calculated.

According to [34], the PDF of the ratio of two exponential variables is as per the below:

$$f(Y_i) = \frac{\sigma_1 . \sigma_2}{(\sigma_1 . Y_i + \sigma_2)^2} \tag{2.35}$$

As per the MLE method applied before, but in this case with 2 dimensions, we need to get the values of σ_1 and σ_2 that maximize the likelihood of the PDF function of the ratio of two exponential variables as per the following:

$$MLE_{\sigma_1,\sigma_2} = Argmax_{\sigma_1,\sigma_2}\left(\frac{\sigma_1 . \sigma_2}{(\sigma_1 . Y_i + \sigma_2)^2}\right) \tag{2.36}$$

Since

$$max\,[f(x)] = min\,[-f(x)]$$

to solve the complex equation (2.35), we adopt the gradient descent algorithm with two dimensions to have the values of σ_1 and σ_2 by minimizing the negative value of (2.36), and with the below constraint referring to (2.30) and (2.31),

$$\sigma_1 = \frac{\sigma_{a1}}{\sigma_{a2}} . \sigma_2 \tag{2.37}$$

In this method, we are minimizing the function $[-MLE_{\sigma_1,\sigma_2}]$ to get the desired σ_1 and σ_2 that maximize $[MLE_{\sigma_1,\sigma_2}]$ value.

In order to avoid the local minimums, and calculate the global minimum value, a dynamic learning rate μ is applied as per the study in [35], and according to the error function J between previous and current values of the function that we are minimizing as per the below conditions:

$$\mu = \mu + 0.1\mu\,, if\ J(previous) > J(current)$$
$$\mu = \mu - 0.5\mu, if\ J(previous) < J(current)$$
$$\mu = \mu, if\ J(previous) = J(current)$$

By applying the above described method to calculate σ_1 and σ_2 using Matlab, we didn't reach a local maximum value for equation (2.36), since we had noticed that for different step values of the gradient descent method, we are getting different maximum values of the MLE. By applying the plot of the solution to extract the maximum values, global maxima were found at straight line $\sigma_2 = 2\sigma_1$ as per Fig. 2.13.

We have introduced the constraint $\sigma_1 = \frac{\sigma_{a1}}{\sigma_{a2}}$. σ_2 of (2.37), in order to define the intersection between the line of straight line of the global maxima, however the two lines do not intersect (unless at null value) as per Fig 2.14, therefore we cannot calculate a unique value for σ_1 and σ_2:

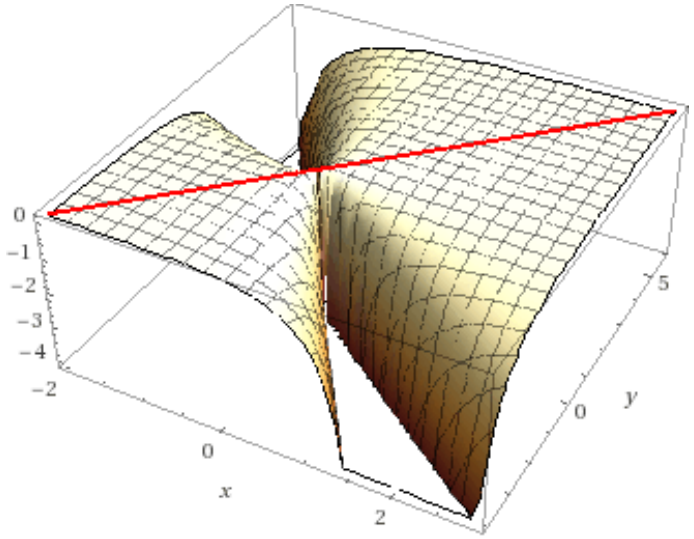

Fig 2.13. MLE of σ_2 in respect to σ_1 in 3D plot with Maxima Values in red line

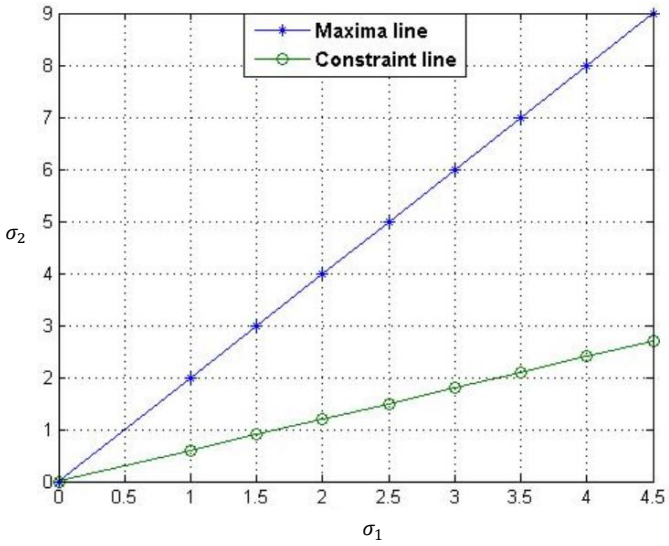

Fig 2.14. Maxima and Constraint lines of σ_2 in respect to σ_1

2.7 Conclusion and potential Use Cases

Our proposed algorithm is able to estimate the load times the attenuation of the 12 overlapped channels of the WiFi 802.11n, based on only 3 observations of non-overlapping channels (1,5 and 9 in our simulation). The accuracy of the algorithm has been measured by the MSE of multiple realizations, in Ideal channel and in white Gaussian noisy channel. We evaluated our work and can conclude a high accuracy level and flexibility in estimating the load of the physical channels with normalized attenuation, thus facilitating the channel assignment based on the minimal load, providing better QoE for the end user and minimized load measurement and channel selection time. Following the same principle, the analysis of 5 GHz spectrum and 802.11ac could be applied, including the channel bonding feature. However, more work should be carried out to estimate the attenuation level which was normalized during our study.

From the analysis of our simulated results, we can notice that in a high level of noise, the number of channels observation and message length could be increased (more than 3 channels observation and 500 t_s respectively) in order to maintain the same accuracy level of the algorithm as per the Ideal channel environment. In addition the proposed averaged calculation method through two simultaneous channels observation is also recommended in

order to minimize the MSE value and increase the precision level of the estimated load in noisy environment.

Furthermore, as described previously, when the user is trying to connect to a suitable AP, interrogation requests are performed in order to detect the available one. Different values of the timers could be set to assure an optimal waiting time for the response of the AP before the connection. Following the application of our algorithm, and where the user terminal is waiting between two timers values to be connected, the measurement of the load by the user terminal could facilitate the selection and thus optimize both the values of the timers, and the battery consumption when compared to long timers duration with no response in congested networks.

Finally, we should note that currently in practical use the overlapped channels analyzed in this study, are not considered usable and typically are not selectable in order to avoid co-channel interference. However, in densely populated networks, and with the future increasing traffic demand, overlapped channels might be needed to resolve the increasing available spectrum demand in Het-Nets towards 5G, where further algorithms and procedures should be analyzed to minimize the anticipated interference.

CHAPTER 3 –

LTE Capacity Management and Resources Allocation

In this chapter the physical layer of LTE network in addition to the resources' distribution are described. Resource allocation along with the modulation technique on the physical interface are described. In addition, we propose how we define the LTE heaviest users that have the highest amount of throughput in terms of Mbps, in order to select the criteria of LTE users offload to WiFi network that will be described in detail in Chapter 4.

Before the standardization for the LTE in 2004, 3GPP highlighted the most important basic requirements for the long-term evolution of UTRAN as following:

- LTE system should be Packet Switched domain optimized.
- A global roaming technology with the inter-system mobility with Global System for Mobile Communication (GSM), Wideband Code Division Multiple Access (WCDMA) and Code Division Multiple Access (CDMA) 2000.
- Enhanced customer experience with high data rates exceeding 100 Mbps in DL and 50 Mbps in UL.
- Reduced latency with radio round trip time below 10 ms and access time below 300 ms
- Scalable bandwidth from 1.4 MHz to 20 MHz
- Increased spectral efficiency
- Reduced network complexity

These specifics are based on the visions of 3GPP that concluded the need of LTE technology to cope up with the growth predictions of the wireless market [36].

3.1 LTE Physical Layer Structure

The LTE radio interface or LTE-Uu interface is the interface between the UE and the Evolved NodeB or eNodeB. The eNodeB is the termination point for the radio protocols and related functionalities in LTE network, considered as a base station that controls all radio related functionalities of the Evolved Packet System (EPS) (Evolved UTRAN (E-UTRAN) and Evolved Packet Core (EPC)). It is the connecting layer between UE and EPC. All of the radio protocols from UE terminate at eNodeB. eNodeB is the essential part of mobility management in EPS. It also performs encryption/decryption of User Plane/Control Plane data and Internet Protocol (IP) header compression/decompression as well to decrease the sending of redundant data in IP header [37].

In addition to these basic functionalities, there are other Radio Resource Management (RRM) functionalities handled by the eNodeB. As a terminating node for the radio protocols, it sets Radio Resource Connection (RRC) and performs radio resource allocations to the users with QoS based prioritization [37].

Comparing it with UTRAN, it can be seen that the eNodeB performs the functionalities of both NodeB and Radio Network Controller (RNC). This simplifies the network structure and also in a way reduces the latency in the network as well. The eNodeBs are connected to their neighboring eNodeBs with the X2 interface. This connection becomes useful during the handover scenarios [37].

3.2 LTE System and Channel Assignment Model

In LTE systems, Orthogonal Frequency Division Multiple Access (OFDMA) is the multiple access technique used in the downlink. However, since it presents a high Peak-to-average Power Ratio, it is not possible to use OFDMA on the uplink. For the uplink, Single Carrier Frequency Division Multiple Access (SC-FDMA) is used [38].

The main difference between an OFDM and OFDMA system is the fact that in the OFDM, users are allocated on the time domain only while using an OFDMA system the user would be allocated by both time and frequency. This is useful for LTE since it makes possible to exploit

frequency dependence scheduling. For instance, it would be possible to exploit the fact that user 1 might have a better radio link quality on some specific bandwidth area of the available bandwidth.

It is not possible to use OFDMA on the uplink since, as told before, it presents a high Peak-to-average Power Ratio. SC-FDMA presents the benefit of a single carrier multiplexing of having a lower Peak-to-average Power Ratio. On SC-FDMA, before applying the IFFT the symbols are pre-coded by a Discrete Fourier Transform (DFT). This way each subcarrier after the IFFT will contain part of each symbol..

With OFDMA and SC-FDMA the radio spectrum is divided up into 15 KHz subcarriers. These are allocated to UEs in groups of 12 known as Resource Blocks (RBs) or Physical Resource Block (PRBs) during one 0.5 ms slot [39]. The total number of those PRBs depends on the LTE bandwidth. A RB is assigned to a user to cater its service demand that can range from few kilobits per second (Kbps) to some megabits per second (Mbps) [40].
The 12 OFDM subcarriers of the RB that are adjacent to each other and each of these sub-time slot utilizes 6 OFDM symbols when normal CP is used and 7 OFDM symbols when extended CP is used.
In RB assignment, the Channel State Information (CSI) plays a significant role [40] and this information is acquired periodically by an eNodeB from its connected users. Based on this information, an eNodeB decides upon the Modulation and Coding Scheme (MCS) and the number of radio blocks that it needs to allocate to its connected users.
However, in LTE downlink, if a user has been assigned to more than one RB, all these RBs must have the same MCS. This increases the complexity of the radio resource allocation problem [40].
Each 1 ms Transmission Time Interval (TTI) consists of two slots. Each user is allocated a number of RBs in the time/frequency grid. The higher the modulation used in the resource elements are and the more RBs a user gets, the higher the bit-rate becomes [41].

The type of modulation used in LTE depends on the radio environment. The UE estimates the quality in the downlink and signals it back to the eNodeB in the Channel Quality Indicator (CQI). The uplink reference signals that are embedded into the uplink transmission are used by the eNodeB to estimate the quality in the uplink. The eNodeB decides which modulation

technique should be used based on the quality of the downlink (DL) and uplink (UL) radio environment through the adaptive modulation technique [38][39].

The supported modulation techniques in the DL and UL are: 64 QAM (6 bits/symbol), 16 QAM (4 bits/symbol), QPSK (2 bits/symbol), used in very good radio conditions till poor ones, yielding to the highest throughput till the lowest one, respectively.

The LTE specifications support number of channel bandwidths ranging from 1.4 to 20 MHz in the DL as per Table 3.1 [41] [43]:

Table 3.1. LTE Channel Bandwidths

Channel Bandwidth (MHz)	1.4	3	5	10	15	20
Number of Subcarriers	72	180	300	600	900	1200
Number of RBs	6	15	25	50	75	100

Finally, Sampling frequency varies under different bandwidth configuration in LTE, where the possible combinations are summarized in Table. 3.2 [41][44]:

Table 3.2. Sampling frequency for different LTE bandwidths (FDD and TDD)

Transmission BW [MHZ]		1.4	3	5	10	15	20
Sub-frame duration		1.0ms					
Sub-carrier spacing		15MHZ					
Sampling frequency (MHZ)		1.92	3.84	7.68	15.36	23.04	30.72
FFT size		128	256	512	1024	1536	2048
Number of occupied sub-carrier		72	180	300	600	900	1200
CP length (μs)	Normal	4.69*6, 5.21*1					
	extended	16.6					

3.3 LTE Schedulers

Scheduling is a process through which the eNodeB decides which UEs should be given RBs, and how many RBs should be given to send or receive data. In LTE, scheduling is done per subframe basis (i.e. every 1 ms). The entity that governs this mechanism is known as scheduler [45].

A scheduler takes input from the operation and maintenance system configuration e.g. which scheduling algorithm is to be enabled and considers QoS information and channel quality information (CQI, Rank, SINR etc) to make the decisions [45].

Scheduling paradigms such as Round Robin (RR), Best Channel Quality Condition or Maximum Channel Quality Indication (Max- CQI), and Proportional Fair (PF) are commonly adopted in current LTE downlink scheduling algorithms [46].
In RR, terminals are assigned one after another without taking any factor into consideration. Although this method results in poor performance, fairness is guaranteed since all terminals are equally scheduled. Max-CQI scheduling assigns RBs to the user with the best radio link conditions. The UEs with the highest CQI therefore become candidates for scheduling thereby increasing the overall cell throughput. The disadvantage of this approach is that UEs with lower CQI are denied scheduling instances, thus being starved for throughput and leading to degraded user experience. On the other hand, PF scheduling tries to maximize total throughput while providing all users at least a minimal level of service. Thus, it balances between throughput and fairness among all the UEs. The PF scheduling performs in such a manner that it considers resource fairness as well as maximizing cell throughput (in addition to other possible performance metrics) [45] [46].
For a Max-CQI scheduling, the sector throughput improves while cell edge throughput drops compared to a PF scheduling where sector throughput may not be as good as Max-CQI, but cell edge throughput thoroughly improves [45].

In our LTE system model proposed in the next chapter, we propose that the PF scheduling is adopted due to its frequent application in such networks. We assume that a minimum level of service or cell capacity is provided to all UEs, while providing a max per user throughput according to the user demand and quality of service. Thus, our definition of the heavy users

who will be offloaded from LTE to WiFi will depend on the users who consume the highest level of transmission power, leading to a highest throughput demand. Therefore, the problem formulation will be power minimization and not throughput maximization as it will be described in details in the next chapter of this thesis.

CHAPTER 4-

WiFi Network Planning for LTE Offload

As mentioned previously, LTE and WiFi cooperation is needed in order to ensure a balanced traffic so that the end user benefits from a maximum bit rate with the same or better QoS, by being transferred to WiFi or LTE seamlessly, with available needed capacity and optimal throughput.

We propose in this chapter a WiFi dimensioning method that will offload LTE. We study the available WiFi capacity and the minimum needed number of WiFi APs that will be able to handle heavy users transferred from LTE advanced to WiFi. The dimensioning method is based on the remaining available capacity of the WiFi network taking into consideration the load of the overlapped channels of the WiFi physical layer, as estimated in Chapter 2 of this thesis.

4.1 Main Drivers of WiFi Offload in 5G Systems

Mobile data offloading transfers cellular users to WiFi networks to relieve the cellular system from the pressure of the ever-increasing data traffic load. This approach was designed many years, since the third generation (3G) networks in years 2010 and 2011 [49], till the fourth generation (4G) and LTE-A networks, and still under analysis in current research areas of HetNets in the roadmap of 5G technology, even though mobile network operators and providers have deployed many small cells or femtocells solutions to cope with the forecasted needed capacity in licensed and unlicensed mode.

To have a preliminary forecast about the data traffic in the upcoming years in mobile data traffic, we represent here below a rough forecasted measures according to Cisco's annual Global Mobile Data Traffic Forecast Update (2017 – 2022) [50]:

- By 2022, there will be more than 12 billion mobile-ready devices and IoT connections, up from about 9 billion in 2017.

- By 2022, mobile networks will support more than 8 billion personal mobile devices and 4 billion IoT connections.
- The average mobile network speeds globally will increase more than three-fold from 8.7Mbps in 2017 to 28.5Mbps by 2022.
- By 2022, mobile video will represent 79 percent of global mobile data traffic, up from 59 percent in 2017.
- By 2022, 79 percent of the world's mobile data traffic will be video, up from 59 percent in 2017.
- Mobile offload exceeded cellular traffic by a ton in 2017; 54 percent of total mobile data traffic was offloaded onto the fixed-line network through WiFi or femtocell in 2017.
- In 2017, 4G already carried 72 percent of the total mobile traffic and represented the largest share of mobile data traffic by network type. It will continue to grow faster than other networks, however the percentage share will go down slightly to 71 percent of all mobile data traffic by 2022.

"As a percentage of total mobile data traffic from all mobile-connected devices, mobile offload increases from 54 percent (13.4 exabytes/month) in 2017 to 59 percent (111.4 exabytes/month) by 2022. Offload volume is determined by smartphone penetration, dual-mode share of handsets, percentage of home-based mobile Internet use, and percentage of dual-mode smartphone owners with WiFi fixed Internet access at home," Cisco said.

Other Wi-Fi predictions from the study of [50]:

- By 2022, 59 percent of global mobile data traffic (cellular) will be offloaded to WiFi or small cell networks, up from 54 percent in 2017.
- By 2022, 51 percent of total IP traffic will be Wi-Fi, 29 percent will be wired, and 20 percent will be mobile (cellular). In 2017, total IP traffic was 48 percent wired, 43 percent WiFi, and 9 percent mobile (cellular).
- Globally, total public Wi-Fi hotspots (including home spots) will grow four-fold from 124 million in 2017 to 549 million by 2022.
- In 2022 the average Wi-Fi connection speed will be 54.2 Mbps, up 2.2 times from 2017 to 2022.

WiFi is as mentioned in many studies as described before, a potential network infrastructure layer that will be supporting mobile systems in the roadmap of 5G technology, especially for non-sensitive services which can tolerate some delay (i.e. email checking, browsing, text messaging…), in respect to the 5G experience expected in the IOT services (i.e. remote health care operations, industrial live operations, streaming services, smart cities management applications, autonomous vehicles and machines,…), or in the indoor locations where WiFi APs deployment is easier to ensure indoor coverage especially when 5G BSs, operating on the higher spectrum bands, may represent certain limitations in the deep indoor penetration. This is due to the fact that 5G will be based on the acquisition of high-frequency bands between 1 GHz and 3 GHz, which will result in smaller wavelength propagation characteristics. This necessitates network designs that are smaller in coverage footprint but will also help support a very dense network that will be low powered and achieve very low noise in the 5G environment [51].

Moreover, the handover to a Wi-Fi network should be seamless, and customers shouldn't be aware that they are receiving their service through WiFi. Indoor, offloaded networks benefit customers by providing a seamless, out-of-the-box experience using their existing phone and phone number, and extending connectivity into areas where cellular and public-safety networks often don't reach. Future improvements in WiFi calling will provide a seamless handover between available Wi-Fi and LTE networks along with high-quality voice and next-generation calling features [51].

Therefore, Mobile device manufacturers and operating system developers may need to add options that allow users to have their default connection method based on speed or quality of network rather than having the decision made for them based on technology. It might be that devices connect to multiple networks at the same time.

In addition, an efficient WiFi APs planning and dimensioning is needed in order to avoid the network gaps or interference or congestions among unplanned distribution of WiFi APs. An efficient WiFi planning is proposed in the next chapter, which could ensure a minimum needed number of WiFi APs that will support efficiently with the same or better QoS the offloaded users.

To note that, the cost of deployment in CAPEX and OPEX for WiFi APs is much cheaper than 5G BSs or small cells that could ensure the same indoor coverage.

A Total Cost of Ownership (TCO) study was presented in [52], where the estimated cost (CAPEX and OPEX) for a WiFi AP and an LTE BS along with a study of two major cities (Manhattan and San Diego) were presented, in order to pinpoint the cost saving when implementing the WiFi offload to support LTE. The study found that a detailed analysis is required for every deployment. The key analysis assumptions, such as expected traffic load, density of subscribers, WiFi coverage, WiFi AP density factors, expected costs, are critical in determining the economic impact of adding WiFi offload into a network deployment plan.

In dense environments, such as New York City, the study showed that an improvement of 7.2% in the TCO can be achieved with an optimized deployment of a WiFi offload network.

In a smaller city, such as San Diego, the economic analysis can pinpoint the optimal combination of WiFi coverage and density that will optimize the Return on Investment (ROI). The key is that every case is different, and an operator must do the detailed business case analysis to understand how WiFi offload can help their deployment plans.

The cost assumptions is presented in Table 4.1 as following [52]:

Table 4.1. WiFi LTE CAPEX & OPEX Assumptions

CapEx Assumptions	WiFi AP	LTE Macro Cell
Cost of 3-Sector BTS		$45,000
Cost of WiFi Access Point	$500	
New Site Acquisition	$600	$150,000
Collocation		$50,000
Backhaul	$300	$5,000
OpEx Assumptions	**WiFi AP**	**LTE Macro Cell**
Monthly Site Rental	$20	$1,000
Site Maintenance /month	$10	$200

From the above analysis, we can visualize the profit from applying the WiFi offload to support LTE systems in the roadmap of 5G networks, where we can ensure additional spectrum and connectivity capacity, in addition to the monetary profit for the long term TCO models.

The cost and profit of the LTE WiFi cooperation has been analyzed in details in our thesis in the next chapters using Shapley value by considering both scenarios: if mobile and WiFi systems are owned by the same operator or by different ones.

4.2 State of the Art

Many studies and researches have tackled the cooperation between WiFi and LTE or future mobile networks technologies in the Heterogeneous Networks (HetNets) architecture. In practice, offloading the cellular data traffic to a WLAN depending on the signal quality is a broadly deployed method to solve networks limitations. Mobile users obtain data through WiFi instead of cellular network; hence, it is the efficient technique to improve the spectrum efficiency and reduce the cellular network congestion. In addition, it is the cost-effective solution that offloads mobile traffic to the existing WiFi networks, where extra needed expansions cost is saved in the cellular networks, which is relatively higher than the needed expansions cost in WLANs.

For those considerations, we propose in this thesis to analyze the benefit of the cooperation between the LTE and WiFi, however through the proper minimum needed planning and dimensioning of the WiFi network that will be handling a certain specified transferred users and data traffic from the mobile network.

Many studies have tackled the planning of the WiFi networks, whereas many others have tackled the offloading scenarios from cellular to WLANs.

For the WiFi network planning, authors in [3], tackled the WiFi offloading solution by analyzing the hypothesis of how many APs are needed to accommodate a proper number of users per WiFi AP without severe performance degradation. They first set the target average per-user throughput when a WiFi network can play a role as an offloading network of a given cellular network. Then, based on this criterion, they proposed the minimum required number of WiFi APs in an overlay network through a mathematical analysis.

The minimum required number of WiFi APs was investigated based on the active users' density of the uniformly distributed users, the overall coverage of the WiFi APs and the transmission probability of a user, without taking into consideration the WiFi network available capacity. The criterion proposed was the target average per-user WiFi throughput, and it is just an example

and it can be adjusted if other performance evaluation metrics such as energy efficiency or delay are employed. Although the results of this paper are based on several assumptions for simplicity of analysis, however it provides intuitive results and basic guidelines to establish a WiFi cell deployment strategy, which has been adopted in our next algorithm as it will be presented in the next sections.

In [53], the authors propose WiFi deployment algorithms based on realistic mobility characteristics of users to deploy WiFi APs for continuous service for mobile users based on maximum continuous coverage. They studied two AP deployment problems that aim to maximize the continuous user coverage and that minimize the AP deployment cost, respectively.

They were driven by the fact of the critical need to satisfy stringent performance requirements of interactive and time-sensitive mobile applications through WiFi networks; therefore they proposed the WiFi deployment to ensure continuous service for mobile users in terms of coverage and throughput, at the same time, to minimize the deployment cost such as the number of APs must be minimized for large-scale WiFi networks. The same principle as well is applied in our next proposed algorithm, however the effective network available capacity was not calculated in this paper, where the dimensioning was based only on the needed QoS offered to the end user. They formulated the Maximum Continuous Coverage and the Minimum Deployment Cost problems, which aim to provide the maximum continuous WiFi coverage to mobile users at the minimum deployment cost. Both problems were formulated based on mobility graphs that capture the statistical movement patterns of users on a map.

In [49], authors proposed and evaluated an integrated architecture to migrate data traffic from cellular networks to metropolitan WiFi APs, by considering the case of bulk file transfer and video streaming over cellular networks and simulate data delivery using real mobility data set of 500 taxis in an urban area. They calculated the number of APs needed for different requirements of quality of service for data delivery in large metropolitan area.

They proposed Delay Tolerant Networking approach by leveraging the fact that a significant amount of mobile data is delay tolerant in nature. Certain uplink data created by sensors, and Machine to Machine (M2M) applications such as remote sensing does not require real-time

data transmission; so, they proposed an integrated architecture Metropolitan Advanced Delivery Network that consists of cellular networks, WiFi networks, and mobile to mobile Pocket Switched Networks

Network architecture and mobility sessions were analyzed, however, authors just provided a feasibility study on such offloading solution through real mobility traces and did not perform any mathematical analysis or dimensioning for this problem.

In [54], authors studied the problem of mobile data offloading via WiFi networks. They analyzed a large-scale real user mobility traces and proposed a deployment algorithm based on the density of user data access requests. They first focused on the deployment of WiFi APs for efficient offloading. To this end, they analyzed a wide city real user mobility traces and proposed an APs deployment scenario. They measured how much offloading can be achieved with different numbers of APs, and they measured the offloading efficiency of proposed deployment for future data usage by network users. They also proposed a framework for the recruitment of available APs owned by private parties. The simulation results demonstrate that the alternative solution is able to provide good offloading ratios without requiring the deployment of new APs.

Although the idea of mobile data offload to WiFi networks has been tackled in many research studies since 2010 till present, based on predefined performance metrics or real traffic traces and use cases; however, the real dimensioning and planning of the WiFi network has not been analyzed in detail upon to our knowledge. In our thesis, a mathematical approach has been proposed to calculate exactly the needed number of WiFi APs, that ensures at least same or better throughput per user when transferred from LTE to WiFi network.

From the other side, many studies have analyzed the benefit or challenges of the offload between LTE and WiFi based on different criteria and assumptions.

In [1], the offload to WiFi was analyzed based on the Remaining Throughput Scheme for WiFi selection, where data is offloaded from U-LTE to WiFi APs. In addition, they proposed a distance-based transfer and speed-based transfer where the transfer process relies on distance and speed of users to be transferred to the WiFi systems or to Licensed LTE systems. They have investigated the network performance in order to evaluate the efficiency of this offload or transfer. Authors in their work discussed the cooperation between U-LTE, licensed

LTE and WiFi where they considered the probability of transmission in a time slot and the successful transmission probability in order to calculate the per user throughput. They considered that the decision of the network saturation and non-saturation depends on the WiFi saturation throughput which is the maximum load a WiFi network can carry in stable conditions. By setting the maximum network capacity, they calculated the maximum number of users that can be offloaded from U-LTE to WiFi. There was no planning or dimensioning for the WiFi/LTE networks, however, the decision of offloading was based on throughput. Similarly, they studied the shortest distance between WiFi AP and the UE in order to decide the transfer based on the shortest distance, as well they investigated the speed of the UE with the specific conditions to be transferred to licensed LTE or WiFi. All those scenarios were evaluated in respect to the offered throughput to the UE.

In [47], cellular-to-mesh data offloading for LTE-A cellular mobile users to WiFi mesh networks was proposed, which are built and managed collaboratively by users. Mobile network operators can lease these mesh networks to offload their traffic and reduce their servicing cost. Authors proposed an analytical framework that determines which mobile users should be offloaded, based on the energy cost incurred to the cellular base stations eNB for serving their demands. The offload was analyzed based on the energy cost incurred to the cellular base stations and according to a routing policy within the overlay network. The policy comprises the data routing decisions for serving a set of users that are offloaded by the cellular network in respect to the average flow (bps) of data transfer over transmission link for the offloaded users, and the WiFi flow for serving locally offloaded traffic, and the Internet average rate of flow from the WiFi node or AP. The mesh network policy is constrained by the respective link capacities. Furthermore, authors in this paper proposed employing the Shapley value profit sharing rule, to reflect the reimbursement offered by the operator that should be dispensed to the different mesh users, according to their contribution and added-value significance.

In [55], the reverse way of offloading was proposed. Authors proposed transferring some WiFi users to be served by the LTE system, in contrast to the traditional mobile data offloading which effectively offloads LTE traffic to the WiFi network, where some unlicensed spectrum resources may be allocated to the LTE system in compensation for handling more WiFi users. Authors believe that a win–win situation would be generated since LTE can generally achieve

better performance than WiFi due to its capability of centralized coordination. They tackled three different user transfer schemes according to the availability of Channel State Information (CSI): the random transfer, the distance-based transfer, and the CSI-based transfer. The minimum required amount of unlicensed time slots under a given transferred user number is first analyzed for each scheme. The number of users that need to be transferred and the amount of unlicensed spectrum that needs to be relinquished to the LTE-U system are jointly determined by negotiation between the two networks. The challenge was that WiFi and LTE-U have contradicting intentions, i.e., WiFi intends to transfer more users to LTE-U and relinquish as less unlicensed spectrum as possible while the expectation of LTE-U is just opposite. Therefore, to achieve an effective balance/tradeoff, authors utilized the Nash bargaining solution to develop a joint user transfer and unlicensed resource allocation algorithm.

In fact, in their work, authors of [55] analyzed the benefit of adopting the offload toward LTE-U instead of the licensed spectrum and mentioned how it is fairly and harmoniously coexisting with the WiFi network deployed in the same unlicensed spectrum. It has been demonstrated that LTE-U would be a better neighbor to WiFi than an additional WiFi network if its transmission is carefully controlled.

This was assessed in detail in [56], since traffic offloading and resource sharing are two common methods for delivering cellular data traffic over unlicensed bands. Authors in [56], first developed a hybrid method to take full advantages of both traffic offloading and resource sharing methods, where cellular base stations offload traffic to WiFi networks and simultaneously occupy certain number of time slots on unlicensed bands. Then, they analytically compared the cellular throughput of the three methods with the guarantee of WiFi per user throughput in the single BS scenario. They demonstrated that traffic offloading can achieve better performance than resource sharing when existing WiFi user number is below a threshold and the hybrid method achieves the same performance as the resource sharing method when existing WiFi user number is large enough.

In [57], authors studied the offload between LTE-U and WiFi and within the same WiFi network between the high busy APs and the less loaded ones.

Since Licensed Assisted Access (LAA) is considered one of the latest groundbreaking innovations to provide high performance in future 5G, authors based their study on the

coexistence between Listen Before Talk protocol (LBT) and the Carrier Sensing and Adaptive Transmission (CSAT) schemes to share spectrums. They proposed a modified LBT-based CSAT scheme which can effectively reduce the collision at the moment when LTE starts to transmit data in CSAT mode. Two-layer Coalition-Auction Game-based Transaction mechanism is proposed in order to optimize the performance of the two systems. In the first layer, a coalition among APs is built to balance the WiFi stations by merging the light-loaded APs with heavy-loaded APs into a coalition; consequently, the data of the overloaded APs can be offloaded to the light-loaded APs. Next, an auction game between the LAA and WiFi systems is used to gain a win-win strategy, in which, LAA BS is the auctioneer and AP coalitions are bidders.

Similar studies have shown the user patterns behaviors and network challenges for mobile offloading as was studied in [58], [59], and [60]. In [58], authors presented a model for defining the behavioral patterns of smartphone users when offloading data from mobile to WiFi networks. The model was generated through analysis of individual characteristics of 298 smartphone users, based on data collected via online survey as well as the amount of data offloaded from mobile to WiFi networks as measured by an application integrated into the smartphone. Users were segmented into categories based on data volume offloaded from mobile to Wi-Fi networks, and numerous user characteristics were explored to develop a model capable of predicting the probability that a user, with given characteristics, will fall into a given category of data offloading. In [59], authors carried out a survey of the practical challenges faced by operators in data traffic offloading to Wi-Fi networks (Availability and limitations of WiFi planning tools, Backhaul limitations, site availability and acquisition issues, device limitations, charging issues, authentication…) and provided recommendations to successfully address these challenges. Finally, in [60], authors in their work reviewed WiFi offloading, as a simple strategy of increasing network capacities. After performing some real-life mobile data rates measurements in different areas of specific city, they gave some recommendations on deploying a WiFi offloading strategy regarding the feasibility and the area-specific necessity behind this method.

In our next proposed algorithm in this thesis, we determined the users that should be offloaded from LTE-A to WiFi, however we proposed a planning for the WiFi network in order

to cope with this number of offloaded users. Furthermore, we have proposed the offload between LTE-A operating on the licensed spectrum toward WiFi in order to fully benefit from both spectrums at the same time, and not to have the unlicensed one shared between both technologies. Finally, in our work, Shapley value was applied to reflect the profit in terms of revenues versus cost of the adopted cooperation between WiFi and LTE systems taking into consideration the needed OPEX and CAPEX for network deployments and the revenues or data subscription fees of the data services.

4.3 Overlay LTE/WiFi Network Model

We describe in this section the adopted network model of our proposed algorithm, in order to pinpoint the WiFi network dimensioning method that will ensure an efficient optimal traffic offload from LTE.

We consider a network where an LTE-A cell, also known as eNB, is covered by K WiFi APs (K unknown to be calculated) that will support the transfer of heavy users from LTE-A to a WiFi network with a sufficient capacity and proper available coverage.
The proposed architecture of the overlay network is depicted in Fig. 4.1 where the eNB serves a set of UEs that also have WiFi interfaces.

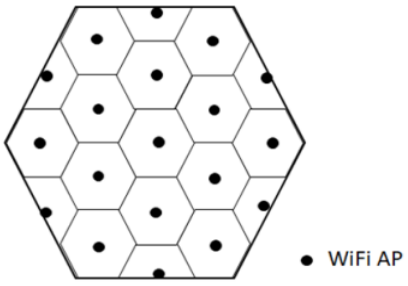

Fig 4.1. An overlay network with 'K' WiFi APs deployment covering a regular hexagonal LTE-A cell

We consider that the UEs are in range with at least one or more WiFi APs. The amount of data to be downloaded or uploaded from/to the internet differs between different users, as well

as for their channel conditions with the BS. The effects of the hidden node problem (that occurs when a node can communicate with an AP but cannot directly communicate with other nodes that are communicating with that AP and are outside their transmission range [61] [62]), and the exposed node problem (that occurs when a node is prevented from sending packets to other nodes because of co-channel interference with a neighboring transmitter [61] [63]) are not considered in our analysis.

In the proposed algorithm, the selection of the transferred users is not random. Instead, it is based on the users with heavy data consumption depending on the requested throughput thus consuming the highest level transmitted power, so the minimum needed number of WiFi APs is calculated to cope with the traffic of those transferred users.

In addition, the offloading decision is not random or based on the probability of WiFi channels occupation or on the CSI either. Instead, it is based on the exact information sent by the WiFi network informing the LTE eNB about its remaining average capacity.

This remaining average capacity depends on the estimated channels load of the physical layer of the WiFi network calculated in Chapter 2 of this thesis. However, in this chapter, we consider the average of the channels load or occupation value of the channels previously calculated, where this value is averaged for several days during the peak hour traffic of the WiFi network. Based on this averaged value, we have a global estimation, calculated through the multiple APs to be collected on a higher control node of the network, to estimate the remaining available capacity and to facilitate the measurements collection and processing time.

Therefore, our framework is divided into two phases to ensure WiFi cooperation in the heterogenous network:

- The first phase is to determine the average number of heavy users who will transmit the highest power. Therefore, we consider the LTE traffic during peak hours for several days, so to have an estimated traffic volume that should be offloaded from the LTE system. Real network statistics could be considered to estimate the traffic that should be offloaded, however we have adopted in this thesis a mathematical approach as it will be explained in the next section in equation (4.1).
- The second phase is WiFi APs dimensioning. This is considered through WiFi APs remaining capacity calculation, and it is based on the remaining throughput of each

WiFi AP based on the average occupation or load value of the physical channels. The heavy users definition and the dimensioning method will be detailed in the following paragraphs.

4.4 Heavy Users Definition

In our study, as previously mentioned, the problem formulation that will be described in this section, is an energy minimization problem and not a throughput maximization problem with the effect of adopting the PF scheduler. Therefore, the energy minimization solution consists by identifying the heaviest users who consume the highest transmission power and thus a high needed throughput. Our approach for the eNB scheduler adopts a greedy method to exclude the costly users. The eNB using our algorithm sorts the mobile users in decreasing order of power consumption and selects the most power consuming ones to be transferred to WiFi. This number of users and the related downloaded volume is averaged for several days during the peak hours of the network, to measure the overall traffic of the LTE cell and to estimate the volume and number of users to be offloaded from this LTE cell to the WiFi network. This is a greedy method for determining the most energy-consuming nodes as it leverages the results and policy that the eNB has to devise for serving its mobile users. Our approach in the evaluation scenario is the simplest one as we desired to showcase the benefits of considering power savings for the eNB by offloading a different number of users.

In order to determine the heaviest users in LTE, the operator needs to determine the resource allocation policy, in terms of RBs assignment and transmission power [47].

We consider the downlink operation of one LTE-A macro cellular Base Station (BS) for a time period of T subframes, possibly expanding over multiple frames. There exists a set of $\mathrm{N_c}$ users within the cell. Each user $\mathrm{n} \in \mathrm{N_c}$, needs to download an amount of $\mathrm{D_n} \geq 0$ in bytes, thus is assigned by the LTE QoS mechanism a data rate of $\mathrm{D_n}/T \geq 0$ in bps, for the current period, based on the used class of service, subscription status, etc [47] [64].

The BS has a set of M available Resource Blocks (RBs) that can be allocated to users in each subframe $(\mathrm{t} = 1,2,\ldots,\mathrm{T})$. The value of M depends on the available spectrum. Hence, there are in total $(\mathrm{M} * \mathrm{T})$ RBs. The system is considered quasi-static, i.e., users do not join or

leave the cell during the current time period, and channels do not change significantly (flat fading). Note that, even if channels change rapidly, the eNB will not be aware of this fact, as users transmit their CQI parameters only once during this time period.

In the beginning of the period, the eNB devises the RB assignment and power allocation policy for serving his users.

Let $x_{nm}(t) \in \{0,1\}$ denotes whether RB $m \in M$ is allocated to user $n \in N_c$ during subframe t or not. $x_{nm}(t) \in \{0,1\}$ was considered randomly in our simulation using Matlab.

Let $P_{nm}(t)$ denotes the respective transmission power. For each RB, the BS can determine a different transmission power. However, the total power consumption should not exceed a maximum level of aggregated transmission power P_{max} (Watt).

Assuming orthogonal allocation of RBs [48], and ignoring inter-cell interference, i.e., we assume that proper Enhanced Inter-Cell Interference Coordination (eICIC) techniques are applied, the bit rate for each user n is calculated by [47]:

$$r_n(t) = \sum_{m=1}^{M} x_{nm}(t).W_b.\log\left(1 + \frac{h_{nm}.x_{nm}(t).P_{nm}(t)}{\sigma^2}\right) \quad (4.1)$$

where W_b is the symbol rate per RB, h_{nm} the channel gain of user n in RB m during the current time period, σ^2 is a parameter considering the variance of the noise. These parameters are estimated through the CQI feedback that is provided by the users, once every period T. Real network statistics could be considered to estimate the values of these parameters, however we have considered $P_{nm}(t)$, in our simulations using Matlab, as a random parameter between the two minimal and maximal possible values of the transmission power of the UEs: 1 dBm and 23 dBm (in Watt). Based on this policy, the operator determines which users consume the highest power and hence are most costly.

With equation (4.1), we can calculate the users bit rate or highest throughputs values that depend on the highest transmission power. The top-heavy users in the LTE cell, are the ones that exceed a certain maximal predefined threshold of this bit rate. Knowing the top-heaviest users, we rely on this value to dimension the WiFi network based on the needed Mbps volume transferred from LTE to WiFi, and to ensure a balanced and beneficial cooperation between both networks.

4.5 WiFi Dimensioning Method

The WiFi network should assure a minimum acceptable and predefined average per user throughput for an efficient LTE offloading. Based on this average per user throughput, we will calculate the minimum required number of WiFi APs in the overlay network.

As mentioned earlier in this thesis, future generation cellular networks are likely to involve multiple RATs over multiple frequency bands, such as LTE, WiFi, and LTE-U. The prime bands today are licensed frequency bands under 3 GHz and over 500 MHz of unlicensed spectrum in the 2.4 GHz and 5 GHz frequency bands [65].

As illustrated in Fig. 4.1, we consider a scenario with one LTE BS and K WiFi APs operating separately in licensed and unlicensed spectrum, respectively.

In our scenario, we assume a coverage area of 802.11n WiFi APs with no interference, each transmitting on an orthogonal channel in the 2.5 GHz unlicensed spectrum selected based on the minimal calculated load value of the channels as proposed in Chapter 2. This model has also been adopted in other literatures, such as [47] and [53]. Following the same principle, the analysis of 5 GHz spectrum and 802.11ac could be applied.

The coexistence of WiFi and LTE could be facilitated by assuming that an inter-system coordinator exists, which performs the WiFi user transfer and resource allocation, as in [47]. To note that our proposed system is very useful for the case where LTE-A and WiFi are deployed by the same network operator. In this case, the inter-system coordinator can be implemented by the cellular network operator itself. Otherwise, it can be implemented by a third-party vendor that provides service enhancement for both WiFi and LTE.

To calculate the WiFi network remaining capacity, we need to measure the network load or occupation level. However instead of adopting the instant CCA information previously described on each WiFi AP on the network to reflect the network occupation, we rely in this thesis on the channel load estimation method previously presented in Chapter 2, which enables to scan and measure the occupation of all WiFi overlapped physical channels simultaneously, collected on a higher control node, instead of the local measurement on each AP. This load estimation method facilitates the occupation measurements aggregation and processing time.

In addition, since initially this value is an instant occupation measure, we consider in this chapter the average value of channels occupation during peak hours for several days within the LTE-WiFi HetNet, so the dimensioning calculations will be based on an averaged occupation value for several days to reflect more accurately the load of the WiFi network.

Let α_i denotes the average load or occupation value of channel i; $(1 - \alpha_i)$ is therefore the available idle capacity of this WiFi channel.

Since WiFi APs operate on the different 12 channels of the 802.11n system based on the minimum load value of the channel, different APs might be operating simultaneously on a specific channel i, taking into consideration that they are not neighbor APs to avoid the inter-channel interference. Therefore, the total available capacity of this channel i will be divided between at least two APs. If we consider t_i as the number of APs operating simultaneously under the frequency i of the WiFi channels$(1 < t_i < 12)$, we can deduce the below equation:

$$K = \sum_{i=1}^{12} t_i \tag{4.2}$$

$K \geq 1$ is the number of WiFi APs to be calculated.

Consequently, we can define the available capacity in terms of bit rate for a WiFi AP L with $L = 1, \ldots, K)$, operating on a channel i, denoted as R_l^i as follows:

$$R_l^i = (R_{w\,max} . \frac{(1-\alpha_i)}{t_i}) \tag{4.3}$$

$$R_{tot} = \sum_{l=1}^{K} \sum_{i=1}^{12} \mu_l^i \, . R_l^i \tag{4.4}$$

where $R_{w_{max}}$ is the maximum throughput of the WiFi APs (considered as same releases and specs), i is WiFi channel number $(i = 1, \ldots, 12)$, R_{tot} is the total remaining capacity or throughput of the WiFi network, and $\mu_l^i = \{0,1\}$ is 1 if the AP l is operating on frequency i, and 0 if the AP l is not operating on frequency i.

From equation (4.4), we can estimate the total available capacity of the WiFi network, and thus dimension the minimum needed number of WiFi APs that will handle the transferred LTE users according to certain throughput criteria.

To ensure the same user experience, the average per-user throughput offered by the WiFi network should be at least equal to or higher than the cellular network throughput.

Based on this constraint, we set the target average per-user WiFi throughput as follows [3]:

$$S_W^{user} \geq S_C^{user} \tag{4.5}$$

where S_W^{user} and S_C^{user} represent the average per-user WiFi throughput and the average per-user cellular throughput, respectively.

We define a maximum throughput threshold within the LTE network, considered in the simulations as 20 Mbps as average [66], where each user exceeding this threshold is considered as heavy user and should be transferred from LTE to WiFi. From equation (4.4) we can conclude the below equation to compute the average per user throughput offered in WiFi network:

$$S_W^{user} = \frac{R_{tot}}{N_w} \tag{4.6}$$

where N_w is the number of the heavy users to be transferred from LTE to WiFi as previously described.

While setting the maximum throughput threshold within the LTE as the minimum needed throughput per user to be ensured by the WiFi network, we calculate the minimum required number of WiFi APs K that achieves the target average per user WiFi throughput.

We can express the mathematical expression of K by:

$$K = \underset{K}{\operatorname{argmin}}(S_W^{user} \geq r_n(t)) \tag{4.7}$$

where $r_n(t)$ is the bit rate value calculated per user in the LTE network as per equation (4.1) and that should be at least offered by the WiFi network to the transferred user.

Therefore, by applying (4.6), we can find K, the minimum number of WiFi APs that are needed to offload the LTE heavy users.

A similar analysis could be done by analyzing the number of users to be re-transferred from WiFi to LTE when we reach a certain maximum number of WiFi APs K, that could not be increased indefinitely, and when the capacity of those APs is fully utilized. Taking into consideration, that in a certain defined coverage area of LTE BS, we have an optimal number of WiFi APs that could be added, and if both K WiFi APs and LTE BS are fully loaded, thus reconsidering the LTE network dimensioning by increasing the number of LTE BS will be a possible solution. This will be tackled in a consecutive work following the current one.

4.6 Simulations results

We consider in our simulations, an LTE system for one eNB cell operating in 1800 MHz with an available bandwidth of 10 MHz [47] [67]. The WiFi network is based on 802.11n system that operates in 2.5 GHz bandwidth with 12 overlapped channels on the physical layer. Every TTI, the eNB makes a scheduling decision to dynamically assign the available time-frequency RBs to the UEs. The eNB scheduler aims at power minimization while also at satisfying UEs demands.

Table 4.2 summarizes the basic system model parameters, while considering a total number N_c of LTE users operating in the heterogeneous network varying from 10 to 100 users per eNB making simultaneously data sessions.

Table. 4.2. Overlay LTE/WiFi system parameters

Parameters	Values
Bandwidth	10 MHz
Duration	10 ms
RBs per Time Slot	50
RBs per TTI	100
Subcarriers per RB	12

Max eNB TX Power	43 dBm
Max UE TX Power	23 dBm
Symbols per RB	7
Number of subframes(T)	20
Block Error Rate	0.1
Channel Gain	6 dB
Max WiFi AP	600 Mbps
Cost of LTE BS (C_{LBS})	45,000 USD
Cost of WiFi AP (C_{WAP})	500 USD
Cost of 1Mbps data traffic (λ)	0.001 USD

Based on the configured setup, we present in this section, numerical results by using MATLAB to analyze the minimum required number of WiFi APs versus LTE and WiFi throughput.

By varying the number of simultaneous active users in the LTE cell from 10 to 100 active users, Fig. 4.2 represents the number of users considered as heavy users and that need to be offloaded to WiFi network.

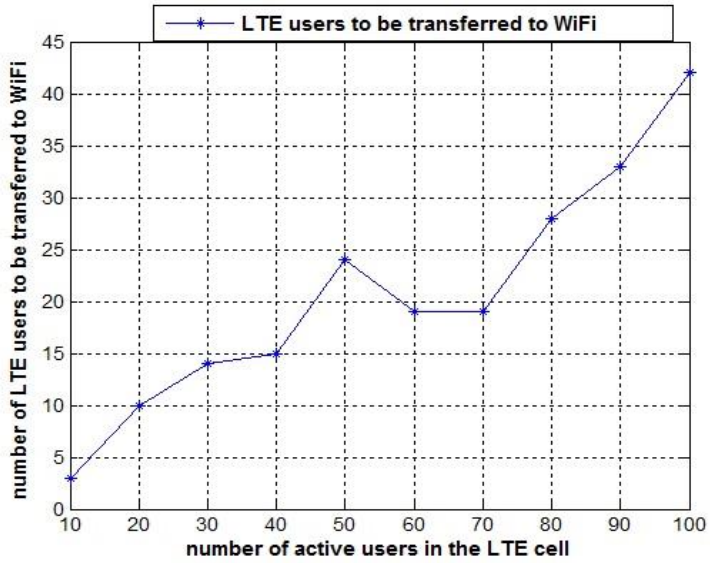

Fig 4.2. Number of users to be offloaded to WiFi with respect to the total number of active users in the LTE cell.

Taking into consideration that the LTE users will be offloaded when their demands exceed the 20 Mbps, considered as the average per user throughput in LTE-A network [66], the minimum needed number of WiFi APs, and the acquired throughput in the WiFi network are shown in Fig. 4.3 and Fig. 4.4 respectively, noting that there is no restriction in this case on the maximum offered throughput per user in the WiFi network.

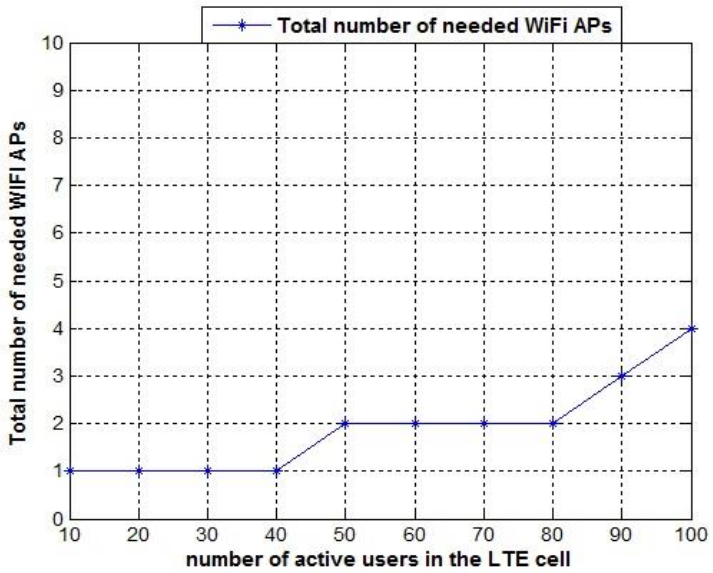

Fig 4.3. Total number of needed WiFi APs with no limitation on average per user WiFi throughput

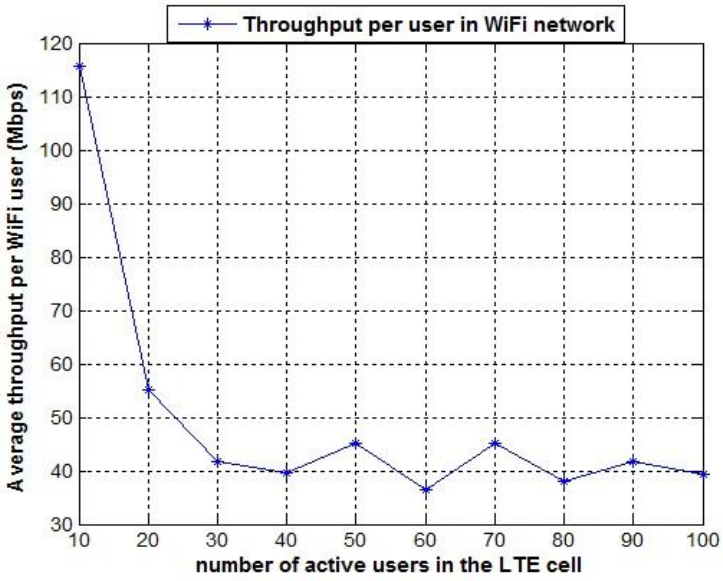

Fig 4.4. Average per user WiFi throughput (Mbps)

As we can observe, with few LTE users to be offloaded, the WiFi network with only one AP can provide up to around 120 Mbps as theoretical value on top of its existing users. The WiFi throughput per user decreases with the additional number of offloaded simultaneous active users, with an average of 40 Mbps, thus greater than the maximum defined threshold in the LTE network (20 Mbps).

By adopting this method, in addition to the saved cost when increasing the WiFi APs in indoors environment, to a maximum of 4 APs as shown in Fig. 4.3, instead of increasing the number of eNBs; the user experience will be enhanced instead of suffering from any possible congestion or throughput deterioration with limited number of LTE eNBs.

If we take the scenario of a restricted threshold of throughput offered to the offloaded users in the WiFi network (e.g. a max of 20 Mbps), the needed number of WiFi APs will be reduced to 3 APs as presented in Fig. 4.5.

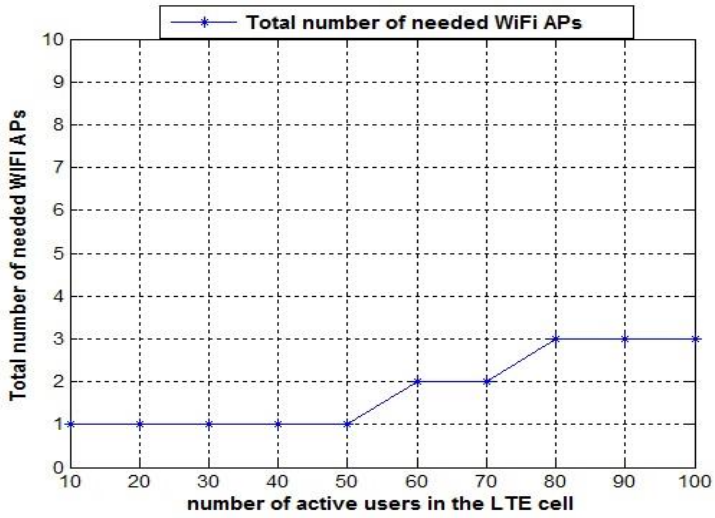

Fig 4.5. Total number of needed WiFi APs with average per user WiFi throughput set to 20 Mbps maximum.

To pinpoint the saving in LTE when applying our proposed dimensioning method, we have measured the average power consumption saving related to the transmitted power after being transferred to WiFi.

Fig. 4.6 and Fig. 4.7 represent the average saved power consumption in the eNB in Watts, and the percentage of power saving in respect to the total consumed power, respectively.

As we can observe, there is on average 40% saving of the total consumed power in the eNB. This saving is expected to grow obviously when the number of offloaded users increase.

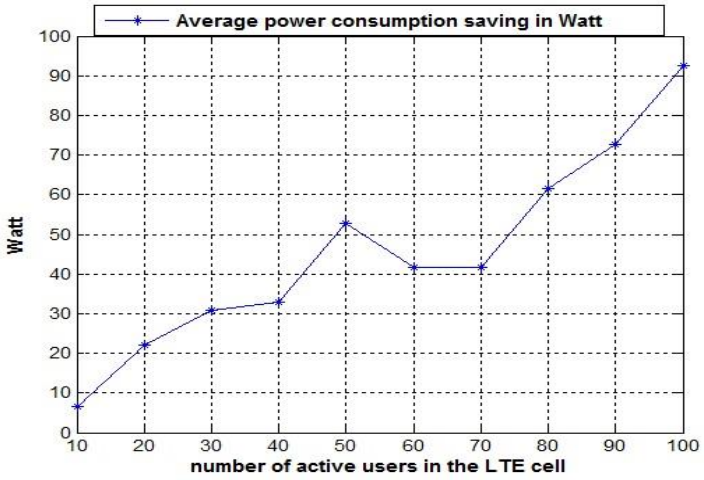

Fig 4.6. Average Power Consumption saving in Watt

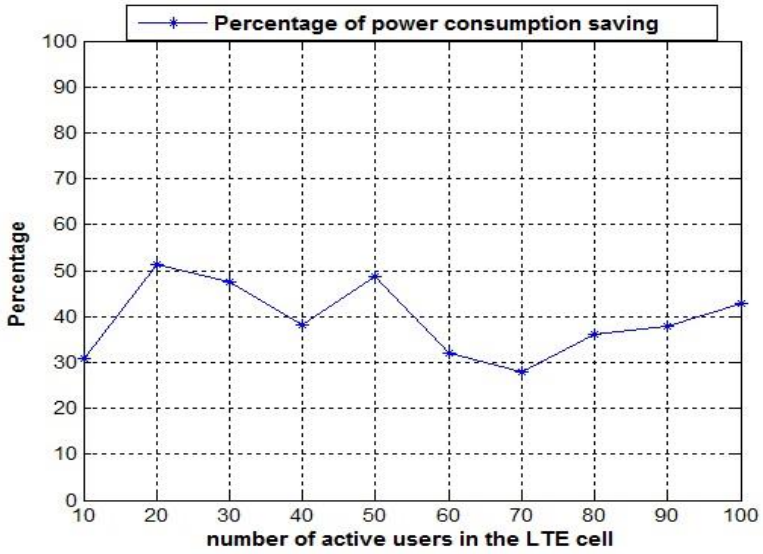

Fig 4.7. Percentage of Power Consumption saving

4.7 Conclusion

We have proposed in this chapter a mathematical approach to find the minimum required number of WiFi APs to support the heavy users' traffic transferred from LTE to WiFi network based on the remaining available capacity of the WiFi network. This capacity was estimated taking into consideration the overlapping characteristics of the physical channels of the WiFi technology in Chapter 2, where we can estimate the average percentage of busy time and idle time of the channels during peak hours traffic and for several days to estimate the global occupation and thus capacity of the WiFi network.

Through this mathematical approach, we can ensure an efficient coexistence between LTE-A and WiFi HetNets, while providing a high level of bit rate to the end users, and with minimum required number of WiFi APs thus a minimum needed hardware and investment cost. The cost investment is presented in details in the next chapter of this thesis, where we perform a detailed cost analysis based on Shapley value, to reflect the benefits of the cooperation in the proposed HetNet.

CHAPTER 5 –

Profit sharing in case of WiFi LTE coexistence

LTE and WiFi operators seek a monetary profit in case of cooperation while heavy users are transferred from LTE to WiFi. Each WiFi or LTE player tries to adopt a network configuration that decreases its own costs in order to maximize its profits. Thus, we evaluate in this chapter the Shapley Value that proved to be very effective in profit sharing in a multiplayer context, where several types of relationships are involved [68]. The idea is that each player will have a profit share proportional to its contribution in the network setting and the added value it brings to the overall value chain.

We estimate in this chapter the profit of LTE and WiFi, taking into account the data bundles subscription revenues as well as the infrastructure capital and operational costs. We calculate for each player the profit share using a coalition game concept Shapley value.

5.1 Shapley Value: Definition and Properties

The Shapley value provides a concept of solution in gaming theory. Basically, in this gaming theory, where a coalition of players are contributing to this game, they can cooperate to obtain a certain overall gain from that cooperation [68]. Since some players could contribute more to the coalition than others, and they may possess different participation power or influence on the whole gain, Shapley reflects the final distribution of the generated surplus or payoff among the players in any particular game.

Consequently, the Shapley value is the share gained by a player i when he is in coalition S. This value $\varphi_i(S,V)$ as defined by Shapley in [68] [69] [70] is given by:

$$\varphi_i(S,V) = \frac{1}{N!}\sum_{\pi\in\Pi}\Delta_i\big(V, S(\pi,i)\big)\ \forall i \in N \quad (5.1)$$

where N is the set of players and S a given coalition formed by a subset of these players, $V(S)$ is the worth function that denotes the weight or payoff of coalition S [68], the worth function V describes the expected payoff the members of S can obtain by cooperation. Π is the set of all $N!$ players permutations, $S(\pi,i)$ is the coalition formed by players from rank 1 till i in a given permutation π $(\pi \in \Pi)$, and $\Delta_i\big(V, S(\pi,i)\big) = V(S) - V(S\backslash\{i\})$ is the marginal contribution of player i in coalition S, defined as the difference between the worth functions of (S) and $(S\backslash\{i\})$ that is the set of players in N which precede i in all players permutations, and representing the benefits or losses that player i could bring if he entered coalition $(S\backslash\{i\})$.

1) Properties: The Shapley value has the following properties [71]:

a. Additivity: If the worth function $V(S)$ can be divided into two components $V(S) = V_1(S) + V_2(S)$, then the Shapley value for a player i is equal to:

$$\varphi_i(S,V) = \varphi_i(S,V_1) + \varphi_i(S,V_2) \quad (5.2)$$

b. Efficiency: There is a conservation of the total value of the coalition:

$$\sum_{i\in S}\varphi_i(S,V) = V(S)$$

c. Balance contribution: For any two players i and j, the Shapley values are balanced as follows:

$$\varphi_i(S,V) - \varphi_i(S\backslash\{j\},V) = \varphi_j(S,V) - \varphi_j(S\backslash\{i\},V)$$

In our model, there are two players only, LTE and WiFi, considered managed by the same operator in scenario 1, and by different operators in scenario 2.

The profit is the difference between the total revenue represented in the equations by r and costs represented in the equations by c, and is to be shared among the different players in the

system. Using the above defined Shapley additivity property in (5.2), the worth function of any coalition S, i.e., its payoff $V(S)$, is simply the difference of the revenue worth function $V_r(S)$ and the cost worth function $V_c(S)$. This yields the profit share of each player i as follows [71]:

$$\varphi_i(S,V) = \varphi_i^r(S,V_r) - \varphi_i^c(S,V_c) \tag{5.3}$$

We now derive closed-form expressions for the Shapley value so as to ease its numerical computation and overcome the exhaustive summation in (5.1).

Since we have 2 players $(N = 2)$, WiFi and LTE, so we have two different permutations $(\Pi = 2)$:

1- LTE, WiFi
2- WiFi, LTE

Let C_L be the cost of the network in presence of LTE only, $C_{L,W}$ the cost in presence of LTE and WiFi, G_L the revenues of the network in presence of LTE only, $G_{L,W}$ the revenues of the network in presence of LTE and WiFi. The cost and revenues shares C_W and G_W respectively in presence of WiFi only are equal to zero, since we are proposing that WiFi exists to support LTE and the presence of WiFi network only is not a scenario to be considered in our study in this chapter, however the scenario where LTE network only exists is considered $(C_L, G_L \neq 0)$ if WiFi does not support LTE.

The share of LTE in the costs according to Shapley value of equation (5.1) is calculated for the different possible permutations:

In case of permutation 1 $(\pi = 1)$ mentioned previously, and since there is no other player that precedes LTE, Δ_{LTE} the difference of cost worth function is:

$$\Delta_{LTE}\big(V, S(1,1)\big) = C_L\,; \qquad (\pi = 1, i = 1) \tag{5.4}$$

In permutation 2 $(\pi = 2)$, WiFi is a player preceding LTE, therefore Δ_{LTE} is:

$$\Delta_{LTE}\big(V, S(2,1)\big) = C_{L,W} - C_W = C_{L,W;} \qquad (C_W = 0), (\pi = 2, i = 1) \tag{5.5}$$

Thus, the share of LTE in the costs φ_L^c is as per equation (5.1) the sum of the different permutations of equation (5.4) and (5.5) over 2! As per the below:

$$\varphi_L^c = \frac{1}{2}.(C_L + C_{L,W}) \tag{5.6}$$

Let us now compute the share of WiFi Δ_{WiFi} in the costs. In the first permutation, it is given as below:

$$\Delta_{WiFi}(V, S(1,2)) = C_{L,W} - C_L; \qquad (\pi = 1, i = 2) \tag{5.7}$$

In the second permutation, the share of WiFi in the costs Δ_{WiFi} is:

$$\Delta_{WiFi}(V, S(2,2)) = C_W = 0; \qquad (\pi = 2, i = 2) \tag{5.8}$$

Therefore, the share of WiFi in the costs φ_W^c is as per equation (5.1) the sum of the different permutations of equation (5.7) and (5.8) over 2! as per the below:

$$\varphi_W^c = \frac{1}{2}.(C_{L,W} - C_L) \tag{5.9}$$

Under the same concept, we consider φ_L^r the share of LTE in the revenues, φ_W^r the share of WiFi in the revenues, $G_{L,W}$ the revenues in the presence of both LTE and WiFi, G_L the revenues in presence of LTE only, G_W the revenues in presence of WiFi only. Therefore, the shares of LTE and WiFi in the revenues are as per the following equations, where $G_W = 0$ as previously described:

$$\varphi_L^r = \frac{1}{2}.(G_L + G_{L,W}) \tag{5.10}$$

$$\varphi_W^r = \frac{1}{2}.(G_{L,W} - G_L) \tag{5.11}$$

5.2 Revenue Sharing

Revenues depend on the pricing of data traffic offered to mobile users, and the volume of this traffic. In general, operators offer various data bundles with a flat rate for each one. Therefore, by having the total number of mobile subscribers within the LTE network, N_L , and the number

of users transferred to the WiFi network, N_W (with N_W included in the total number of LTE users N_L), along with their related average Mbps volume per month, the operator can estimate the related revenues.

Let γ_L and γ_w be the total average volume in Mbps per month per user connected on LTE and per user transferred to WiFi, respectively. This volume is calculated based on an average value per month calculated from equation (4.1). λ is the price per Mbps per user in LTE or WiFi network as presented in Table 4.1.

We consider in the revenues calculations that both WiFi and LTE networks exist, and the heavy users $\mathrm{N_W}$ are transferred from LTE to WiFi.

Let ($\mathrm{G_L}$) be the revenues of the network in presence of LTE only, defined in the previous section as the revenues generated from LTE network only without considering the participation of WiFi in the game. Let ($G_{L,W}$) be the revenues of the network in presence of both LTE and WiFi where WiFi is participating in the game. $\mathrm{G_L}$ and $G_{L,W}$ are calculated as per the below equations, through two different scenarios:

Scenario 1: In case WiFi supports LTE in the revenues sharing:

$$\mathrm{G_L} = (\mathrm{N_L} - \mathrm{N_W}) * \gamma_\mathrm{L} * \lambda \tag{5.12}$$

$$G_{L,W} = (N_L - N_W) * \gamma_L * \lambda + N_W * \gamma_W * \lambda \tag{5.13}$$

Scenario 2: In case WiFi does not support LTE in the revenues sharing, therefore equations (5.12) and (5.13) become:

$$G_L = N_L * \gamma_L * \lambda \tag{5.14}$$

$$G_{L,W} = N_L * \gamma_L * \lambda \tag{5.15}$$

Indeed, in the scenario where WiFi does not support LTE, WiFi will not be participating in the users offload or the revenues sharing, therefore the total LTE users N_L will stay connected to the LTE network, and therefore G_L and $G_{L,W}$ are equal.

Therefore, the shares of both LTE φ_{L}^{r} and φ_{W}^{r} WiFi in the revenues, according to the different permutation of the two players calculated as per the equations (5.10) and (5.11).

5.3 Cost Sharing

The cost of equipment and related operations expenditure for the LTE BS and WiFi AP are C_{LBS} and C_{WAP} respectively presented in table 4.1.

The cost of the network in presence of LTE only (C_L), and in presence of LTE and WiFi ($C_{L,W}$) are calculated as per the below equations:

$$C_L = L \,.\, C_{LBS} \tag{5.16}$$

$$C_{L,W} = (K.\, C_{WAP}) + (L.\, C_{LBS}) \tag{5.17}$$

K is the number of WiFi APs calculated in (4.6), and L is the number of LTE BSs that will assure an average throughput per user greater than 20 Mbps for around 100 simultaneous active users [66] (minimum values for L are considered as follow: $L = 1$ in case of WiFi support, $L = 2$ in case WiFi does not support LTE).

Therefore, the shares of both LTE φ_{L}^{c} and WiFi φ_{W}^{c} in the costs, and according to the different permutations of the two players are calculated as per the equations (5.6) and (5.9).

5.4 Profit Sharing

The profit distribution of each player is simply the difference between its revenue and cost share as per (5.3).

We consider as previously described two scenarios:

- Scenario 1: the case of a single, joint LTE/WiFi operator.
- Scenario 2: the case where the LTE and WiFi operators are separate.

For both scenarios, we calculate the profit in case WiFi APs supports LTE for its heavy users and in case there is no WiFi support.

In scenario 1, we consider the total cost share, revenue share and profit share as per the below equations:

$$\varphi^c = \varphi_L^c + \varphi_W^c \quad (5.18)$$

$$\varphi^r = \varphi_L^r + \varphi_W^r \quad (5.19)$$

$$\varphi = \varphi^r - \varphi^c \quad (5.20)$$

Whereas in scenario 2, the profit share is calculated separately for LTE and WiFi as per the below equations:

$$\varphi_L = \varphi_L^r - \varphi_L^c \quad (5.21)$$

$$\varphi_W = \varphi_W^r - \varphi_W^c \quad (5.22)$$

Due to its fairness, the profit distribution under Shapley value is appealing in cooperative games. Each player is rewarded a profit proportional to its contribution in the overall profit. This is demonstrated in the simulation results section, where the profit started to be positive or beneficiary, in case of WiFi support, earlier than the case of without WiFi support. This is due to the fact that the cost of investment in WiFi is much less than the additional cost of investment for the LTE BSs, with same subscribers' revenues and offered throughput per user.

5.5 Simulations Results

By applying the Shapley value calculations in our Matlab simulation using the previously calculated minimal number of WiFi APs K, the results of the profit calculations are presented in Fig. 5.1 and Fig. 5.2 for the scenario 1 (joint operator) and scenario 2 (separate operators), respectively.

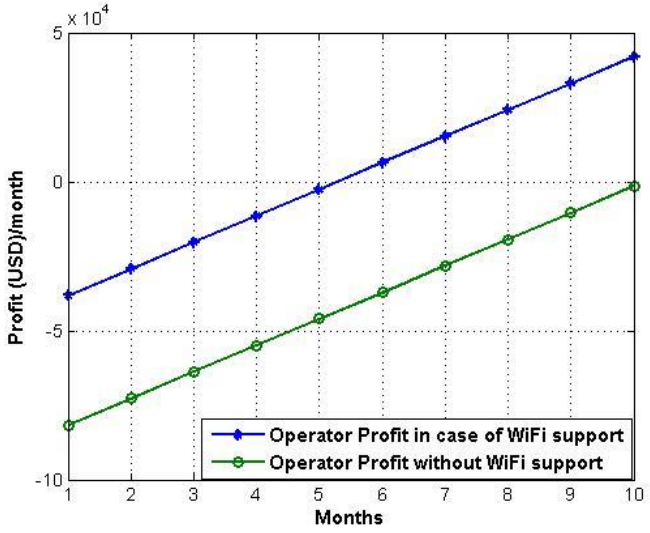

Fig. 5.1 Profit in case of Joint WiFi/LTE operator

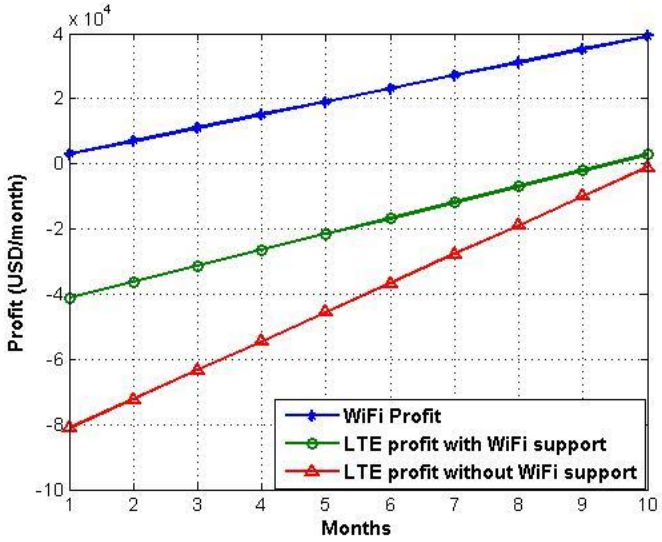

Fig. 5.2 Profit in case of separate WiFi and LTE operators

The study is split over 10 months only, where we consider that the number of subscribers is constant during this period without additional growth on LTE network. In this case we consider that a minimum of 1 BS is needed for 100 simultaneous active users with WiFi network support, and 2 BSs are needed in case of no WiFi support. After 10 months, the growth of subscribers and consequently the growth of revenues will affect both the LTE and WiFi dimensioning, but

if there is no need for an additional LTE BS, the profit of LTE in case of no WiFi support could be the same as if there is WiFi support after 10 months as per Fig. 5.2, however this analysis is not considered in our study at this stage.

In case of joint operator in Fig. 5.1, we can observe that the profit is becoming positive or beneficiary starting almost the 5th month where the revenues share become higher than the investment cost in case WiFi supports LTE. However, this gain is much more delayed for almost several additional months in case there is no WiFi support.

In the case of separate operators in Fig. 5.2, the profit starts to be positive or beneficiary on almost the 9th month whereas staying less than the profit in case of WiFi support for joint operator.

Thus, we can conclude that the Return on Investment (RoI) is maximum in the scenario where the operator owns both WiFi and LTE networks and while WiFi is providing support to LTE.

Finally, we can as well observe that the profit of the WiFi is always positive in case of separate operators as shown in Fig. 5.2, since the traffic transferred to WiFi is directly covering the investment expenses or cost.

5.6 Conclusion

We have analyzed in this chapter, the benefit of the proposed WiFi dimensioning method, which cooperates with LTE to handle the heavy users' traffic, through the profit share calculations by applying the cooperative game theory and the Shapley Value.

Two scenarios were considered, the first one where the same operator owns both WiFi and LTE networks, and the second one where both networks are owned by different operators.

The estimated profit using Shapley value is obviously increasing in time for both WiFi and LTE in both scenarios in case WiFi presents support to LTE to offload its heavy users. This profit is maximal when the same operator owns both systems.

CHAPTER 6-

Conclusion and Future Directions

This chapter presents the general conclusion of the different work described in this thesis report. We summarize the main contributions in Section 6.1, and we give future directions and topics in Section 6.2, related to the HetNet resource allocation and planning, where our contributions can be exploited in an efficient way.

6.1 Summary of Contribution

The exponentially growing demand for mobile broadband communications has made the dense deployment of cellular networks with aggressive frequency reuse a crucial need. HetNets between LTE cells and WiFi APs are considered as good architecture to ensure additional spectrum margin between LTE-A and WiFi to use both licensed and unlicensed spectrum simultaneously. However, this dense deployment, will lead to complicated channel assignment model and criteria. In this context, the focus of this thesis is to introduce dynamic radio resource allocation methods in WiFi networks based on the overlapped physical channels estimated load. This increases system available channels and energy efficiency, in addition we were able to deduce a WiFi network dimensioning algorithm to support LTE systems and to handle the traffic of the LTE heavy users.

Our first contribution, addresses the problem of the channel assignment in WiFi network. Our algorithm analyses the channels overlapping on 802.11 system, and based on the overlapped intersections, we were able to estimate the occupation time or load of each channel. In our algorithm, through the analysis of 3 non-overlapped channels only of 802.11n systems, we estimated the load of the entire 12 overlapped channels multiplied by the attenuation of the

channel. Based on the minimal load value, the channel could be allocated to an end user. However, the problem of channel attenuation factor and inter channel interference was not presented here, and this will be tackled in further analysis, although our algorithm was analyzed in noisy environment, where we have proven that in the presence of white Gaussian noise channel, the accuracy of the proposed algorithm is still reliable to estimate the channels load.

Based on this load estimation, we proposed another algorithm and method to dimension the WiFi network with a minimum number of WiFi APs that will support an LTE-A network. In this algorithm, we defined the users who are demanding the highest throughput in the LTE network on the downlink, and thus transferred them to the WiFi network. According to the estimated transferred load, the minimal number of WiFi APs was calculated based on the available network capacity calculated from the channels load of the first algorithm.

Having the minimal needed number of WiFi APs, we demonstrated the profit of such architecture or cooperation between WiFi and LTE through gaming theory and the Shapley value. With this cooperation, the operator will have minimum investment in CAPEX and OPEX and thus will increase its ROI.

6.2 Future Directions

In fact, the integration of heterogeneous wireless environment consisting of multiple Radio Access Technologies (RATs) is proliferating within 5G networks. The optimization and the inter cell or inter channel interference management of heterogeneous data networks is one of these challenges to tackle in future research issues. Our current contribution can be extended to include the channel attenuation problem while calculating the channel load values, and to tackle new algorithms to minimize and manage the overlapped channels interference.

As well, we can easily extend our proposed WiFi dimensioning algorithm to include the transfer of users from WiFi to LTE to ensure both directions cooperation, or the transfer of LTE users to WiFi based on the coverage area and distance between the APs and the transferred users. In addition, we can consider the performance degradation due to hidden and exposed node problems and investigate the impact of practical traffic patterns and multiple modulation and coding scheme (MCS) levels on WiFi cell deployment.

Finally, with the deployment of Internet of Things, uplink traffic will drastically increase. Therefore, uplink resource allocation in mobile networks will become also a crucial problem to solve. Therefore, the load association between LTE-A and WiFi could be analyzed in the uplink as well, which can be different than the downlink as it is proposed in this thesis to provide more flexibility. In general, in the downlink, the UE is associated to the best coverage eNB with the highest received signal strength, which favors the choice of LTE macro cell serving with the highest transmitting power. Consequently, the macro cell will attract more UEs which degrade its capacity and resource availability. The serving macro cell in the downlink may be not ideal for uplink traffic. It is interesting to study the improvement of the downlink/uplink decoupling on throughput efficiency and power economy.

French Summary

Introduction

Il est devenu évident depuis des années que le taux du trafic mobile des données ne fait qu'augmenter. Cette augmentation pousse à développer encore et toujours de nouvelles interfaces radio dans les réseaux mobiles adaptées aux contraintes amenées par les dits usages.

Ce développement rapide annonce l'arrivée de la technologie cinquième génération (5G). En substance, pour répondre aux besoins futurs du trafic, et pour supporter la demande croissante des utilisateurs, la 5G doit fournir un débit de données plus élevé et une capacité beaucoup plus grande que la quatrième génération (4G). Ceci impose de nouvelles méthodes pour renforcer les capacités comme l'intégration de petites cellules, ou ajouter des nouvelles fréquences sans licence, ou utiliser les réseaux Wireless Fidelity (WiFi) pour former des réseaux hétérogènes. La coopération entre WiFi et 4G ou Long Term Evolution (LTE) est nécessaire, et peut permettre à l'utilisateur de bénéficier d'un débit de données maximal, avec une même ou meilleure qualité de service.

Dans cette thèse, différents algorithmes ont été proposés pour contribuer à la coopération optimale entre WiFi et 4G dans le domaine des réseaux hétérogènes.

On propose un algorithme qui calcule la charge des canaux de la couche physique du système 802.11n. La charge représente le taux d'occupation du canal durant la transmission par rapport au temps global d'allocation du canal. A partir uniquement de trois observations des canaux indépendants, qui ne se chevauchent pas frequentiellement, on peut estimer la charge des 12 canaux qui se chevauchent. Ainsi, durant la phase de la recherche des canaux pour établir la connexion, le canal avec la valeur minimale de la charge peut être réservé.

Ayant cette valeur de la charge du canal, on présente notre second algorithme qui dimensionne un réseau WiFi pour supporter un réseau 4G en déchargeant les utilisateurs 4G qui consomment le plus haut niveau de débits de données. A partir de la valeur de la charge des canaux physiques, on calcule la capacité du réseau WiFi, et puis on calcule le nombre minimal de points d'accès nécessaire pour supporter le trafic des utilisateurs déchargés du LTE.

Dans la dernière partie de cette thèse, on calcule le profit de la coopération entre WiFi et LTE en utilisant la valeur de Shapley, et en se basant sur les données du coût d'investissement et le coût du service. Le coût, les revenus et le profit ont été analysés, dans les 2 cas :

- Le même operateur gère les 2 systèmes WiFi et LTE
- Deux opérateurs possèdent les deux systèmes séparément.

PARTIE 1 : Estimation de la charge multipliée par l'atténuation de la couche physique des réseaux WiFi

Afin de réduire le temps de découverte d'un Point d'accès WiFi (PA), et ainsi d'optimiser les valeurs des différents timeurs du système WiFi sur couche physique et couche 'Media Access Control' (MAC), nous proposons dans cette partie un nouvel algorithme qui estime la charge ou temps d'occupation multiplié par l'atténuation de chaque canal. Cet algorithme exploite le chevauchement des canaux de la couche physique WiFi. Cet algorithme permet à partir de quelques observations des canaux non chevauchés, d'estimer la charge multipliée par l'atténuation de tous les canaux de la couche physique.

Notons que par charge de canal, nous entendons le pourcentage d'utilisation du canal en temps (ou temps occupé) par rapport au temps de mesure total du canal (temps occupé et inactif total). La connaissance de la charge de chaque canal facilite la décision de l'utilisateur pour sélectionner le canal ayant la charge minimale.

De nombreux algorithmes ont été proposées pour définir les critères de sélection des canaux dans les réseaux sans fil, afin de minimiser le temps de découverte des PA. En général, ces algorithmes ont été basés sur des procédures de balayage optimal pour ajuster les valeurs des timeurs du système WiFi en fonction des conditions du canal et des caractéristiques du réseau tout en tenant compte des besoins des utilisateurs. De plus, d'autres méthodes ont été proposées pour mesurer la charge des canaux en se basant sur les paramètres d'occupation des canaux du standard WiFi.

Notre algorithme proposé dans cette partie, est appliqué sur la couche physique des réseaux 'Wireless Local area Network' (WLAN), avant d'établir toute connexion entre le PA WiFi et la station de l'utilisateur. Comme nous l'avons déjà indiqué, nous proposons d'estimer la valeur a_i (i est le numéro du canal ($i = 1, \dots, 12$)) de la charge multipliée par l'atténuation des 12 canaux superposés de l'IEEE 802.11n fonctionnant sous 2,4 GHz, en effectuant 3 observations uniquement, et ce sur les canaux non superposés, c'est-à-dire les canaux 1, 5 et 9. En effet, en observant le canal 1, la valeur a_i de la charge multipliée par l'atténuation des canaux 2, 3 et 4 est estimée. De même, l'observation du canal 5 conduit à estimer la valeur des canaux chevauchés 2, 3, 4 et 5, 6, 7 et 8. L'observation du canal 9 conduit à estimer la valeur des canaux chevauchés 6, 7, 8 et 9, 10, 11 et 12 comme le montre la figure 1.1 suivante :

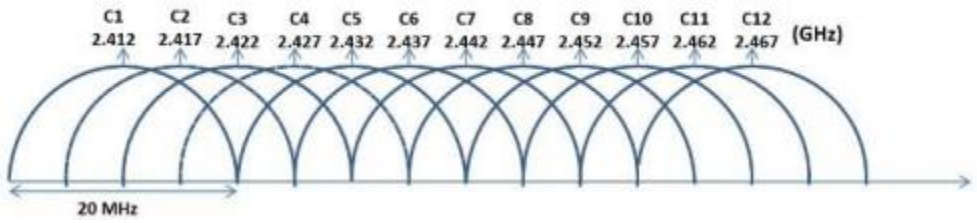

Fig. 1.1 Canaux de la couche physique du 802.11n

Afin de simplifier les notations, nous présentons la méthode en utilisant l'observation du canal 1. La généralisation à l'ensemble des canaux 5 et 9 est aisée.

Soit $\Gamma^1(f)$ le spectre du signal acquis dans le canal 1. Du fait du recouvrement spectral des canaux, ce spectre peut provenir de signaux se trouvant dans les canaux 1, 2, 3, et 4. Notons que le recouvrement de deux canaux adjacents est de $3B/4$ où B est la bande d'un canal Wifi. Soit $S(f)$ le spectre d'un signal théorique d'un signal Wifi en bande de base qui émet d'une manière continue. Si le signal n'émet plus de façon continue, mais possède une charge égale à α_i, et en supposant un canal flat fading sur la durée d'observation du signal, alors le signal observé est de plus atténué par λ_i, et le spectre s'exprime par :

$$(\lambda_i^2(f).\alpha_i).S(f)$$

La valeur du spectre $S(f)$, est calculée comme suit et représente le spectre d'un signal OFDM:

$$S(f) = \frac{\sigma_c^2}{MT_S}\sum_{k=0}^{N-1}\left(sinc\left[\left(f - k\Delta_f\right)MT_S\right]\right)^2 \quad (1.1)$$

On peut exprimer alors $\Gamma^1(f)$ en fonction de $S(f)$, et de la valeur de la charge multipliée par l'atténuation du canal a_i.

Nous découpons le spectre $S(f)$ en quatre parties :

$$\begin{aligned} S_1(f) &= S(f)\ pour\ f\ \epsilon\ [-B/2; -B/4] \text{ et } 0 \text{ sinon} \\ S_2(f) &= S(f)\ pour\ f\ \epsilon\ \left[-\tfrac{B}{4};\ 0\right] \text{ et } 0 \text{ sinon} \\ S_3(f) &= S(f)\ pour\ f\ \epsilon\ [0; B/4] \text{ et } 0 \text{ sinon} \\ S_4(f) &= S(f)\ pour\ f\ \epsilon\ [B/4; B/2] \text{ et } 0 \text{ sinon} \end{aligned} \quad (1.2)$$

avec le vecteur $\mathbb{S} = [S_1(f), S_2(f), S_3(f), S_4(f)]$.

De même

$$\begin{aligned} \gamma_1^j(f) &= \Gamma^j(f)\ pour\ f\ \epsilon\ [-B/2; -B/4] \text{ et } 0 \text{ sinon} \\ \gamma_2^j(f) &= \Gamma^j(f) pour\ f\ \epsilon\ \left[-\tfrac{B}{4}; 0\right] \text{ et } 0 \text{ sinon} \\ \gamma_3^j(f) &= \Gamma^j(f)\ pour\ \ f\ \epsilon\ [0; B/4] \text{ et } 0 \text{ sinon} \\ \gamma_4^j(f) &= \Gamma^j(f)\ pour\ f\ \epsilon\ [B/4; B/2] \text{ et } 0 \text{ sinon} \end{aligned} \quad (1.3)$$

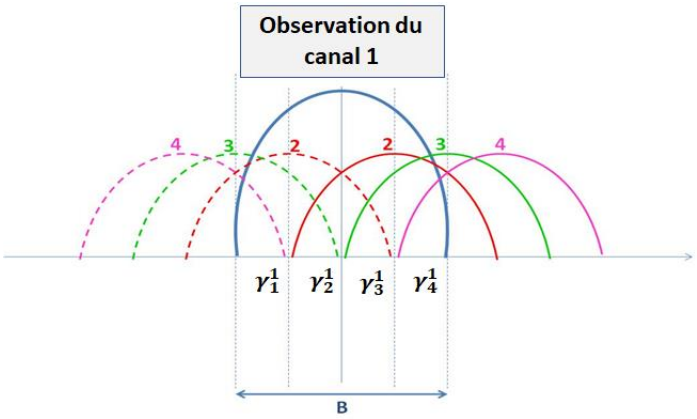

Fig. 1.2. Modèle d'observation du canal 1

avec j est le numéro du canal observé (1, 3, ou 5), avec $j = 1$ dans notre analyse dans cette partie, et le vecteur $\Gamma^j(f) = [\gamma_1^j(f); \gamma_2^j(f); \gamma_3^j(f); \gamma_4^j(f)]$. En se basant sur la figure 1.2, on aura le système d'équations suivant :

$$\gamma_1^1(f) = 2.a_1.S_1(f) + a_2.S_2(f) + a_3.S_3(f) + a_4.S_4(f) \quad (1.4)$$

$$\gamma_2^1(f) = 2.a_1.S_2(f) + a_2.\big(S_1(f) + S_3(f)\big) + a_3.S_4(f)$$

$$\gamma_3^1(f) = 2.a_1.S_3(f) + a_2.\big(S_2(f) + S_4(f)\big) + a_3.S_1(f)$$

$$\gamma_4^1(f) = 2.a_1.S_4(f) + a_2.S_3(f) + a_3.S_2(f) + a_4.S_1(f)$$

Ainsi,

$$\Gamma^1(f) = \begin{bmatrix} \mathbb{S} & 0 & 0 & 0 \\ 0 & \mathbb{S} & 0 & 0 \\ 0 & 0 & \mathbb{S} & 0 \\ 0 & 0 & 0 & \mathbb{S} \end{bmatrix} \cdot \begin{bmatrix} 2 & 0 & 0 & 0 \\ 0 & 1 & 0 & 0 \\ 0 & 0 & 1 & 0 \\ 0 & 0 & 0 & 1 \\ 0 & 1 & 0 & 0 \\ 2 & 0 & 0 & 0 \\ 0 & 1 & 0 & 0 \\ 0 & 0 & 1 & 0 \\ 0 & 0 & 1 & 0 \\ 0 & 1 & 0 & 0 \\ 2 & 0 & 0 & 0 \\ 0 & 1 & 0 & 0 \\ 0 & 0 & 0 & 1 \\ 0 & 0 & 1 & 0 \\ 0 & 1 & 0 & 0 \\ 2 & 0 & 0 & 0 \end{bmatrix} \cdot \begin{bmatrix} a_1 \\ a_2 \\ a_3 \\ a_4 \end{bmatrix} \quad (1.5)$$

avec

$$\mathbb{B}_1 = \begin{bmatrix} \mathbb{S} & 0 & 0 & 0 \\ 0 & \mathbb{S} & 0 & 0 \\ 0 & 0 & \mathbb{S} & 0 \\ 0 & 0 & 0 & \mathbb{S} \end{bmatrix} . \begin{bmatrix} 2 & 0 & 0 & 0 \\ 0 & 1 & 0 & 0 \\ 0 & 0 & 1 & 0 \\ 0 & 0 & 0 & 1 \\ 0 & 1 & 0 & 0 \\ 2 & 0 & 0 & 0 \\ 0 & 1 & 0 & 0 \\ 0 & 0 & 1 & 0 \\ 0 & 0 & 1 & 0 \\ 0 & 1 & 0 & 0 \\ 2 & 0 & 0 & 0 \\ 0 & 1 & 0 & 0 \\ 0 & 0 & 0 & 1 \\ 0 & 0 & 1 & 0 \\ 0 & 1 & 0 & 0 \\ 2 & 0 & 0 & 0 \end{bmatrix} \quad (1.6)$$

et

$$\Gamma^1(f) - \mathbb{B}_1 . a^1 = 0 \quad (1.7)$$

avec $a^1 = [a_1, a_2, a_3, a_4]$. On note les valeurs estimées de a^1 par $[\hat{a}_1^1, \quad \hat{a}_2^1, \quad \hat{a}_3^1, \quad \hat{a}_4^1]$, alors on aura :

$$\begin{bmatrix} \hat{a}_1^1 \\ \hat{a}_2^1 \\ \hat{a}_3^1 \\ \hat{a}_4^1 \end{bmatrix} = \underset{a^1}{\text{Argmin}}(\|\Gamma^1(f) - \mathbb{B}_1 . a^1\|) \quad (1.8)$$

Pour avoir l'estimation de la charge des douze canaux, il suffit de concaténer de la même manière l'observation du canal 5 et 9.

Deux méthodes pour calculer la valeur a_i ont été proposées : la méthode de calcul directe, et la méthode de calcul moyenné. Par la méthode de calcul directe, les valeurs de a_i ont été calculées directement de l'observation d'un seul canal, et par la méthode de calcul moyenné, les valeurs de a_i ont été calculées comme valeur moyenne entre l'observation de deux canaux selon la proportion de chevauchement entre ces canaux.

Ainsi, par la méthode directe, les valeurs $a_1, a_2, a_3,$ et a_4 sont directement calculées par l'observation du canal 1, les valeurs $a_5, a_6, a_7,$ et a_8 sont directement calculées par l'observation du canal 5, et les valeurs $a_9, a_{10}, a_{11},$ et a_{12} sont directement calculées par l'observation du canal 9.

Soit a_i^j, la valeur a_i du canal i observé dans le canal j. En utilisant, la méthode de calcul moyenné on aura a_i :

$$a_1^1 = a_1^1$$

$$a_2^{1,5} = \left(\frac{3}{4}.a_2^1\right) + \left(\frac{1}{4}.a_2^5\right)$$

$$a_3^{1,5} = \left(\frac{1}{2}.a_3^1\right) + \left(\frac{1}{2}.a_3^5\right)$$

$$a_4^{1,5} = \left(\frac{1}{4}.a_4^1\right) + \left(\frac{3}{4}.a_4^5\right)$$

En application les simulations sur Matlab, on obtient les résultats suivants:

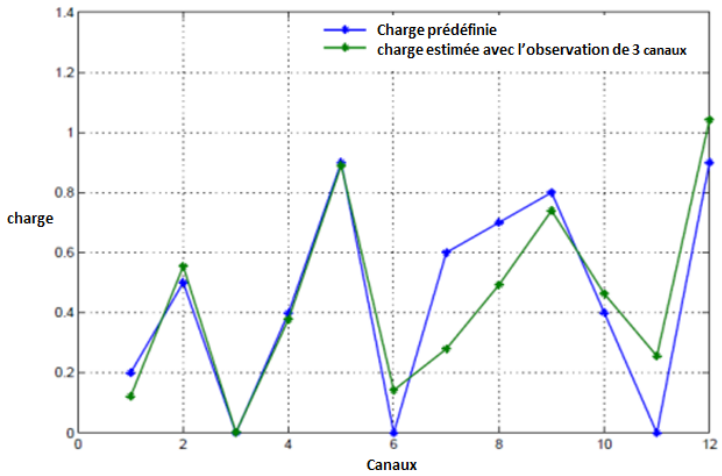

Fig.1.3. Charge estimée par rapport à la charge réelle ou prédéfinie avec l'observation de 3 canaux – cas d'un canal idéal

Figure 1.3 montre que la charge estimée est presque la même par rapport à la charge prédéfinie ou réelle, avec durée de 100 symboles comme un signal d'entrée, un rapport SNR égal à 10 dB et la méthode de calcul directe, dans les conditions d'un canal idéal.

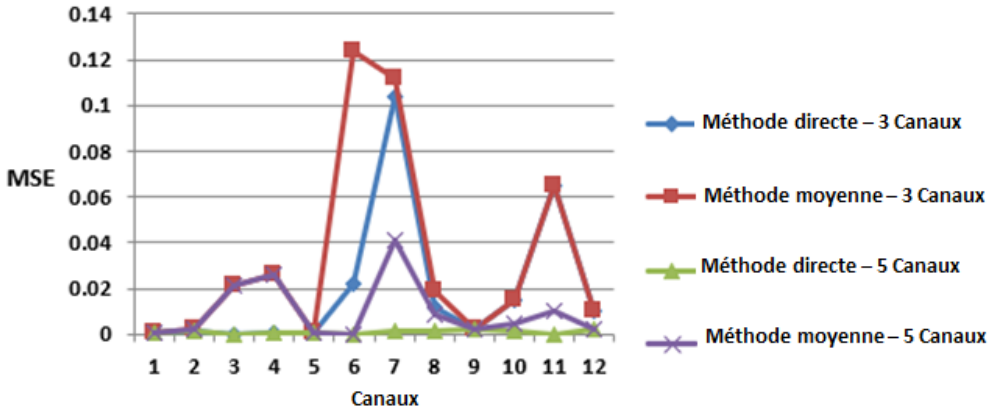

Fig.1.4. Charge estimée par rapport à la charge réelle avec les 2 méthodes de calcul

Dans la figure 1.4, une comparaison entre l'observation de 3 canaux et l'observation de 5 canaux avec les deux méthodes de calcul est effectuée. Les performances en termes de l'erreur quadratique moyenne ou Mean Squared Error (MSE), à travers plusieurs simulations sont présentés. Comme nous pouvons le voir, la MSE diminue avec l'observation de 5 canaux; nous pouvons donc conclure qu'avec un nombre supplémentaire d'observations de canaux, le niveau de précision de l'algorithme est augmenté. La durée du signal est 100 symboles ou 0.3 ms avec rapport signal sur bruit ou Signal to Noise Ratio (SNR) égal à 10 dB.

Afin d'analyser l'effet du bruit sur la précision de notre algorithme, les mêmes simulations ont été réalisées pour différents niveaux de bruit. La valeur MSE moyenne est représentée par rapport au SNR dans la figure 1.5. On peut remarquer que la précision de l'algorithme est affectée par un niveau de bruit élevé ; cependant une marge d'erreur acceptable peut encore exister avec un SNR autour de 3 dB.

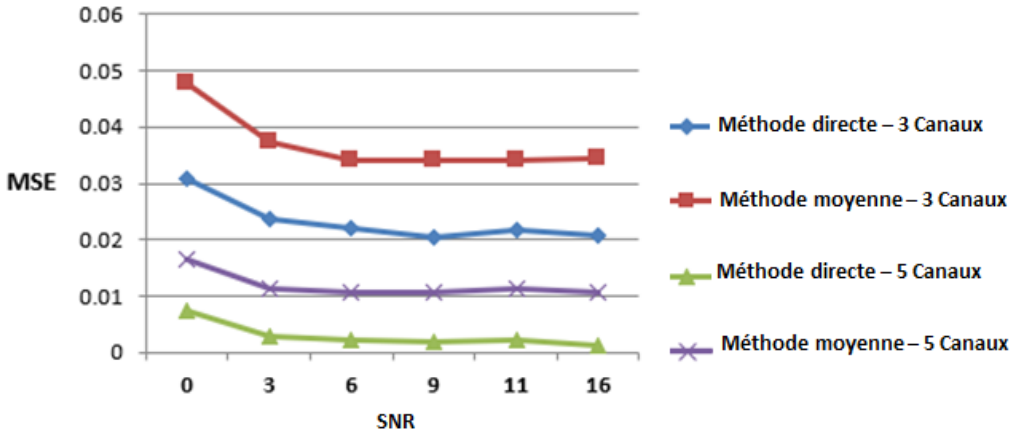

Fig.1.5. charge estimée par rapport à la charge réelle en fonction du SNR

Dans la figure 1.5, la durée du signal est 100 symboles ou 0.3 ms

De plus, nous avons analysé l'effet de la longueur du signal (c'est-à-dire le nombre de symboles OFDM) à l'entrée d' un canal sans erreur. Différentes réalisations ont été réalisées afin de refléter le MSE moyen avec une augmentation du nombre de symboles: 100 * ts (avec la durée du symbole (ts) = 3,2 μ s), 200 * ts, 300 * ts, 400 * ts et 1000 * ts. La valeur MSE moyenne diminue avec un nombre plus grand de symboles OFDM comme montré dans la Fig. 1.6. De plus, la précision de la charge estimée augmente avec la longueur du message.

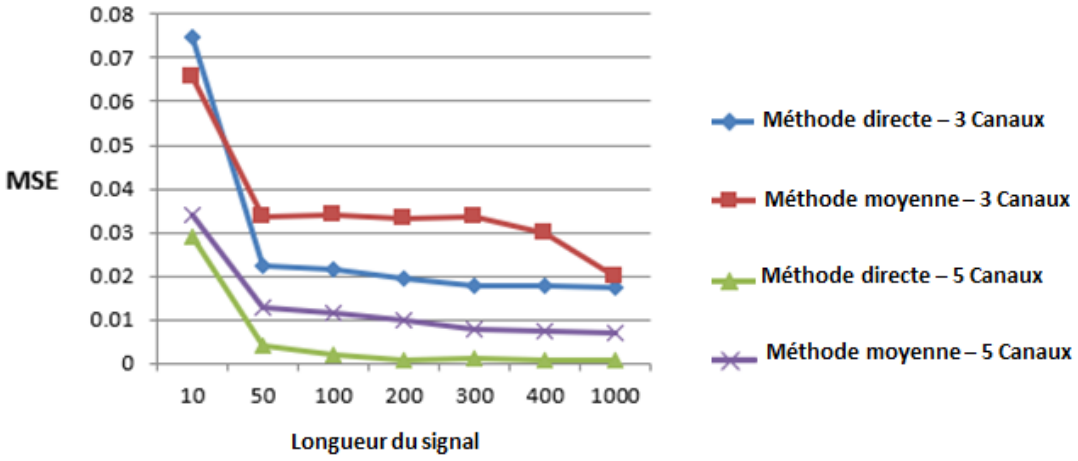

Fig.1.6. Charge estimée par rapport à la charge réelle en fonction de la longueur du signal

Finalement, on a appliqué nos simulations en présence des canaux à trajets multiples Rayleigh pour mesurer la performance de l'algorithme dans des conditions non parfaites.

La probabilité de densité de Rayleigh est comme suit :

$$f(x;\sigma) = \frac{x}{\sigma^2} . e^{-x^2/(2\sigma^2)} \quad (1.9)$$

où $x\ et\ \sigma > 0$, σ est le paramètre de la distribution.

On considère le canal de Rayleigh le vecteur $H = [h_0, h_1, \dots, h_{K-1}]$ et le signal transmis S, alors le signal reçu est le signal R définit par l'équation :

$$R = H \otimes S \quad (1.10)$$

où le symbole $\otimes$ est l'opérateur de convolution discrète.

L'espérance de la variable aléatoire Rayleigh est donnée par :

$$E(X) = \sigma * \sqrt{\frac{\pi}{2}} \quad (1.11)$$

Pour le k^{ième} coefficient de Rayleigh h_k de la réponse impulsionnelle, on définit l'espérance suivant le profil de puissance des trajets exponentiellement décroissante, alors :

$$E(h_k) = e^{-k\lambda} \quad (1.12)$$

avec λ un paramètre prédéfinie pour chaque simulation.

Pour générer les différents taps du canal multi-trajets, on calcule le paramètre de la distribution Rayleigh comme suit en se referrent sur l'équation (1.11) :

$$\sigma_k = \frac{E(h_k)}{\sqrt{\frac{\pi}{2}}} = \frac{e^{-k\lambda}}{\sqrt{\frac{\pi}{2}}} \tag{2.26}$$

Nous normalisons le vecteur H pour avoir $||H||^2 = 1$, pour refléter la PSD effective et ainsi calculer la charge des canaux comme expliqué précédemment dans le premier algorithme de cette thèse. Les résultats des simulations sont comme suit :

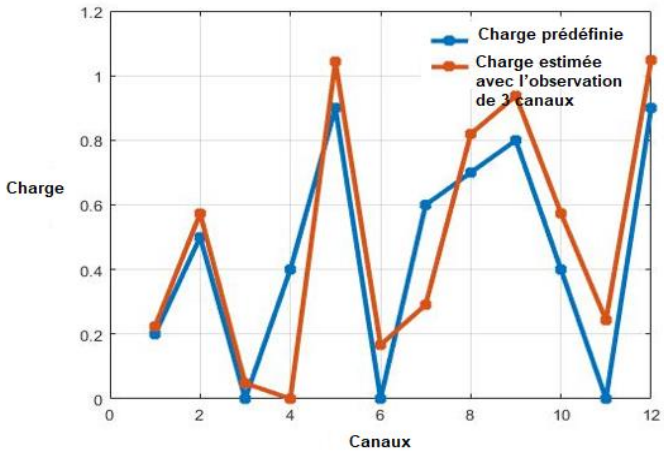

Fig.1.7. Charge estimée par rapport à la charge réelle ou prédéfinie avec l'observation de 3 canaux – canaux à trajets multiples

Dans la figure 1.7, la marge de précision a été réduite par rapport au cas de canal idéal, mais notre algorithme est toujours fiable pour les différents 12 canaux WiFi avec 10 taps de canal et un profil de puissance des trajets exponentiellement décroissante avec le paramètre λ égal à 1, malgré certains facteurs d'atténuation.

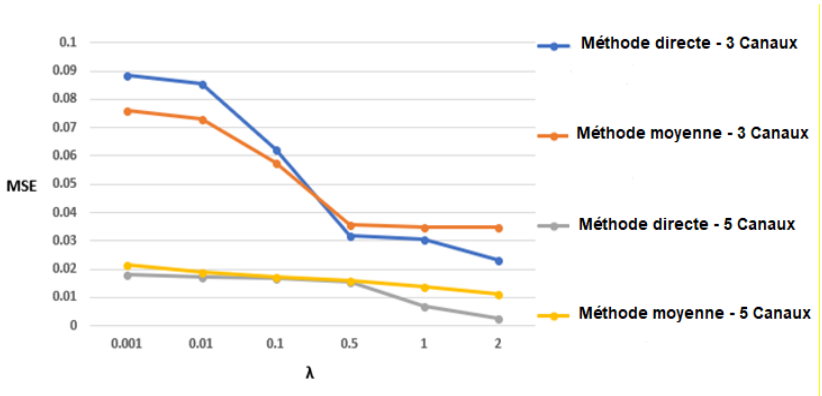

Fig.1.8. Charge estimée par rapport à la charge réelle en fonction du λ – canaux à trajets multiples

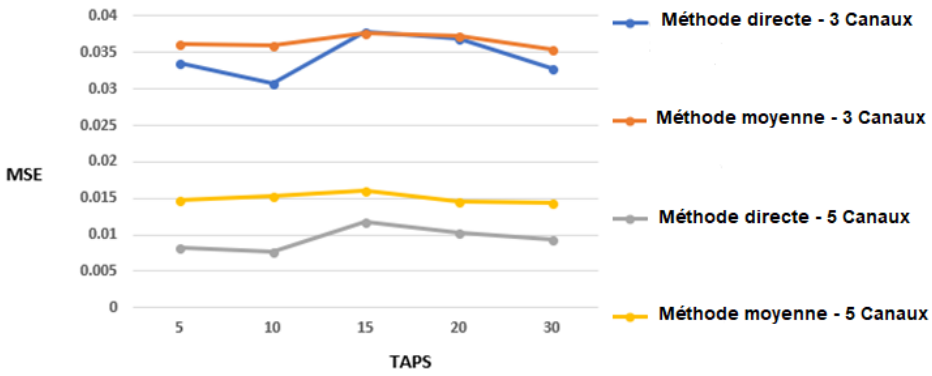

Fig.1.9. Charge estimée par rapport à la charge réelle en fonction du nombre de taps – canaux à trajets multiples

Nous pouvons observer dans les figures 1.8 et 1.9 la valeur du MSE par rapport aux différentes valeurs de λ et le nombre de taps respectivement. La valeur MSE décroît avec une valeur croissante du paramètre du profil du canal à puissance exponentiellement décroissante, et est presque la même pour tous les nombre des taps.

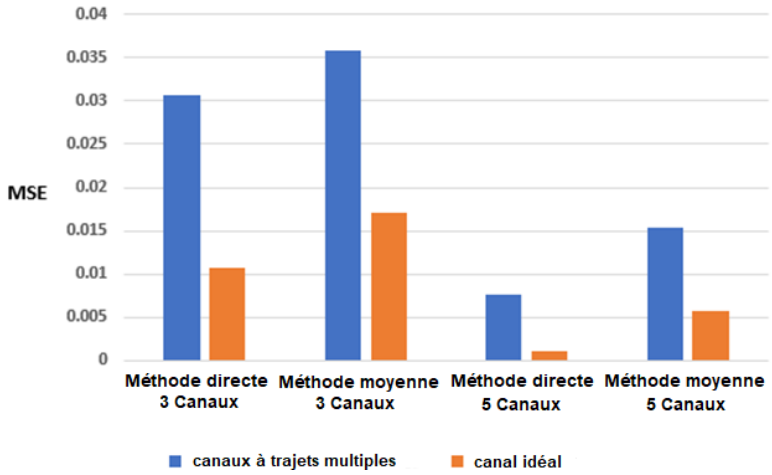

Fig.1.10. Charge estimée par rapport à la charge réelle – canaux à trajets multiples et canal idéal

Finalement, comme on peut voir dans la figure 1.10, évidement la valeur du MSE est plus faible dans le cas d'un canal idéal.

PARTIE 2 : Calcul du nombre minimal de PA WiFi pour décharger le réseau LTE

Comme présenté précédemment, la coopération entre LTE et WiFi est nécessaire pour augmenter la capacité des réseaux mobiles, et assurer une même ou meilleure qualité de service à l'utilisateur tout en étant transféré du LTE au WiFi d'une manière transparente.

De nombreuses études ont abordé la coopération entre WiFi et LTE. Les utilisateurs mobiles obtiennent des données via WiFi au lieu du réseau cellulaire ; c'est donc une technique efficace pour améliorer l'efficacité du spectre et réduire la congestion du réseau cellulaire. En général, le déchargement du trafic de données cellulaires vers un WLAN a été analysé en fonction de la qualité du signal, la densité d'utilisateurs actifs et des utilisateurs uniformément répartis, la couverture globale des PA WiFi et la probabilité de transmission d'un utilisateur, sans tenir compte de la capacité disponible du réseau WiFi.

Nous proposons dans cette partie une méthode de dimensionnement du réseau WiFi pour décharger le réseau LTE. Nous étudions la capacité moyenne disponible du réseau WiFi et le nombre minimal nécessaire de PA WiFi pour supporter le trafic des utilisateurs lourds à transférer de LTE vers WiFi. La méthode de dimensionnement est basée sur la capacité disponible restante du réseau WiFi en considérant la valeur de la charge des canaux WiFi estimée dans la première partie de cette thèse.

Nous considérons un réseau où une cellule LTE, également connue sous le nom d'eNB, est couverte par K points d'accès WiFi (K inconnu à calculer) qui prend en charge le transfert d'utilisateurs lourds de LTE vers un réseau WiFi avec une capacité suffisante et couverture disponible appropriée.

L'architecture proposée du réseau est représentée par la figure 2.1.

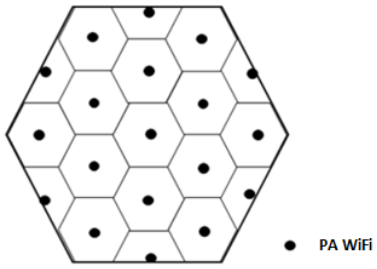

Fig 2.1. Un réseau avec déploiement de K points d'accès WiFi couvrant une cellule LTE-A hexagonale régulière

Notre analyse est divisée en deux phases pour assurer la coopération entre le WiFi et LTE dans le réseau hétérogène :

- La première phase consiste à déterminer le nombre moyen d'utilisateurs lourds qui transmettent la puissance la plus élevée. Pour cela, nous considérons uniquement les heures de pointe du trafic et ce trafic est moyenné sur plusieurs jours. Cela nous permet d'obtenir une estimation du trafic moyen à décharger de LTE vers WiFi.

- La deuxième phase est le dimensionnement des PAs WiFi. Ceci est pris en compte par le calcul de la capacité restante du réseau WiFi, et il est basé sur la capacité restante de chaque PA WiFi en fonction de l'occupation moyenne ou la valeur de la charge des canaux physiques.

Afin de déterminer les utilisateurs les plus lourds en LTE, l'opérateur doit déterminer la politique d'allocation des ressources, en termes d'attribution des 'Ressource Blocks' (RB) et de puissance de transmission en adoptant la formule suivante :

$$r_n(t) = \sum_{m=1}^{M} x_{nm}(t).W_b.\log\left(1+\frac{h_{nm}.x_{nm}(t).P_{nm}(t)}{\sigma^2}\right) \quad (2.1)$$

r_n	Débit de données (instant rate in bps) instantané de l'utilisateur
M	Nombre de RB pendant une durée T de sous-trame (subframe)
$x_{nm}(t)$	{0, 1} est la possibilité si l'utilisateur 'n' a un RB 'm' ou non
$P_{nm}(t)$	Puissance de transmission de l'utilisateur n dans le RB m
W_b	Taux ou débit de symboles par RB
h_{nm}	Gain du canal de l'utilisateur 'n'dans le RB 'm'
σ^2	Variance du bruit

Le réseau WiFi doit garantir un débit de données moyen minimal et acceptable par utilisateur pour un déchargement efficace du réseau LTE. Le débit offert par le réseau WiFi doit être au moins égal au débit offert par LTE ou meilleur. Ainsi :

$$S_W^{user} \geq S_C^{user}$$

S_W^{user}	Débit de données ou throughput de l'utilisateur dans le réseau WiFi
S_C^{user}	Débit de données ou throughput de l'utilisateur dans le réseau LTE

La capacité restante du réseau WiFi est calculée en se basant sur notre premier algorithme pour calculer la charge des canaux WiFi α_i .

Pour calculer la capacité disponible du réseau WiFi, nous proposons les formules :

$$K = \sum_{i=1}^{12} t_i \quad (2.2)$$

$$R_l^i = \left(R_{w\,max}.\frac{(1-\alpha_i)}{t_i}\right) \quad (2.3)$$

$$R_{tot} = \sum_{l=1}^{K}\sum_{i=1}^{12} \mu_l^i\,.\,R_l^i \quad (2.4)$$

$$S_W^{user} = \frac{R_{tot}}{N_w} \quad (2.5)$$

avec

K	Nombre de PAs à calculer
t_i	Le nombre de PAs qui fonctionnent simultanément sur la fréquence *i*
$R_{w\,max}$	La capacité maximale du PA du réseau WiFi
R_l^i	La capacité restante du PA *l* fonctionnant sur la fréquence *i*
R_{tot}	La capacité restante totale du réseau WiFi
α_i	La charge du canal *i* calculée précédemment
μ_l^i	1 si le PA *l* fonctionne sur la fréquence *i*, 0 si le PA *l* ne fonctionne pas sur la fréquence *i*
N_w	Le nombre d'utilisateurs lourds transférés du LTE au WiFi

Alors le nombre minimal de PAs est calculé par :

$$K = \underset{K}{\operatorname{argmin}}(S_W^{user} \geq r_n(t)) \tag{2.6}$$

En simulant notre algorithme sur Matlab, nous avons obtenu les résultats suivants :

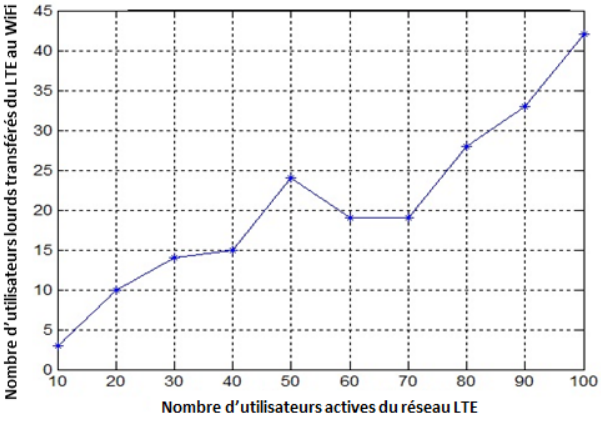

Fig 2.2. Nombre d'utilisateurs transférés au réseau WiFi

En faisant varier le nombre d'utilisateurs actifs simultanés dans la cellule LTE de 10 jusqu'à 100, la figure 2.2 représente le nombre d'utilisateurs considérés comme des utilisateurs lourds et qui doivent être déchargés sur le réseau WiFi.

Le nombre minimal de PA et le débit de données acquis dans le réseau WiFi sont indiqués dans la Fig. 2.3 et la Fig. 2.4 respectivement :

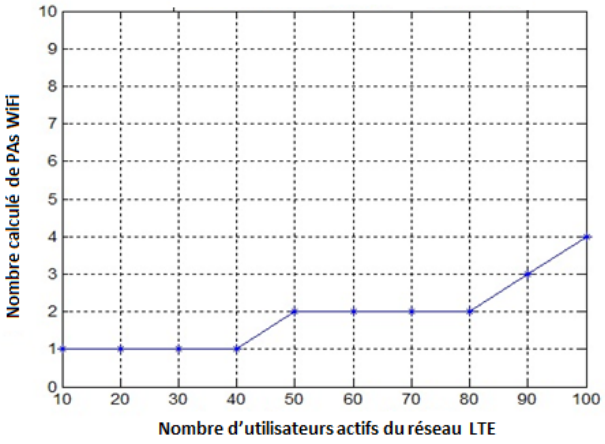

Fig 2.3. Nombre de PAs calculé pour décharger le LTE

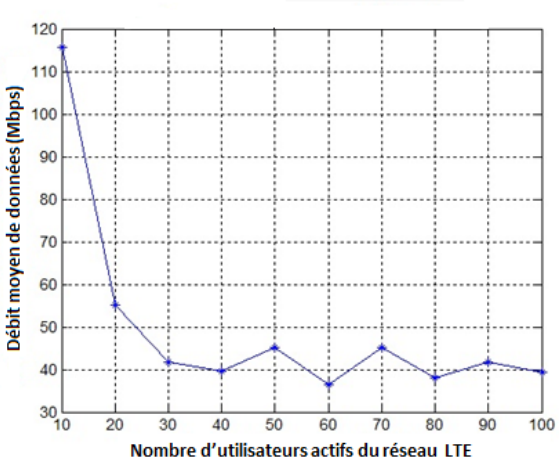

Fig 2.4. Débit moyen de données (Mbps) par l'utilisateur dans WiFi

Le nombre de PAs WiFi nécessaire pour décharger le LTE est 4 PAs comme indiqué dans la figure 2.3. En installant ces 4 PAs WiFi, il n'est pas nécessaire d'augmenter le nombre de cellules LTE comme la cellule qui existe n'est pas saturée. De plus, l'expérience des utilisateurs s'est améliorée pour avoir un débit moyen de 40 Mbps comme par la figure 2.4.

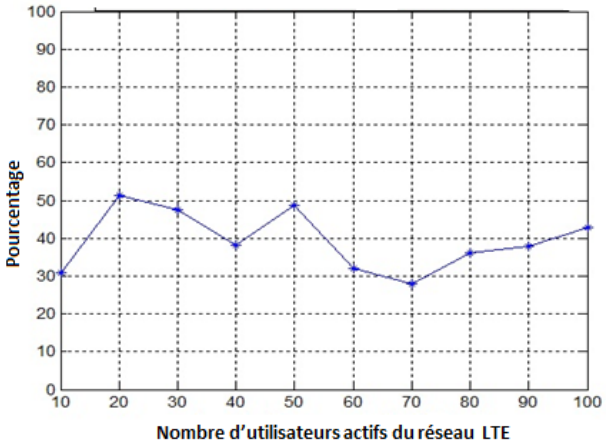

Fig 2.5. Pourcentage de la Puissance moyenne économisée dans la cellule LTE

Finalement, comme nous pouvons l'observer dans la figure 2.5, il y a en moyenne 40% d'économie de la puissance totale consommée dans la cellule LTE. Cette économie devrait augmenter de façon évidente lorsque le nombre d'utilisateurs déchargés augmentera.

PARTIE 3 : Calcul du Profit Financier entre LTE et WiFi

Les opérateurs LTE et WiFi cherchent un profit monétaire en cas de coopération dans les réseaux hétérogènes lorsque les utilisateurs lourds sont transférés du LTE vers le WiFi. Nous modélisons dans cette partie le problème par un jeu ou chaque joueur va estimer son profit une fois il participe au jeu (coopération entre WiFi et LTE) ou non.

Alors, chaque joueur WiFi ou LTE essaie d'adopter une configuration du réseau qui diminue ses propres coûts afin de maximiser ses profits. Pour ces raisons, nous évaluons dans cette partie la valeur de Shapley qui a démontré une efficacité dans le calcul du partage du profit dans un contexte multijoueurs, où plusieurs types de relations sont impliquées. L'idée est que chaque joueur aura une part des bénéfices proportionnelle à sa contribution dans le jeu et à la valeur ajoutée qu'il apporte à la chaîne globale du système.

La valeur de Shapley peut être calculée par :

$$\varphi_i(S,V) = \frac{1}{N!}\sum_{\pi\in\Pi}\Delta_i\big(V, S(\pi,i)\big)\ \forall i \in N \tag{3.1}$$

$v(S)$	La fonction caractéristique du jeu qui donne la valeur maximum de la coalition S
N	Nombre de joueurs
Π	L' ensemble de $N!$ permutations de N joueurs

Le profit est donné par :

$$\varphi_i(S,V) = \varphi_i^r(S,V_r) - \varphi_i^c(S,V_c) \tag{3.2}$$

avec

φ_i^r	La valeur de partage de Shapley des revenues
φ_i^c	La valeur de partage de Shapley des coûts

Pour calculer les valeurs du coût et du revenu des réseau LTE seul, ou LTE en présence du WiFi on a les formules suivantes :

$$\varphi_{\mathrm{L}}^{\mathrm{c}} = \frac{1}{2}.(C_L + C_{L,W}) \tag{3.3}$$

$$\varphi_{\mathrm{W}}^{\mathrm{c}} = \frac{1}{2}.(C_{L,W} - C_L) \tag{3.4}$$

$$\varphi_L^r = \frac{1}{2}.(G_L + G_{L,W}) \tag{3.5}$$

$$\varphi_{W}^{r} = \frac{1}{2}.\ (G_{L,W} - G_L) \quad (3.6)$$

avec

φ_{L}^{c} La valeur Shapley du coût par rapport à LTE

φ_{W}^{c} La valeur Shapley du coût par rapport à WiFi

φ_{L}^{r} La valeur Shapley de la revenue par rapport à LTE

φ_{W}^{r} La valeur Shapley de la revenue par rapport à WiFi

$C_L\ (G_L)$ coût (Gain) du LTE seul

$C_{L,W}\ (G_{L,W})$ coût (Gain) du LTE and WiFi

$C_W\ (G_W)$ coût (Gain) du WiFi seul = 0

Le coût du réseau en présence de LTE seulement, et en présence de LTE et WiFi:

$$\mathrm{C_L} = \mathrm{L}\,.\,\mathrm{C_{LBS}} \quad (3.7)$$

$$\mathrm{C_{L,W}} = (\mathrm{K}.\,\mathrm{C_{WAP}}) + (\mathrm{L}.\,\mathrm{C_{LBS}}) \quad (3.8)$$

L Nombre de eNB

$\mathrm{C_{LBS}}$ Coût d'un eNB (~ 45,000 USD)

K Nombre de PA WiFi calculé

$\mathrm{C_{WAP}}$ Coût d'un PA WiFi (~500 USD)

Les revenus du réseau en présence de LTE seulement, et en présence de LTE et WiFi :

Si le WiFi supporte le LTE:

$$\mathrm{G_L} = (\mathrm{N_L} - \mathrm{N_W}) * \gamma_L * \lambda \quad (3.9)$$

$$G_{L,W} = (N_L - N_W) * \gamma_L * \lambda + N_W * \gamma_W * \lambda \quad (3.10)$$

Si le WiFi ne supporte pas le LTE:

$$G_L = N_L * \gamma_L * \lambda \quad (3.11)$$

$$G_{L,W} = N_L * \gamma_L * \lambda \quad (3.12)$$

λ prix d'un Mbps (~0.001 USD)

γ_W (γ_L) volume de données déchargé dans le réseau WiFi (LTE)

N_L Nombre d'utilisateurs dans le LTE; N_W nombre d'utilisateurs déchargés dans le réseau WiFi

Le Profit φ au cas où les 2 réseaux sont possédés par le même opérateur :

$$\varphi^c = \varphi_L^c + \varphi_W^c \quad (3.13)$$

$$\varphi^r = \varphi_L^r + \varphi_W^r \quad (3.14)$$

$$\varphi = \varphi^r - \varphi^c \quad (3.15)$$

Le Profit du LTE φ_L , et le profit du WiFi φ_W au cas où les 2 réseaux sont possédés par des opérateurs différents :

$$\varphi_L = \varphi_L^r - \varphi_L^c \quad (3.16)$$

$$\varphi_W = \varphi_W^r - \varphi_W^c \quad (3.17)$$

En simulant nos équations sur Matlab, nous avons obtenu les résultats suivants :

Cas où le même opérateur possède les deux réseaux LTE et WiFi :

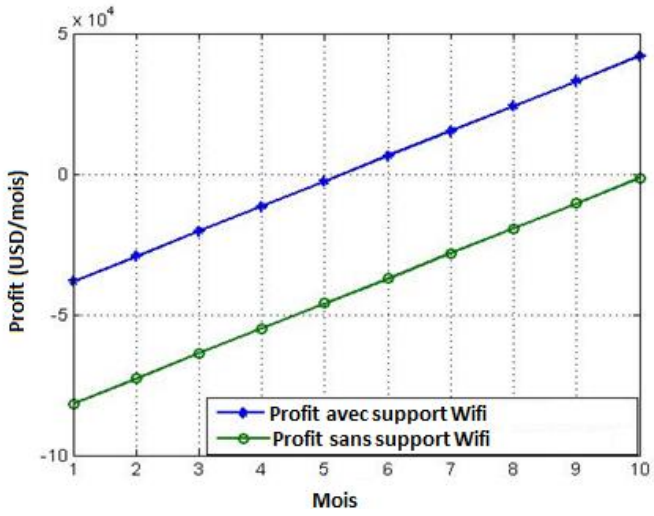

Fig 3.1. Profit du réseau au cas où le même operateur possède LTE et WiFi

Nous pouvons observer dans la figure 3.1, que le profit devient positif ou bénéficiaire à partir du 5ème mois dans le cas où le WiFi supporte le LTE. Cependant, ce gain peut être retardé de plusieurs mois en absence du support WiFi.

Cas où deux opérateurs différents possèdent les réseaux LTE et WiFi :

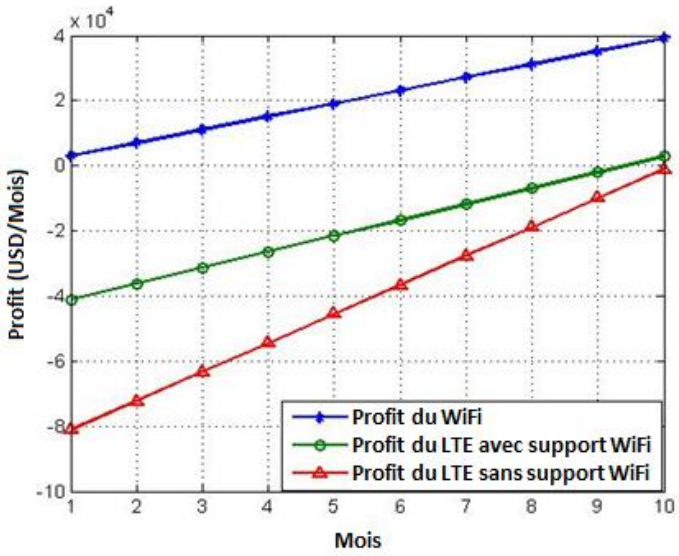

Fig 3.2. Profit du réseau au cas où deux operateurs possèdent LTE et WiFi

Dans la figure 3.2, le profit du WiFi est toujours positif (i.e. il gagne des utilisateurs), mais le profit du LTE commence à être positif ou bénéficiaire à partir du 9ème mois. Cependant le profit dans le cas où le Wifi supporte le LTE reste toujours plus grand.

PARTIE 4 : Conclusion et Perspectives

La demande exponentiellement croissante de trafic de données dans les réseaux de communications mobiles a rendu le déploiement de réseaux cellulaires, avec une réutilisation agressive des fréquences, un besoin crucial. Les réseaux HetNets entre les cellules LTE et les points d'accès WiFi ont été considérés comme une bonne architecture pour garantir une marge de spectre supplémentaire entre LTE-A et WiFi, et pour utiliser simultanément le spectre sous licence et sans licence.

Cependant, ce déploiement dense entraîne un modèle et des critères d'attribution de canal compliqués. Dans ce contexte, l'objectif de cette thèse est d'introduire des méthodes dynamiques d'allocation de ressources radio dans les réseaux WiFi basées sur la charge estimée des canaux physiques qui se chevauchent. Cela augmente les canaux disponibles du système, en plus nous avons pu déduire un algorithme de dimensionnement du réseau WiFi pour décharger le réseau LTE au Wifi et gérer le trafic des utilisateurs lourds du LTE.

Dans la première partie de cette thèse, nous avons proposé un algorithme qui analyse les canaux qui se chevauchent sur le système 802.11, où nous avons pu estimer le temps d'occupation ou la charge multipliée par l'atténuation de chaque canal. Dans notre algorithme, grâce à l'analyse de 3 canaux non superposés uniquement des systèmes 802.11n, nous avons estimé la charge de l'ensemble des 12 canaux superposés. Sur la base de la valeur de charge minimale, le canal pourrait être attribué à un utilisateur final. Cependant, le problème du facteur d'atténuation du canal et des interférences entre canaux n'a pas été présenté ici, et cela sera abordé dans une analyse plus approfondie, bien que notre algorithme ait été analysé dans un environnement bruité, où nous avons simulé qu'en présence d'un canal à trajet multiple, la précision de l'algorithme proposé reste fiable pour estimer la charge des canaux.

En se basant sur cette estimation de charge, nous avons proposé un autre algorithme dans la deuxième partie de cette thèse, pour dimensionner le réseau WiFi avec un nombre minimal de points d'accès WiFi permettant de décharger un réseau LTE. Dans cet algorithme, nous avons défini les utilisateurs lourds qui exigent le débit le plus élevé dans réseau LTE, moyennés sur un certain nombre de jours, pendant les heures pointes de trafic. Cela, nous permet d'avoir une idée du trafic moyen à transférer vers le WiFi. Le nombre minimal de points d'accès WiFi, nécessaire pour supporter ce trafic, a été calculé en se basant sur la capacité disponible du réseau WiFi, calculée à partir de la charge des canaux du premier algorithme.

Dans la troisième partie de la thèse, ayant le nombre minimal de PA WiFi, nous avons calculé le profit d'une telle coopération entre WiFi et LTE à travers la théorie des jeux et la valeur Shapley. Grâce à cette coopération, l'opérateur aura un investissement financier minimum et augmentera ainsi son profit.

Finalement, notre contribution actuelle peut être étendue pour inclure le problème d'atténuation de canal lors du calcul des valeurs de charge de canal, et pour analyser de nouveaux algorithmes pour minimiser et gérer les interférences de canaux qui se chevauchent.
De plus, nous pouvons facilement étendre notre algorithme de dimensionnement WiFi proposé pour inclure le transfert dynamique d'utilisateurs du WiFi vers le LTE pour assurer la coopération dans le sens inverse. De plus, nous pouvons analyser le transfert des utilisateurs LTE vers le WiFi en fonction de la zone de couverture et de la distance entre les points d'accès et les utilisateurs transférés. Comme le trafic sur uplink augmentera considérablement dans les réseaux 5G, ou pourra étendre notre analyse de dimensionnement par rapport au trafic uplink des réseaux mobiles qui deviendra également un problème crucial à résoudre.

Publications

- Danielle Saliba, Rodrigue Imad, Sebastien Houcke, and Bachar El Hassan, “Planning and Profit Sharing in Overlay WiFi and LTE Systems toward 5G Networks”, Journal of Software Engineering and Applications (JSEA), Nov 2019.
- Danielle Saliba, Rodrigue Imad, Sebastien Houcke, and Bachar El Hassan, “WiFi Dimensioning to offload LTE in 5G Networks”, IEEE Computing and Communication Workshop and Conference (CCWC), LAS Vegas, USA, Jan 2019.
- Danielle Saliba, Rodrigue Imad, and Sebastien Houcke, “Channels Load Measurement in WiFi Networks”, 24th International Scientific Conference “Sciences, Social Equity and Sustainable Development”, Balamand, Lebanon, Apr 2018.
- Danielle Saliba, Rodrigue Imad, and Sebastien Houcke, “Wifi Channel Selection Based on Load Criteria”, International Symposium on Wireless Personal Multimedia Communications WPMC, Yogyakarta, Indonesia, Dec 2017
- Danielle Saliba, Rodrigue Imad, and Sebastien Houcke, “Overlapped Physical Channels Load Measurement in 802.11 Networks,” International Journal of Advanced Research in Computer Science, Sep 2017.

References

[1] Ibrahim Elgendi, Kumudu S. Munasinghe, and Abbas Jamalipour, “Traffic Offloading for 5G: L-LTE or Wi-Fi”, IEEE Conference on Computer Communications Workshops (INFOCOM WKSHPS): IECCO: Integrating Edge Computing, Caching, and Offloading in Next Generation Networks, 2017.

[2] M. Paolini, “Beyond Data Caps-An Analysis of the Uneven of Growth in Data Traffic”, Senza Fili Consulting, 2011.

[3] JaYeong Kim, Nah-Oak Song, Byoung Hoon Jung, Hansung Leem, and Dan Keun Sung, “Placement of WiFi Access Points for Efficient WiFi Offloading in an Overlay Network,” IEEE 24th International Symposium on Personal, Indoor and Mobile Radio Communications: Mobile and Wireless Networks, 2013.

[4] Gavin Phillips, “the Most Common WiFi Standards and Types Explained”, Mar 2019.

[5] Richard Van Nee et al, “The 802.11n MIMO-OFDM Standard for Wireless LAN and Beyond”, Wireless Personal Communications 37: 445–453, 2006.

[6] Matthew Gast, book “802.11 Wireless Networks: the definitive Guide, 2nd Edition”, June 2009.

[7] Jim Geier, book “Designing and Deploying 802.11n Wireless Networks”, June 2010.

[8] Wi-Fi: Overview of the 802.11 Physical Layer and Transmitter Measurements. Tektronix, 2013.

[9] Bach Duy Vo, “802.11n Wireless Communication System Simulation Using Matlab and Implementation on FPGA”, Faculty of Worcester Polytechnic Institute, 2009.

[10] J. P. Amit Kachroo and H. Kim, “Channel assignment with transmission power optimization method for high throughput in multi-access point wlan,” IEEE, ICT and Future Planning as Global Frontier Project (CISS-2014011066), 2015.

[11] T. van Waterschoot, V. L. Nir, J. Duplicy, and M. Moonen, "Analytical expressions for the power spectral density of cpofdm and zp-ofdm signals," IEEE Signal Processing Letters.

[12] Iyappan Ramachandran and Sumit Roy, "Clear Channel Assessment in Energy-constrained Wideband Wireless Networks", Dep. of Electrical Engineering University of Washington, July 2006.

[13] Laudin Alessandro Molina Troconis, "Techniques et métriques non intrusives pour caractériser les réseaux Wi-Fi", Ecole Nationale Superieure Mines Telecom Atlantique Bretagne Pays De La Loire - IMT Atlantique, July 2018.

[14] Jianjun Lei, "Channel Assignment Mechanism for Multiple APs Cochannel Deployment in High Density WLANs", Wireless Communications and Mobile Computing, Feb 2018.

[15] M. Z. Dawei Gong and Y. Yang, "Channel assignment in multirate 802.11n wlans," IEEE Wireless Communications and Networking Conference, 2013.

[16] A. A. M. Nicolas Montavont and G. Castignani, "On the selection of scanning parameters in ieee 802.11 networks," IEEE 24th International Symposium on Personal, Indoor and Mobile Radio Communications: Mobile and Wireless Networks, pp. 2137–2141, 2013.

[17] Laudin Molina, Alberto Blanc, Nicolas Montavont, and Ljiljana Simić, "Identifying Channel Saturation in Wi-Fi Networks via Passive Monitoring of IEEE 802.11 Beacon Jitter", 15th ACM International Symposium on Mobility Management and Wireless Access, Nov 2017.

[18] Behrouz Shahgholi Ghahfarokhi, "Distributed QoE-aware channel assignment algorithms for IEEE 802.11 WLANs" Wireless Network (vol.21), pp.21–34,(2015).

[19] Mohamad Haidar et al, "Channel Assignment in an IEEE 802.11 WLAN based on signal-to-interference ratio", CCECE/CCGEI May 2008.

[20] Arunesh Mishra, Suman Banerjee, and William Arbaugh , "Weighted coloring based channel assignment for WLANs", ACM SIGMOBILE Mobile Computing and Communications Review Homepage archive, Volume 9 Issue 3, July 2005.

[21] Salim Eryigit ; M. Sarper Gokturk, “Cloud-assisted channel selection for wireless mesh networks”, 2017 IEEE International Black Sea Conference on Communications and Networking, June 2017.

[22] C. Thorpe, S. Murphy, and L. Murphy, “Analysis of variation in ieee802.11k channel load measurements for neighbouring wlan systems,” in ICT Mobile and Wireless Communications Summit (ICTMobileSummit’08), Jun. 2008.

[23] Ashish Kumar and Dr. M.Nandhini, “An efficient least congested distributed channel selection algorithm with associated and interfering stations in WLAN”, International Journal of Advanced Research in Computer Science, Feb 2017.

[24] Ram Krishana, Vijay Laxmi, “IEEE 802.11 WLAN Load Balancing for Network Performance Enhancement”, 3rd International Conference on Recent Trends in Computing 2015.

[25] Emmanuel A. Panaousis et al, “Optimizing the channel load reporting process in IEEE 802.11k-enabled WLANs”, 16th IEEE Workshop on Local and Metropolitan Area Networks, Sep 2008.

[26] Haeyoung Lee, Seiamak Vahid, and Klaus Moessner, “Traffic-aware Resource allocation with aggregation in Heterogeneous Networks with WLANs”, 2018 European Conference on Networks and Communications (EuCNC), Jun 2018.

[27] Nemesio A. Macabale , “Load Aware Routing in Wireless Mesh Networks: Which is the Right Metric?”, IEEE 42nd Conference on Local Computer Networks Workshops, 2017.

[28] Mehmet Karaca and Bjorn Landfeldt “Learning based Channel Load Measurement in 802.11 Networks”, arXiv:1301.2750v3, Apr 2016.

[29] P. D.Welch, “The use of fast fourier transform for the estimation of power spectra: A method based on time averaging over short, modified periodograms,” IEEE Trans. Audio and Electroacoust., vol. 15, pp. 70–73, June 1967.

[30] R. M. Hansa Rani Gupta, “Power spectrum estimation using welch method for various window techniques,” International Journal of Scientific Research Engineering and Technology (IJSRET), vol. 2, no. 6, p. 389 392, Sep 2013.

[31] J. C. M. B. Jie Chen, Cedric Richard and P. Honeine, “Nonnegative least-mean square algorithm,” IEEE Transactions on Signal Processing, vol. 59, no. 11, pp. 5225–5235, Nov 2011.

[32] M. Shakil and M. Ahsanullah, “Record values of the ratio of rayleigh random variables,” Pak. J. Statist., vol. 27, no. 3, pp. 307–325, 2011.

[33] “Theorem The square of a Rayleigh random variable is an exponential random variable”, college of William and Mary, Williamsburg, Virginia.

[34] Oguntunde et al, “On a Modified Ratio of Exponential Distributions”, technical report, Covenant University.

[35] M. Pandey and B. L. Pal, “Adaptation to best fit learning rate in batch gradient descent,” International Journal of Science and Research (IJSR), vol. 3, no. 8, Aug 2014.

[36] 3GPP ETSI TR 125.913 V8.0.0 Release 8. 2009. Requirements for Evolved UTRA (E-UTRA) and Evolved UTRAN (E-UTRAN).

[37] Prabhat Man Sainju, “LTE Performance Analysis on 800 and 1800 MHz Bands”, Tampere University of Technology, 2012.

[38] Rafael Lopes Conde dos Reis, “4G – LTE/LTE-A”, Federal University of Rio de Janeiro Polytechnic school.

[39] Harri Holma, and Antti Toskala, “WCDMA for UMTS: HSPA Evolution and LTE”, 5th Edition, Sep 2010.

[40] Amit Kachroo, Mehmet Kemal Ozdemir, Hatice Tekiner-Mogulkoc, “Optimization of LTE Radio Resource Block Allocation for Maritime Channels”, IEEE 37th Sarnoff Symposium at Newark, Aug 2018.

[41] Zewdu Gurmu, Long Term Evolution (LTE) Radio Network Dimensioning, Addis Ababa University, June 2015.

[42] Noman Shabbir, Muhammad T. Sadiq, Hasnain Kashif and Rizwan Ullah, “Comparison of radio propagation models for long term evolution (LTE) network,” International Journal of Next-Generation Networks (IJNGN), 2011, Vol.3, No.3.

[43] Mahdi Ezzaouia, "Allocation de ressource opportuniste dans les réseaux sans fil multicellulaires", Réseaux et télécommunications [cs.NI], Ecole nationale supérieure Mines-Télécom Atlantique, Université de Tunis El Manar, 2018.

[44] Lin Guangpu, Dong Fei, Ying Weimin, He Gang, Tan Zhu, “Guide: Long Term Evolution (LTE) Radio Access Network Planning,” huawei technologies CO., LTD, 2011.

[45] Techplayon, "LTE eNodeB Scheduler and Different Scheduler Type", Aug 2018

[46] Mohamad Omar Kayali, Zeinab Shmeiss, Haidar Safa, and Wassim El-Hajj, "Downlink scheduling in LTE: Challenges, improvement, and analysis", 13th International Wireless Communications and Mobile Computing Conference (IWCMC), 2017.

[47] Apostolos Apostolaras, George Iosifidis, Kostas Chounos, Thanasis Korakis, Leandros Tassiulas, “C2M: Mobile Data Offloading to Mesh Networks,” IEEE Global Communications Conference, 2014.

[48] Stefania Sesia, Issam Toufik and Matthew Baker, “The UMTS Long term Evolution – From Theory to Practice”, 2011.

[49] Savio Dimatteo, Pan Hui, Bo Han, and Victor O.K. Li, “Cellular Traffic Offloading through WiFi Networks,” IEEE MASS, 2011.

[50] Cisco’s annual Global Mobile Data Traffic Forecast Update (2017 – 2022).

[51] Greg Najjar, Mark Reynolds, Don Bach, and Luke Lucas, “The 5G Paradox: The Need for More Offloading Options in the Next-Generation Wireless Era”, WIA Innovation & Technology Council, Feb 2019.

[52] “ROI Analysis of WiFi Offloading”, Wireless 20|20, WiFi offloading, 2015.

[53] Tian Wang, Guoliang Xing, Minming Li, and Weijia Jia, “Efficient WiFi Deployment Algorithms based on Realistic Mobility Characteristics,” IEEE MASS, Dec 2010.

[54] Eyuphan Bulut, and Boleslaw K. Szymanski, “WiFi Access Point Deployment for Efficient Mobile Data Offloading”, ACM Workshop PINGEN at Mobicom’12, Aug 2012.

[55] Qimei Chen, Guanding Yu, Amine Maaref, Geoffrey Ye Li, and Aiping Huang, “Rethinking Mobile Data Offloading for LTE in Unlicensed Spectrum,” IEEE Transactions on Wireless Communications, VOL. 15, NO. 7, July 2016.

[56] Qimei Chen et al, “Cellular Meets WiFi: Traffic Offloading or Resource Sharing?”, IEEE Transactions on Wireless Communications, 2016.

[57] Yan Li and Shaoyi Xu, “Traffic Offloading in Unlicensed Spectrum for 5G Cellular Network: A Two-Layer Game Approach”, Entropy, Jan 2018.

[58] Sinisa Husnjak, Dragan Perakovic, and Ivan Forenbacher, “Data Traffic Offload from Mobile to Wi-Fi Networks: Behavioural Patterns of Smartphone Users”, Wireless Communications and Mobile Computing, Mar 2018.

[59] A. Aijaz, N. Uddin, O. Holland, A. H. Aghvami, "On Practical Aspects of Mobile Data Offloading to Wi-Fi Networks", Networking and Internet Architecture, arXiv:1508.01926, 2015.

[60] Irena Malolli, “Wi-Fi Offloading Strategies for Facing Mobile Data Traffic Challenges”, International Journal of Computer Science and Network, Volume 6, Issue 2, April 2017.

[61] Viral V. Kapadia, Sudarshan N. Patel and Rutvij H. Jhaveri, "Comparative study of hidden node problem and solution using different techniques and protocols", Journal of computing, Volume 2, issue 3, March 2010.

[62] Jaha Mvulla, Eun-Chan Park, Muhammad Adnan, and Ju-Hyung Son, "Analysis of Asymmetric Hidden Node Problemin IEEE 802.11ax Heterogeneous WLANs", International Conference on Information and Communication Technology Convergence (ICTC), Oct 2015.

[63] Javad Jafarian, Khairi A. Hamdi, "Analysis of the Exposed Node Problem in IEEE 802.11 Wireless Networks", Academia, 2010.

[64] Apostolos Apostolaras et al, "A Mechanism for Mobile Data Offloading to Wireless Mesh Networks", IEEE Transactions On Wireless Communications, Vol 15, Sep 2016.

[65] Zhiyi Zhou et al, "Allocation of Licensed and Unlicensed Spectrum in Heterogeneous Networks", Australian Communications Theory Workshop, 2016.

[66] Kishor Pratap Singh, Pradeep Kumar Chopra, “Throughput Computation of LTE-A Network for Urban Area,” International Journal of Advanced Research in Electronics and Communication Engineering (IJARECE) Volume 3, Issue 11, Nov 2014.

[67] Pierre Bertrand, “Channel Gain Estimation from Sounding Reference Signal in LTE,” IEEE 73rd Vehicular Technology Conference (VTC Spring), 2011.

[68] Tatsuro Ichiishi, "Game Theory for Economic Analysis", A volume in Economic Theory, Econometrics, and Mathematical Economics Book, 1983.

[69] L. Shapley, Contributions to the Theory of Games II, ser. Annals of Mathematics Studies. Princeton University Press, 1953, vol. 28, ch. A Value for n-Person Games, pp. 307–317.

[70] Sander Muns, "A note on the Shapley value for characteristic functions on bipartitions", Aug 2018.

[71] Amal Abdel Razzac, Salah Eddine Elayoubi, Tijani Chahed, and Bachar ElHassan, “Dimensining and Profit Sharing in Hybrid LTE/DVB Systems to Offer Mobile TV Services”, IEEE Transactions on Wireless Communications, Vol 12, No 12, Dec 2013.

Titre : Intégration WiFi et LTE dans le domaine du système 5G

Mots clés : 5G, Réseaux hétérogènes, décharge et coexistence du LTE et WiFi, sélection des canaux dans le réseau WiFi, couche physique du 802.11n, Valeur de Shapley

Résumé : suite à l'augmentation continue du trafic de données mobiles, la technologie 5G a été introduite pour offrir une capacité et un débit de données plus élevé. Ceci impose de nouvelles méthodes pour renforcer les capacités comme l'intégration de petites cellules, ou ajouter des nouvelles fréquences sans licence, autour de 2.4 et 5 GHz des réseaux WiFi pour former les réseaux hétérogènes. Pour ces raisons, la coopération entre WiFi et 4G ou Long Term Evolution (LTE) est nécessaire.

Dans cette thèse, différents algorithmes ont été proposés pour assurer une coopération optimale entre WiFi et 4G dans le chemin du système 5G pour les réseaux hétérogènes. Notre premier algorithme calcule la valeur de la charge des canaux de la couche physique du 802.11n. Ayant cette valeur, nous présentons notre second algorithme qui propose de dimensionner un réseau WiFi pour décharger le réseau 4G en transférant les utilisateurs, qui consomment le plus de débits de données, au réseau WiFi. Finalement, nous avons calculé le profit de la coopération entre WiFi et LTE en utilisant la valeur de Shapley.

Title: WiFi Integration with LTE in the Roadmap of 5G Networks

Keywords: 5G, Heterogeneous Networks, LTE WiFi offload and coexistence, WiFi Channel selection, 802.11n physical layer, Shapley Value profit sharing.

Abstract: Following the continuous increase of the mobile data traffic, the 5G technology has been introduced to offer additional capacity and higher data rate. WiFi APs integration with mobile networks are considered as potential candidate towards the heterogenous networks.

We first propose in this thesis an algorithm for the estimation of the WiFi physical channels load through the observation of the non-overlapped channels and estimating as a result the load of the entire physical channels. Then, in our second proposed algorithm, we propose to dimension the WiFi network to offload LTE network and transfer the users that consume the high level of transmission power. The algorithm calculates the minimum needed number of APs that will support the extra offloaded LTE traffic.

Finally, we evaluate the benefit of the cooperation by estimating the profit share of LTE and WiFi. We calculate for each player the profit using a coalition game concept based on Shapley value.